Lecture Notes in Economics
and Mathematical Systems 630

Björn Lutz

Pricing of Derivatives on Mean-Reverting Assets

Springer

Dr. Björn Lutz
Hauck & Aufhäuser Asset
Management GmbH
Löwengrube 18
80333 München
Germany
bjoern.lutz@haam.de

ISSN 0075-8442
ISBN 978-3-642-02908-0 e-ISBN 978-3-642-02909-7
DOI 10.1007/978-3-642-02909-7
Springer Heidelberg Dordrecht London New York

Library of Congress Control Number: 2009930466

Cover design: SPi Publishing Services

Printed on acid-free paper

Springer is part of Springer Science+Business Media (www.springer.com)

To Inge and Karl

Foreword

As already mentioned by Lo and Wang (1995) there is an apparent paradox if we derive standard option pricing formulae for an underlying mean-reverting drift. While the drift has an influence on the long-run behavior of the underlying, the option price becomes independent of the drift of the price process itself. Using the continuous-time pricing framework this leads to option prices which are much too large for more distant maturities. One possible solution for this paradox is the assumption that the market is incomplete. As shown by Ross (1997), in an incomplete market the mean reversion remains in the drift of the risk-adjusted process under the equivalent martingale measure. However, mean reversion in the drift complicates the solution process for option pricing considerably.

Lutz contributes to this research in several respects. Using state-of-the-art Fourier inversion techniques he extends the mean-reverting one-factor diffusion setting of Schwartz (1997) and Ross (1997) and discusses processes with stochastic volatility, different jump components, a stochastic equilibrium level and deterministic seasonalities. This leads to new and rather complex models, where the resulting Riccati systems are difficult to solve. While giving new analytic solutions in some cases Lutz shows that numerical procedures for the Riccati systems are often superior in terms of numerical efficiency.

I recommend this research monograph to everybody who deals with the specific peculiarities of mean-reversion in option pricing.

Tübingen, *Rainer Schöbel*
May 2009

Acknowledgements

The research presented in this Ph.D. thesis has been carried out at the College of Economics and Business Administration at the Eberhard Karls University Tübingen.

Many people have helped me in the course of my research in writing this thesis, and any merit in it is in large measure due to them. First and foremost, I would like to thank my academic supervisor and first referee of this thesis, Prof. Dr.-Ing. Rainer Schöbel, and the second referee, Prof. Dr. Joachim Grammig.

During my time as a student and research assistant in Tübingen, some of my colleagues have become friends. I am deeply indebted to Dr. Detlef Repplinger, Robert Frontczak, Dr. Wolfgang Kispert, Dr. Josef Schürle, Vera Klöckner and Heiko Wöner for reading and fruitful comments to this work, for interesting discussions, the provision of empirical data and, most importantly, all the fun we had together. I would like to thank you for your support and I hope we will enjoy each other's company in the years to come.

Last but not least, I wish to thank my entire family for providing a loving environment for me. My sister, Dr. Eva Huber, and my cousin, Benjamin Kansy, were particularly supportive. Most importantly, my gratitude goes to my parents Ingeborg and Karl Lutz for their never-ending support. To them I dedicate this thesis.

München, *Björn Lutz*
May 2009

Contents

List of Figures

List of Tables

List of Notations and Symbols

DFT	Discrete Fourier transform
FFT	Fast Fourier transform
FPDE	Fundamental partial differential equation
FRFT	Fractional fast Fourier transform
IFFT	Inverse fast Fourier transform
MC	Monte-Carlo
ODE	Ordinary differential equation
OU	Ornstein–Uhlenbeck
RK	Runge–Kutta
SDE	Stochastic differential equation

γ	Parameter of exponential and Γ-distribution
δ	Dampening parameter
η	Adjustment speed of the mean-reverting price process
κ	Adjustment speed of the mean-reverting subordinated process
μ	$\overline{X}/\eta$; drift parameter in the Tahani model
$\mu_{\mathfrak{X}}$	Drift term parameter of subordinated stochastic mean process
μ_J	Determines together with σ_J the mean of the logarithm of jump size J
π	pi $= 3.14159\ldots$
ϕ	Fourier parameter
ρ	Correlation coefficient
σ	Instantaneous volatility
$\sigma_{\mathfrak{X}}$	Standard deviation of subordinated stochastic mean process
σ_J	Standard deviation of the logarithm of jump size J
θ	Equilibrium level of the subordinated process
χ	Market price of risk
χ_t^*	Short term component in Schwartz and Smith (2000)
λ	Jump intensity or eigenvalue
φ	Density function
ξ	Second parameter of Γ-distribution
ξ_t^*	Long term component in Schwartz and Smith (2000)
ζ	Volatility of variance (volatility) process
τ	$T - t$
Λ_j	Seasonality component parameter

Π_1	Option's delta
Π_2	Risk-neutral exercise probability of a call option
Φ	Characteristic function
Υ	Moment-generating function
Ξ	Convenience yield
Ω	Probability space
h	Step size in ODE integration schemes
i	$\sqrt{-1}$
k	$\ln(K)$
r	Risk-free instantaneous interest rate
t	Actual date
$B(t,T)$	Zero bond with time to maturity $T-t$ and a face value of 1
C_t	Price of a call option at time t
$D(t,T)$	$\exp\{-\int_t^T r_s ds\}$
$\mathfrak{D}$	Discounted value of a call option
F	Futures price
F_m	m-th element of the discrete Fourier transform
$\mathcal{F}$	Filtration generated by S_t
FW	Forward price
$J(.)$	Bessel function of the first kind
J	Jump size variable
$\mathbf{J}$	Jacobi matrix
K	Strike price
M	Kummer function of the first kind
N_t	Poisson process
$N(.)$	Normal cumulative distribution function
$\mathcal{O}(h)$	Term of order h
P_t	Jump process
S_t	Spot price
$\overline{S}$	Equilibrium level of S_t
$\mathfrak{S}$	Seasonality component
T	Maturity date
U	Kummer function of the second kind
V_t	Instantaneous variance
W_t	Wiener process
$\mathfrak{W}$	Portfolio wealth
X_t	$\ln(S_t)$
$\overline{X}$	Constant equilibrium level of X_t
$\mathfrak{X}_t$	Stochastic equilibrium level of X_t
Y	Bessel function of the second kind
Z	Radon-Nikodym derivative
$\mathbb{N}$	The set of natural numbers
$\mathbb{P}$	Original probability measure
$\mathbb{Q}$	Risk-neutral probability measure
$\mathbb{R}$	The set of real numbers
$\mathbb{1}$	Indicator function

Chapter 1
Introduction

The commodity derivatives market has strongly increased in recent years, both in trading volume and the variety of offered products. Adequate models to price and hedge commodity futures and options are required and a multitude of models are already proposed. However, the derivative pricing theory developed for financial assets cannot be utilized for commodity derivatives without some adaptations, since it is important that the models capture the empirical properties of commodity price processes. The most important among these are mean reversion in spot and futures prices and backwardation in futures prices for some commodities.[1] Backwardation is an implication of mean reversion and may be used as a predictor for mean-reverting spot prices.[2]

Unlike financial assets, supply and demand for commodities are to a large extent influenced by production costs and consumer behavior. When prices are low, consumption will increase and high-cost producers will leave the market. This leads to an increase in prices. When prices are relatively high, consumers and producers will react vice versa, putting a downward pressure on prices.[3] Additionally, the level of inventories plays an important role in determining the value for storable goods.[4] The owner of the good decides whether to consume it immediately or store it for future disposal. Hence, the price of the commodity is the maximum of its current consumption and asset values.[5]

In Fig. 1.1 and 1.3, the behavior of futures prices can be seen for two commodity futures traded at the New York mercantile exchange (NYMEX). The graphs show

[1] (Strong) backwardation refers to (discounted) futures prices which are lower than the current spot price. A consumer has the possibility to buy the good now and store it until it is needed for consumption. In this case, he faces storing costs and foregone interest as opportunity costs. The second alternative is to buy the corresponding futures contract where payment and delivery is deferred to the maturity date. One would expect that the futures price is in contango, i.e. is above the current spot price, since it incorporates the costs of the first alternative. Therefore, situations of backwardation can only arise when the immediate disposition is worthy.

[2] French (2005).

[3] See Schwartz (1997).

[4] The theory of storage traces back to Kaldor (1939) and Working (1948, 1949).

[5] Routledge, Seppi, and Spatt (2000).

B. Lutz, *Pricing of Derivatives on Mean-Reverting Assets*,
Lecture Notes in Economics and Mathematical Systems,
DOI 10.1007/978-3-642-02909-7_1,

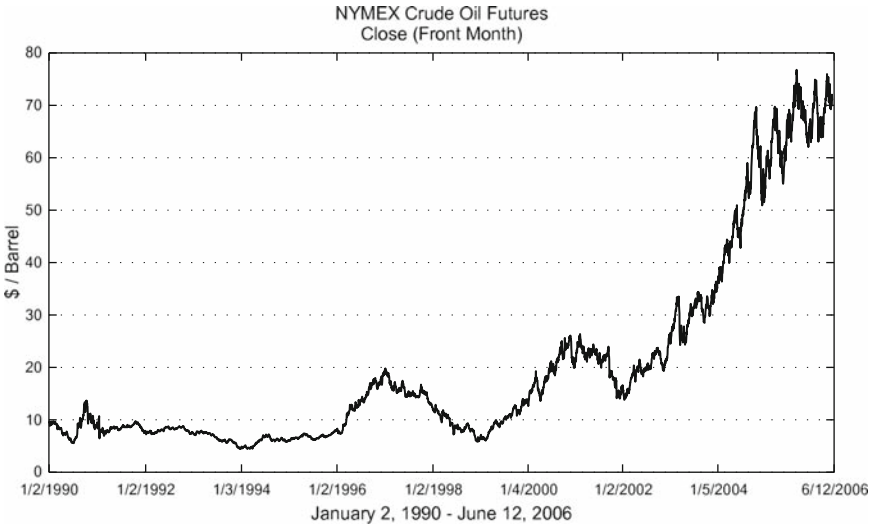

Fig. 1.1 NYMEX crude oil futures prices from 01/02/1990 to 06/12/2006
Source: Bloomberg data

the closing price variations of the nearest-to-deliver futures contract for crude oil and natural gas.

It can be seen that particularly the crude oil futures price behavior experienced a regime shift in the last few years. In the period before 2002, the futures price clearly shows a mean-reverting pattern, though the average amplitude of the price peaks increased at the end of the 1990's. From 2002 to 2006, the futures price increased sharply from 13.8$ per barrel to round about 70$ per barrel (68.68$ per barrel were already reached on 10/15/2004). The reason for this regime change is twofold. Firstly, considering oil supply, the current limit of the oil production capacity is fairly reached and there exists uncertainty about the remaining global oil resources. Secondly, considering oil demand, particularly the oil demand of China increased tremendously. The large impact of the new supply/demand-ratio can be seen in the 400%-price rise within 3 years.

Figure 1.2 displays the oil price trend for a one-year period. When comparing Figs. 1.1 and 1.2, one observes that models with a mean-reverting oil price process could be appropriate for short-term oil futures, while long-term models should additionally incorporate the risk of regime shifts.[6] In the foreseeable future, the regime shift risk in oil price behavior could also affect oil substitutes such as natural gas, though the price history of natural gas shows mean-reverting behavior with large peaks and did not yet experience such a regime shift as the oil price did.

[6] In Chap. 6, we propose models with a stochastic equilibrium level. A jump component in the subordinated equilibrium level process could account for the risk of a regime shift.

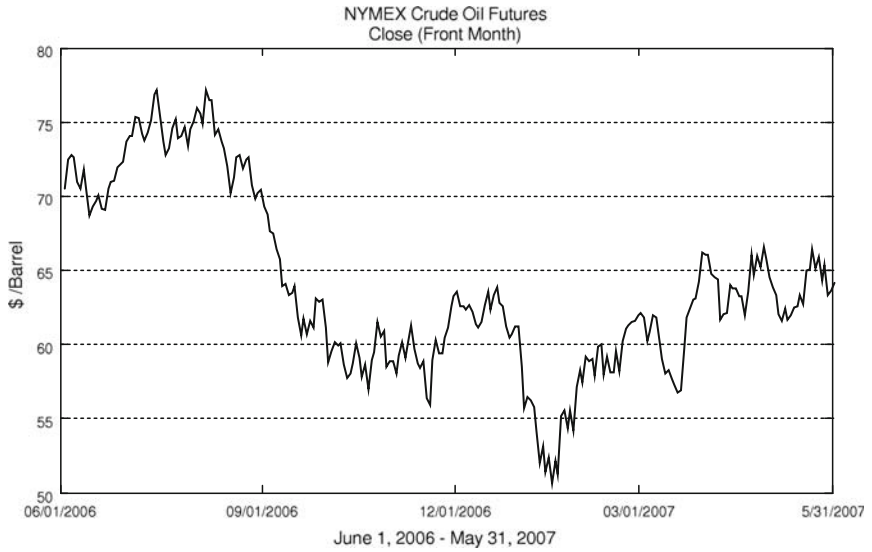

Fig. 1.2 NYMEX crude oil futures prices from 06/01/2006 to 05/31/2007
Source: Bloomberg data

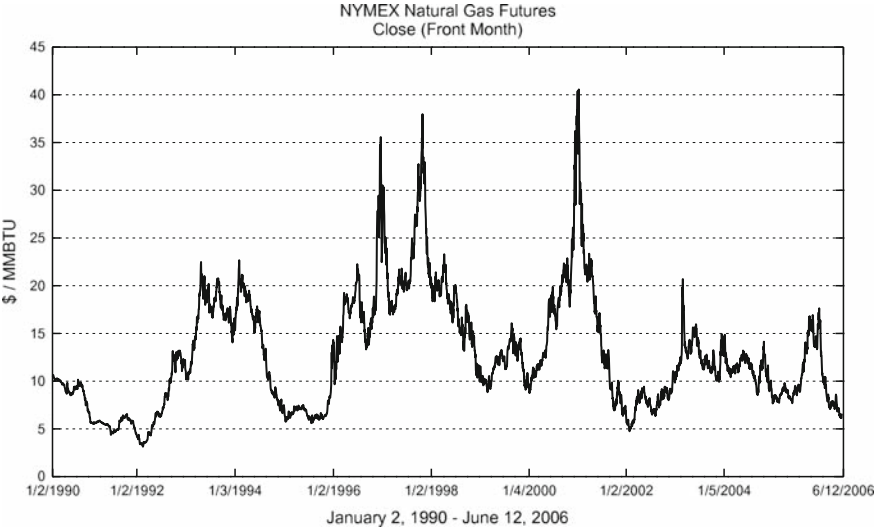

Fig. 1.3 NYMEX natural gas futures prices from 01/02/1990 to 06/12/2006
Source: Bloomberg data

The main reason for short-term price peaks is that consumption and demand are quite inelastic for some products. This may lead to a shortage of the good when production shows an intense decline, e.g. due to crop failures in case of agricultural commodities, unstable political situations in oil producing countries in case of

crude oil, or when dealing with electricity, consider heat waves which lead to a shutdown of nuclear power plants because the cooling water of the rivers is overheated. Since storage is limited, such situations drive the inventory level to zero while prices increase dramatically. In case of electricity, storage is virtually impossible (excluding hydro power) and therefore, the buffering effect of inventories is not existent, leading to large peaks in prices which decay as fast as they arrived when the reason for the shortage is eliminated.[7]

In periods of shortage, the owner of the physical commodity clearly has an advantage compared with the owner of a contract for future delivery.[8] The advantage arises both from price variations and from the ability to maintain a consumption plan or production process. The sum of these "convenient" effects for the holder of the physical good is called convenience yield. As already stated by Kaldor (1939) and Working (1948, 1949), the magnitude of the convenience yield depends inversely on inventories. Routledge, Seppi, and Spatt (2000) follow this approach. They model the level of inventories endogenously in discrete time. The resulting price process is regime-shifting, including one regime with positive inventories and one with zero inventories. A plausible assumption is that the convenience yield in their model is an output variable.

Bühler, Korn and Schöbel (2004) also implement the short-sale constraint in a two-regime pricing model for crude oil futures prices. They take the spot price as exogenous variable and model the futures price in a continuous time two-regime setting, where low spot prices correspond to the cost-of-carry model and high spot prices correspond to the Schwartz (1997) model 1. While the former model assumes that the futures price is only determined by the spot plus storage costs and interest, the latter model assumes a mean reverting spot price process due to convenience yield effects.[9]

Schwartz (1997) proposes three model settings for the spot price process of commodities. In all three types, the mean reverting property of the price process is considered, either directly in a price process of Ornstein–Uhlenbeck type as in model 1 or indirectly through a subordinated convenience yield process as in models 2 and 3. Model 3 incorporates also stochastic interest rates. While models 2 and 3 are based upon standard arbitrage theory, model 1 is similar to Ross (1997).[10]

Ross postulates that frictions in the commodity market inhibit derivative security pricing according to the cost-of-carry model. One may think of high costs for storing and holding of the good, limited storing both in volume and in time (e.g. in case of perishable agricultural goods) or the absence of storing possibilities (e.g. when

[7] See Geman and Roncoroni (2006). The buffering effect of inventories can be seen in the graphs of electricity prices in this paper, since the price peaks are considerably smaller in an energy pool with a large amount of hydro power.

[8] See Brennan (1991). As a result of this, futures prices can be backwardated.

[9] The setup of the model 1 in Schwartz was already considered in Schöbel (1992) as well as Bjerksund and Ekern (1995).

[10] Ross assumes mean-reversion in the price process, whereas Schwartz's model 1 is based on mean-reversion in the log-price process.

dealing with electricity as underlying). These properties result in a price process which is mean reverting under the equivalent martingale measure.[11]

The papers of Ross and Bühler, Korn and Schöbel are representative for a series of papers which investigate the crisis of the German company Metallgesellschaft in 1993. Metallgesellschaft had a program of selling long-dated fuel and oil supply commitments to end-users and hedged these commitments by rolling over short-term futures contracts. In complete and frictionless markets, such a hedging strategy is promising. In fact, things are different and Metallgesellschaft experienced liquidity problems due to large variation margin calls on the futures, finally leaving the company with a loss of USD 1.3 bn after unwinding all of the outstanding positions. After the Metallgesellschaft case, the pricing and hedging of commodity (and especially crude oil) futures contracts became an interesting and vivid subject in financial research.

The purpose of this thesis is an extension of the one-factor models of Schwartz and Ross. Hence, we combine mean reversion in the underlying price process with other stochastic factors such as stochastic volatility and stochastic equilibrium level. Discontinuous jump events and deterministic seasonality effects are also included. The derived solutions can be applied for European type derivatives on assets which show mean-reverting behavior, namely commodity derivatives, electricity contracts, currency options or credit spread options.[12]

The above-mentioned model extensions were already introduced in other papers, though the combination of some of the factors is new in this work. As for the stochastic volatility extension, there exist various papers which deal with stochastic volatility, but not with mean-reverting price processes. Heston (1993) introduces the square-root process as subordinated variance process. Stein and Stein (1991) adopt the Ornstein–Uhlenbeck process as volatility process. Schöbel and Zhu (1999) and Zhu (2000) extend Stein and Stein (1991) and allow for non-zero correlation. Tahani (2004) was first in combining mean reversion in the underlying with square-root and Ornstein–Uhlenbeck stochastic volatility, following Longstaff and Schwartz (1995) and Zhu (2000).[13] However, the Tahani approach has some shortcomings. Due to a slightly different model setup, we are able to remedy the deficiencies of the Tahani model and provide a closed-form solution based on hypergeometric functions in the square-root stochastic volatility case.

Concerning jump components, there is already a multitude of models proposed in various papers, amongst others Bates (1996a, 1996a, 2000), Bakshi et al. (1997), Hilliard and Reis (1998, 1999), Duffie et al. (2000), Zhu (2000) and Eraker (2004). Textbook references on this topic are Cont and Tankov (2003) and Shreve (2004), for instance. However, all of these papers consider financial assets as underlying

[11] Cf. Ross (1997).

[12] The mean-reverting property of exchange rates is addressed in Sørensen (1997), Anthony and MacDonald (1998, 1999) and Hui and Lo (2006), among others. As for credit spread options, cf. Longstaff and Schwartz (1995) and Tahani (2004).

[13] Longstaff and Schwartz (1995) deal with a mean-reverting price process without stochastic volatility.

and deal with non-mean reverting asset prices.[14] The combination of mean reverting price processes with jumps can be found in Das (2002), who models jumps in interest rate processes, as well as in Kamat and Oren (2002), Kispert (2005) and Geman and Roncoroni (2006), among others. The latter references all deal with the modeling of electricity futures prices. However, the authors do not combine mean reversion, jumps and stochastic volatility. Closed-form solutions for this model setup are also not presented in this work, but due to the use of numerical integration algorithms for systems of ordinary differential equations, we are able to provide fast and accurate solution methods also for this case.

The combination with a stochastic equilibrium level is discussed in Schwartz and Smith (2000), Korn (2005) and Realdon (2007). Schwartz and Smith (2000) work with a price process which is additionally composed of an increasing long-term factor and a zero-mean Ornstein–Uhlenbeck process as short-term factor. We firstly extend model 1 in Schwartz (1997) by making the equilibrium level stochastic. In this model setup, the long-term equilibrium level follows a Brownian motion process with drift. This specification is based on a subordinated process, but nearly equivalent to the Schwartz and Smith (2000) setup. Korn (2005) follows Schwartz and Smith by working with a long-term and a short-term price component, but the long-term component in his setup is specified by an Ornstein–Uhlenbeck process. Realdon (2007) deals with a subordinated equilibrium level process which is also mean-reverting. We extend Realdon (2007) as for the presentation of a closed-form solution and a special case solution. We further extend both specifications of the stochastic mean by implementing stochastic volatility. Finally, the combination with jump elements is considered.

Seasonality effects are obviously a feature of commodities which are subject to cyclical fluctuations, e.g. the harvesting cycle in case of agricultural commodities or the season cycle in case of electricity derivatives. Hence, papers incorporating seasonality effects in the price process focus on the pricing of either agricultural commodity derivatives (e.g. Sørensen (2002) and Richter and Sørensen (2002)) or electricity derivatives (Lucia and Schwartz (2002), Elliott et al. (2003), Weron et al. (2003) and Kispert (2005), among others). The specifications of the seasonal component in the papers dealing with electricity are all very similar. It consists of one sine function with a frequency of one year. The approach of Richter and Sørensen (2002) is more flexible, since it consists of a combination of weighted sine and cosine functions.

We follow Richter and Sørensen (2002) as for the specification of the seasonal component. However, the authors work with a non-mean-reverting price process. The seasonality effect in their subordinated variance process is associated with an exponential function, which inhibits closed-form solutions. We discuss seasonal components in the mean-reverting underlying and the variance process. We show that the structure of the solution remains unchanged by the incorporation

[14] An exception is Hilliard and Reis (1998, 1999) who model jumps in commodity price processes. However, their model specification is also non-mean reverting.

of deterministic seasonality effects. Hence, we are able to provide closed-form solutions for some model setups which are not too complex. We also present an alternative specification of the seasonality component in the variance process which allows closed-form solutions. The incorporation of seasonality effects in the model setups of the preceding chapters is also considered.

The remainder of this thesis is organized as follows. In Chap. 2, we firstly deal with empirical findings concerning the sources of mean reversion. Chapter 3 develops the fundamentals of derivative pricing to provide a framework for the model specifications of the following chapters. In Chap. 4, we generalize model 1 of Schwartz (1997) to square-root and Ornstein–Uhlenbeck stochastic volatility. We compare our findings with a similar attempt of Tahani (2004) and provide a comparison with numerical Monte Carlo results. This verification of accuracy via Monte Carlo results is repeated for the most important models in the following chapters. Chapter 5 addresses the integration of different jump components in the stochastic volatility framework. In Chap. 6, the standard Ornstein–Uhlenbeck model is extended by a stochastic equilibrium level. We propose two different specifications for the subordinated equilibrium level process. The combination with the model extensions of the previous chapters is also discussed. Chapter 7 deals with seasonality effects in the price and variance processes. We address extensions of previously discussed model propositions with seasonal components. Chapter 8 concludes.

Chapter 2
Mean Reversion in Commodity Prices

2.1 Sources of Mean Reversion

In this chapter, we discuss the sources, empirical evidence and implications of mean reversion in asset prices. As for the sources of mean reversion, there are three aspects to be discussed. Firstly and most importantly, the correlation between the convenience yield and spot prices accounts for mean reversion. Secondly, spot price level dependent time-varying risk premia have a mean-reverting impact on prices and thirdly, a negative relation between interest rates and prices induces mean reversion. In this section, we will tackle the link between mean reversion and convenience yields as well as with time-varying risk premia.[1]

2.1.1 Convenience Yields

We will focus on commodity markets, where mean reversion is mainly induced by convenience yields. The convenience yield is the sum of all effects which evolve from the ownership of the physical commodity compared to the ownership of a futures contract.[2] Hull (2006) explains the convenience yield as reflecting "the market's expectations concerning the future availability of the commodity. The greater the possibility that shortages will occur, the higher the convenience yield." In case of shortage of the good, one may think of convenience yield as non-existent transportation costs since the good is already available or the value of the ability to profit from local shortages of the commodity, which involves both price variations when the good is sold or the convenience of being able to maintain a production process when inventories are used for own purposes. It is evident that the magnitude of such effects depends inversely on the overall level of inventories. Since the theory of

[1] Mean reversion arising from a negative relation between interest rates and prices arises in the case of commodities which mainly serve as a store of value, i.e. precious metals. This feature is addressed in Sect. 2.2.

[2] Cf. also Brennan (1991).

B. Lutz, *Pricing of Derivatives on Mean-Reverting Assets*,
Lecture Notes in Economics and Mathematical Systems,
DOI 10.1007/978-3-642-02909-7_2,

storage traces back to Kaldor (1939) and Working (1948, 1949), Brennan (1991) calls this finding the Kaldor–Working-hypothesis.[3]

In our model setup in the subsequent chapters, we implement mean reversion directly in the price process by means of an Ornstein–Uhlenbeck (OU) process. An alternative approach of working with mean reverting spot prices is to assume a subordinated convenience yield process where the convenience yield may depend on spot prices. The setup for the underlying price process conforms in the simplest case to the Black–Scholes stochastic differential equation (SDE). However, mean reversion in spot prices may be induced by the subordinated convenience yield process. In some cases, both model formulations can be equivalent.[4] Casassus and Collin-Dufresne (2005) point out that models which imply mean reversion of spot prices under the risk-neutral measure can be interpreted as "arbitrage-free models of commodity spot prices, where the convenience yield is a function of the spot price."

Let us give a short overview of stochastic convenience yield models. This model class does not examine the behavior of inventory levels, but makes use of the fact that the convenience yield will depend on spot prices, since low inventories correspond to high spot prices and high convenience yields. A common assumption in this model class is constant correlation between the stock price and the convenience yield (see Gibson and Schwartz (1990), Brennan (1991), Amin et al. (1995), Schwartz (1997) and Hilliard and Reis (1998)). However, it is important to mention the fact that the correlation between spot prices and convenience yields is unlikely to be constant.[5]

Brennan proposes four types of convenience yield models. In three of these models, the convenience yield depends on the spot price. The easiest setting among these is a linear dependency of the spot price as in Brennan and Schwartz (1985). The fourth specification is called "autonomous convenience yield model" where the convenience yield follows a mean reverting process which is independent of the spot price. The commodities which are involved in the empirical investigation are four precious metals (gold, silver, platinum and copper), heating oil, lumber and plywood. The best empirical performance is asserted for the autonomous convenience model, though the models with dependence from the spot price level performed well for precious metals, but not for the other commodities.

Casassus and Collin-Dufresne (2005) present a three factor model of commodity futures prices. The authors call their model "maximal" in the sense that it allows for the most general three factor model setting. On this account, the Casassus and Collin-Dufresne model nests some of the models we already mentioned, namely Gibson and Schwartz (1990), Brennan (1991), Schwartz (1997), Ross (1997) and Schwartz and Smith (2000). The convenience yield is allowed to depend both on interest rates and spot prices. Additionally, they follow Duffee (2002) and model risk

[3] The empirical results of Brennan (1991) concerning the Kaldor–Working hypothesis are discussed in in the next subsection.

[4] See the comparison of models 1 and 2 in Schwartz (1997), p. 927. This equivalence is only given when the subordinated convenience yield process depends linearly on spot prices.

[5] Routledge, Seppi, and Spatt (2000), p. 1300.

premia as linear functions of the state variables, so extending models with constant risk premiums.

2.1.2 Kaldor–Working Hypothesis

The Kaldor–Working hypothesis postulates that the convenience yield depends inversely upon the level of inventories. Models which are directly build up on the Kaldor–Working-hypothesis are Deaton and Laroque (1992, 1996), Schöbel (1992) and Routledge, Seppi, and Spatt (2000), among others. The model setup in these papers is based on modeling the level of inventories.

In his empirical investigation, Brennan (1991) tests the null hypothesis that the convenience yield is zero against the Kaldor–Working hypothesis. For that purpose, the author estimates a non-linear regression of the convenience yield against the inventory/sales ratio. He finds strong evidence for an inverse dependency of the inventory level and the convenience yield for all involved commodities except for platinum.[6] The reason for the insignificant result concerning platinum is that very low inventory levels for this good were only observed during the interference of the Hunt brothers in the silver market in 1980. This speculative period is excluded in the analysis of Brennan. However, when the 1980 data for platinum is considered, one observes a high rate of convenience yield in line with the Kaldor–Working hypothesis. Hence, it is likely that the Kaldor–Working theory applies for all seven commodities analyzed by Brennan, whereas the strength of the inverse relationship between convenience yield and inventory level increases with the consumption purposes of the commodity in relation to its asset purposes.

A similar finding is reported in Casassus and Collin-Dufresne (2005). The authors test their model using futures price data for crude oil, copper, gold and silver. Since the authors do not work with inventory and sales data, the Kaldor–Working hypothesis can only be verified indirectly. Low inventory levels should correspond to high spot prices, which are induced by high convenience yields. For crude oil and copper, the authors assert a significant positive relation between spot price and convenience yield, therefore confirming the theory of storage. Hence, for commodities which serve as consumption good, the relations between convenience yield, spot prices and inventory levels are strong. As for gold and silver, which serve to a large extent as a store of value, the relation between spot price and convenience yield is marginal.

The results of Brennan together with Casassus and Collin-Dufresne suggest that for commodities with both financial and commercial purposes, there exist also both financial and commercial inventories. When commercial inventories are driven to zero, one observes an increase in convenience yields accompanied by an increase in prices according to the Kaldor–Working theory. On the other hand, a variation in

[6] The involved commodities are gold, silver, platinum, copper, heating oil, lumber and plywood.

prices is not obligatory due to low inventory levels since prices may be driven to a large extent by financial investors.[7] Hence, for commodities with both financial and commercial purposes, price levels cannot always be taken as an indicator for the convenience yield and inventory level.

Sørensen (2002) also tests for the empirical evidence of the Kaldor–Working hypothesis based on U.S. data for agricultural commodities, i.e. wheat, corn and soybeans. The methodology is similar to Brennan (1991). The estimation results for all three commodities are significant and document the negative relation between convenience yield and the inventory level.[8] The Kaldor–Working theory seems also to be valid for agricultural commodities, though the regression curve of the net convenience yield against the stocks of inventory turns out to be concave for corn and wheat and is only convex for soybeans.[9] Sørensen explains this pattern with the fact that storage costs were ignored and postulates that the incorporation of storage costs would lead to convex regression curves for all commodities under account.

2.1.3 Time-Varying Risk Premia

Fama and French (1987) use a regression approach as described in Fama (1984) and test for time-varying risk premia. For that matter, they consider a linear regression of changes in the spot price and the forward premium on the basis.[10] The results of the empirical analysis are the following: Only for some agricultural commodities as well as lumber and plywood, there exists reliable statistical evidence for time-varying risk premia. Especially for precious metals, the regression evidence is unreliable, because the basis variances are too small relative to the variances of premiums and the changes in spot prices, though basis variances may be large in absolute terms.

Casassus and Collin-Dufresne (2005) allow risk premia to be time-varying and motivate this specification with the findings of Fama and French. They point out that "mean reversion under the risk-neutral measure is due to convenience yield, whereas mean reversion under the historical measure results from both the convenience yield and the time variation in risk premia."[11] The assumption of time varying risk premiums is therefore important when working with time series of futures prices. The importance of the convenience yield component, respectively the risk premium component, on the overall mean reversion effect in spot prices depends on the type

[7] For instance, prices for gold and silver are to a large amount influenced by interest rates (see also the discussion of Bessembinder et al. (1995) in Sect. 2.2)

[8] Sørensen normalizes the inventory data with respect to total production in the U.S. and not relating to sales data as in Brennan (1991).

[9] A convex regression curve is expected since low inventories should lead to a large increase in convenience yield while the convenience yield should level off at zero when the good is well available.

[10] The basis is the difference of futures and spot price (see also Fama and French (1987), p. 56).

[11] Cassasus and Collin-Dufresne (2005), p. 2285.

of commodity under account. The authors observe for commodities which serve mainly as a consumption good (e.g. crude oil, copper) a higher contribution of the convenience yield effect to mean reversion compared to commodities which may also serve as a store of value (e.g. gold, silver), where the mean reversion in spot prices is mainly due to negative correlation between risk premia and spot prices.

2.2 Empirical Evidence of Mean Reversion

Bessembinder et al. (1995) provide a test which examines whether investors expect the prices of different assets to revert. For that matter, they work with price data from futures contracts with different maturities. The nearest-to-deliver futures contract is taken as a proxy for the spot, which leads to applicability of the test even for assets without reliable spot price data.[12] The assets under account are agricultural commodities (wheat, live cattle, orange juice, world sugar and domestic sugar), crude oil, metals (gold, silver and platinum) and financial contracts (the S&P 500 index and treasury bonds). The data set ranges from 1982 to 1991.

As indicator for mean reversion, the authors use the relationship between actual spot price level and slope of the term structure of futures prices. When markets imply mean reversion, the mean-reverting behavior of prices is reflected in the slope of the term structure of futures prices as follows. For a spot price which is placed above the long-term equilibrium level, prices are expected to fall. This expectation will lead to a negative slope of the term structure of futures prices. This argument holds also vice versa.

Bessembinder et al. (1995) point out that their test can detect mean reversion arising from correlation between convenience yields and prices and correlation between interest rates and prices, but not from a negative relation between prices and risk premia.[13]

As for commodity markets, the results are clear without ambiguity. For metals, crude oil and agricultural commodities, the slope of the term structure of futures prices is significantly negatively related to the level of spot prices. Hence, spot prices on all involved commodity markets imply mean reversion.

In the crude oil and agricultural commodity markets, the source of mean reversion is the convenience yield, while the impact of interest rate changes is not significantly different from zero. For the precious metals, mean reversion in prices arises both from convenience yields and a negative correlation between interest rates and prices.

[12] One often observes a lack of reliable spot price data in commodity markets. Hence, working with the nearest-to-deliver futures contract as a proxy is a standard technique when working with empirical data for commodities.

[13] Bessembinder et al. (1995) do not consider mean reversion arising from risk premia since their test is based on the cross section of contemporaneous futures prices.

A different result is obtained for financial markets. The results are insignificant when working with the complete data set, though there is very weak evidence for mean reversion. After the exclusion of the 1987 crash period, the regression coefficient for the second nearest contract is significantly positive, while the coefficient for the fourth nearest contract is significantly negative. The interpretation of this finding is that financial asset prices tend to be mean-reverting on the long run, while they show opposed behavior on the short run.

This conclusion is at least partially supported by Poterba and Summers (1988) as well as by Fama and French (1988). In their study, Poterba and Summers find evidence for positive autocorrelation in stock prices over short periods and for negative autocorrelation over large periods. Furthermore, the results indicate that the return standard deviation over long horizons increases less than proportionally with time, which would be the case if the random walk hypothesis applies. Fama and French (1988) examine first order autocorrelations for stock prices. The authors conclude that the autocorrelations are U-shaped: starting from positive values over short return horizons, autocorrelations decay as the return horizon increases. The minimum value for 3-5-year returns is negative. For longer return horizons, autocorrelations increase and approach zero. Poterba and Summers as well as Fama and French work with a data set ranging from 1926 to 1985. In both papers, the evidence for mean reversion weakens when the data before 1940 is excluded.[14] Vice versa, the indication of mean reversion strengthens when the newer data is ruled out. Fama and French argue that it is possible that temporary price components which are accountable for mean reversion are less important after 1940. Hence, mean reversion mainly is a feature of commodity prices.

2.3 Mean Reversion and Volatility: The Samuelson Hypothesis

Samuelson (1965) stated that "it is a well known rule of thumb that nearness to expiration date involves greater variability or riskiness per hour or per day or per month than does farness." Hence, the so-called Samuelson hypothesis postulates that futures prices are less volatile with increasing time to maturity.

This pattern is especially important for the valuation of options on futures since the option price is strongly affected by the volatility of the underlying. In markets where the Samuelson hypothesis holds, not only the actual futures volatility but also the time to maturity of the underlying futures contract is important. One motivation for this theory could be that the information flow increases as the delivery date approaches and therefore, decreasing uncertainty leads to higher volatility of futures contracts.[15] In the case of agricultural commodities, the link between increasing information flow and futures price volatility can be interpreted as follows.

[14] The data from 1926 to 1939 includes the regression period in the 1930s.

[15] See Anderson and Danthine (1983).

A year before the harvest, there is only little information available about the harvest and the future spot price. Hence, futures prices with 1 year to maturity do not fluctuate strongly. As the harvest approaches, uncertainty about weather conditions is resolved and the information about temperatures and rainfall is reflected in futures prices, leading to increasing volatility every time when new information is incorporated in prices.

Conversely, Bessembinder et al. (1996) argue that the variance of futures price changes may be influenced by three factors. Based on the cost-of-carry relation $F(t,T) = S_t \exp\{(r_t - \Xi_t)(T-t)\}$, Bessembinder et al. (1996) consider the changes in the log futures price to identify the sources of (log-) futures price volatility. The change in the log futures price is given by $\ln(F(t+1,T)) - \ln(F(t,T)) = \pi_t + \ln(S_{t+1}/\mathbb{E}_t[S_{t+1}]) + \Delta s_t(T-t)$. The three elements are ex ante spot market risk premium π_t, unexpected log spot price changes and changes in the slope of the term structure of futures prices $\Delta s_t = \Delta(r_t - \Xi_t)$ weighted with time to maturity $T-t$, where r is the risk-free interest rate and Ξ denotes the convenience yield.

Apart from unexpected spot price changes, there are two factors left. Firstly, the variance in spot price changes influences the futures price volatility and is governed itself by the flow of information. This property is at first sight in line with the above-mentioned reasoning of Anderson and Danthine (1983). However, Bessembinder et al. (1996) illustrate that since there are multiple futures contracts with different maturity dates among the year, the increasing information flow conducted with one near-to-deliver futures contract should also have impact on the volatility of the other futures contracts with a larger time to maturity. Consequently, all futures contracts would experience an increase in volatility when a near-to-deliver contract matures, which would result in a saw-toothed volatility pattern.[16] However, empirical observations do not support such a behavior.

Secondly, the time variation in risk premia could account for changes in futures price volatility. At first, the authors do not focus on the risk premium component. When the risk premium component is removed, the only reason for the Samuelson hypothesis is negative covariation between unexpected spot price changes and the slope of the term structure of futures prices. As already stated in Bessembinder et al. (1995) and Sect. 2.2, such negative covariation is equivalent to a mean-reverting behavior of spot prices. Considering risk premia, Bessembinder et al. (1996) point out that "mean reversion in spot prices that is associated exclusively with variation in the risk premiums will not induce the negative comovement between the futures term slope and unexpected returns that is required for the success of the hypothesis."

The empirical analysis in Bessembinder et al. (1996) supports these findings. For commodities with mean-reverting spot prices such as agricultural commodities and crude oil, the authors assert strong evidence for the Samuelson hypothesis. The mean reversion for these commodities is mainly due to negative correlation between convenience yield and spot prices. As for metals, where mean reversion in prices arises both from time-varying risk premia and negative correlation of convenience

[16] Bessembinder et al. (1996), p. 49.

yield and prices, the support of the hypothesis weakens with the importance of the risk premium component in overall spot price mean reversion. For financial contracts, there is no evidence for the Samuelson hypothesis to be found.

In line with Bessembinder et al. (1996), Richter and Sørensen (2002) as well as Sørensen (2002) report decreasing standard deviations in futures prices for increasing maturities concerning contracts on agricultural commodities, i.e. corn, soybeans and wheat. Other papers supporting the Samuelson hypothesis in agricultural commodity futures markets are Benavides (2002) (addressing corn and wheat), Adrangi and Chatrath (2003) (coffee, sugar and cocoa) and Chatrath et al. (2002) (soybeans, corn, wheat and cotton).

The modeling of a subordinated stochastic volatility process with a long-term mean which is higher than the actual volatility level is adequate to capture the empirical findings as discussed in this section. We address stochastic volatility models for commodity derivative pricing in Chap. 4.

Chapter 3
Fundamentals of Derivative Pricing

In this chapter, we discuss the basics for the pricing of European options and futures in a generalized setting. We begin with some technical preliminaries to provide a framework which is based on an underlying price process with subordinated stochastic volatility process. This framework can also be generalized to a multifactor model without changing the solution methods, as done in Chap. 6.

3.1 Derivative Pricing Under the Risk-Neutral Measure

3.1.1 Introduction

Black and Scholes (1973) and Merton (1973) showed in their seminal papers that a derivative security can be priced by creating a replicating portfolio, i.e. a portfolio of primitive securities which matches the payoff of the derivative at maturity. Since both the replication portfolio and the derivative offer the same payoff at maturity, they have to have the same price at any preceding time. Deviations from this equality lead to arbitrage possibilities. Hence, the pricing by duplication procedure inhibits arbitrage by construction. Harrison and Kreps (1979) (in a discrete time setting) and Harrison and Pliska (1981) (in a continuous time setting) demonstrate that the replication-based price is equivalent to the calculation of the discounted expected value of the derivative's payoff under the equivalent martingale measure $\mathbb{Q}$. Delbaen and Schachermayer (1994, 1998) extend Harrison and Pliska to more sophisticated unbounded stochastic processes.

In complete markets, $\mathbb{Q}$ is the measure under which the discounted value of the derivative under account is a martingale, i.e. it is a stochastic process whose expected future value is its current value.[1] Hence, buying and holding the derivative corresponds to the participation at a fair game under $\mathbb{Q}$ since the expected change of value is zero.[2]

[1] The definition of a martingale process can be found in Baxter and Rennie (1996).

[2] See also Malliaris and Brock (1991), p. 17.

B. Lutz, *Pricing of Derivatives on Mean-Reverting Assets*,
Lecture Notes in Economics and Mathematical Systems,
DOI 10.1007/978-3-642-02909-7_3,

Equivalence of the physical measure $\mathbb{P}$ and the above-mentioned measure $\mathbb{Q}$ means that both measures have the same zero subsets. In other words, the two measures agree on what is possible and what is not possible, merely the probabilities of a possible event may be different. In fact, they are different, unless there is no risk adjustment. Under the measure $\mathbb{Q}$, the expected return of all assets is the same. Under the assumption of a risk-free asset with known rate of return r, this argument holds also for the risk-free bond and therefore, all assets have an expected return of r under $\mathbb{Q}$.[3] A risk-neutral investor would be indifferent between the investment in the risk-free bond or a risky asset with the very same rate of return, regardless of the risk he or she takes by following the latter alternative. Hence, the measure $\mathbb{Q}$ is also called the risk-neutral measure.

Consider S_t as price process of the underlying. S_t is a $\mathcal{F}$-adapted stochastic process defined on a filtered probability space $(\Omega, \mathcal{F}, \mathbb{P})$ with filtration $\mathcal{F}$ and probability measure $\mathbb{P}$.[4] The evolution of the process under the physical measure is given by the following stochastic differential equation (SDE):

$$dS_t = a(S_t, V_t)\, S_t\, dt + \sqrt{V_t}\, S_t\, dW_t^S + S_t\, dP_t^S \tag{3.1}$$

with subordinated variance process

$$dV_t = b(V_t)\, dt + c(V_t) dW_t^V + dP_t^V\,, \tag{3.2}$$

where S_t is the spot price and V_t denotes the instantaneous variance of the process at time t. $a(S_t, V_t) : \mathbb{R}^2 \to \mathbb{R}$, $b(V_t) : \mathbb{R} \to \mathbb{R}$ and $c(V_t) : \mathbb{R} \to \mathbb{R}$ are adapted functions which are specified by constant parameters and additionally may or may not depend on S_t and V_t, respectively.[5]

One needs to ensure that a unique solution to the SDE system described by (3.1) and (3.2) exists. Hence, we assume that Lipschitz and growth conditions as described in Appendix E in Duffie (2001) hold.[6]

W_t^S and W_t^V both are one-dimensional standard Brownian motions and P_t^S and P_t^V are one-dimensional jump processes with different jump size distribution

[3] See also Sundaram (1997).

[4] The definition of a probability space, probability measures and measurability is given Malliaris and Brock (1991) and Bauer (1992). For the definition of a filtration, see e.g. Shreve (2004), p. 51.

[5] In this case, the functions are Itô processes themselves. Different process specifications are given in the following chapters.

[6] We also presume the square-integrability condition for Itô integrals (see Shreve (2004), p. 133.):

$$\mathbb{E}\left[\int_0^T V_t\, dt\right] < \infty$$
$$\mathbb{E}\left[\int_0^T c^2(V_t)\, dt\right] < \infty\,,$$

where T is the maturity of the derivative security.

defined on the probability space $(\Omega, \mathcal{F}, \mathbb{P})$.[7] The two Wiener processes are allowed to be correlated via

$$dW_t^S \cdot dW_t^V = \rho \cdot dt.$$

The two jump processes are independent from each other and from the continuous part.[8]

3.1.2 Change of Measure for Diffusion Processes

To change the measure from the physical measure $\mathbb{P}$ to the risk-neutral measure $\mathbb{Q}$, we firstly omit the two jump processes. Under the physical measure $\mathbb{P}$, the SDEs of the underlying price process together with the subordinated variance process are then given by

$$\begin{aligned} dS_t &= a(S_t, V_t)\, S_t\, dt + \sqrt{V_t}\, S_t\, dW_t^S \\ dV_t &= b(V_t)\, dt + c(V_t)\, dW_t^V . \end{aligned} \tag{3.3}$$

Now define the Brownian motions under $\mathbb{Q}$

$$\begin{aligned} d\tilde{W}_t^S &= dW_t^S + \chi_t^S(S_t, V_t)\, dt \\ d\tilde{W}_t^V &= dW_t^V + \chi_t^V(V_t)\, dt , \end{aligned} \tag{3.4}$$

where χ^S, χ^V are the risk premiums of the underlying and the variance process, respectively. As mentioned above, the measure $\mathbb{Q}$ is characterized by the fact that all assets have an expected return which equals the risk-free interest rate. In order to achieve an expected return of r, the price process must transform via[9]

$$\chi_t^S(S_t, V_t) = \frac{a(S_t, V_t) - r}{\sqrt{V_t}} . \tag{3.5}$$

[7] For a definition of Wiener processes, see e.g. Björk (2005), p. 36. Firstly, we will focus on the continuous part of the jump-diffusion process. We will provide a definition of the jump processes when we explicitly address jump components.

[8] In Sect. 5.4.2, we incorporate the case where the two jump sizes are allowed to be correlated (see also Duffie et al. (2000)). The independence between the jump and the continuous part is also given in this context.

[9] Considering the variance risk premium, Heston (1993) illustrates how a risk premium proportional to V can be obtained. The key assumption according to Breeden (1979) is $\chi^V = \varsigma \mathrm{Cov}[dV, dY/Y]$, where ς is the relative risk aversion of an investor and Y_t is the consumption rate, which is driven by a Cox et al. (1985) process. Another possibility to obtain the variance risk premium is via a hedge portfolio as described in the appendix of this chapter.

Girsanov's theorem assures that $\tilde{W}_t^S$ and $\tilde{W}_t^V$ really are Brownian motions under $\mathbb{Q}$ when the adapted processes χ_t^S and χ_t^V fulfill Novikov's condition[10]:

$$\mathbb{E}^{\mathbb{Q}}\left[\exp\{\frac{1}{2}\int_0^T (\chi_u^S(S_u, V_u))^2 du\}\right] < \infty$$
$$\mathbb{E}^{\mathbb{Q}}\left[\exp\{\frac{1}{2}\int_0^T (\chi_u^V(V_u))^2 du\}\right] < \infty, \tag{3.6}$$

Embedded in the Girsanov theorem is the concept of the Radon-Nikodym derivative Z.[11] It is defined by

$$Z = \frac{d\mathbb{Q}}{d\mathbb{P}},$$

and in the case of (3.4), the Radon-Nikodym derivative reads

$$Z = \exp\left\{-\int_0^T \overrightarrow{\chi_u}\, d\overrightarrow{W_u} - \frac{1}{2}\int_0^T \left(\overrightarrow{\chi_u}\right)^2 du\right\},$$

where $\overrightarrow{\chi_u} = (\chi_u^S(S_u, V_u)); \chi_u^V(V_u)))$ and $d\overrightarrow{W_u} = (dW_u^S; dW_u^V)$ are vector processes. To change measure from $\mathbb{P}$ to $\mathbb{Q}$, one uses the Radon-Nikodym derivative. Let $\hat{Y}$ be an $\mathcal{F}$-measurable random variable. Then the expectations of $\hat{Y}$ under $\mathbb{P}$ and $\mathbb{Q}$ are linked via

$$\mathbb{E}^{\mathbb{Q}}\left[\hat{Y}\right] = \mathbb{E}^{\mathbb{P}}\left[\hat{Y} \cdot Z\right].$$

Provided that the technical conditions in (3.6) hold, the Brownian motions under $\mathbb{P}$ in (3.3) are replaced according to (3.4) and (3.5). Equation (3.3) changes to

$$dS_t = r\, S_t\, dt + \sqrt{V_t}\, S_t\, d\tilde{W}_t^S$$
$$dV_t = \tilde{b}(V_t)\, dt + c(V_t)\, d\tilde{W}_t^V, \tag{3.7}$$

with

$$\tilde{b}(V_t) = b(V_t) - \chi_t^V(V_t)\, c(V_t), \tag{3.8}$$

where the (3.7) now describe the evolution of the price process and its instantaneous variance under the risk-neutral measure $\mathbb{Q}$.

[10] Girsanov's theorem and Novikov's condition are defined in Sundaram (1997). Another more technical reference is Øksendal (2000).

[11] See e.g. Shreve (2004), p. 212.

Let us now consider a European call option C as derivative security.[12] The actual price C_t is the expected discounted value under $\mathbb{Q}$ of the payoff at maturity of the option, C_T:

$$C_t = \mathbb{E}^{\mathbb{Q}}[D(t,T)C_T], \tag{3.9}$$

where $D(t,T) = \exp\{-\int_t^T r_s ds\}$ is the discount factor with the risk-free interest rate r. The payoff of the derivative is a function of S_t, V_t and t, i.e. $C = f(S_t, V_t, t)$.[13] The application of the Itô formula leads to the dynamics of the derivative under $\mathbb{Q}$ as follows.[14]

$$\begin{aligned} dC = \Bigg[&\frac{\partial C}{\partial t} + r\, S_t \frac{\partial C}{\partial S} + \frac{1}{2} V_t\, S_t^2 \frac{\partial^2 C}{\partial S^2} + \tilde{b}(V_t) \frac{\partial C}{\partial V} + \frac{1}{2} c^2(V_t) \frac{\partial^2 C}{\partial V^2} \\ &+ \rho\, c(V_t) \sqrt{V_t} \frac{\partial^2 C}{\partial S \partial V} \Bigg] dt + \sqrt{V_t}\, S_t \frac{\partial C}{\partial S}\, d\tilde{W}_t^S + c(V_t) \frac{\partial C}{\partial V}\, d\tilde{W}_t^V \end{aligned} \tag{3.10}$$

As shown in the appendix of this chapter (Sect. 3.6, see (3.82)), the risk-adjusted generator in (3.10) can be simplified by[15]

$$\begin{aligned} \Bigg[&r\, S_t \frac{\partial C}{\partial S} + \frac{1}{2} V_t\, S_t^2 \frac{\partial^2 C}{\partial S^2} + \tilde{b}(V_t) \frac{\partial C}{\partial V} + \frac{1}{2} c^2(V_t) \frac{\partial^2 C}{\partial V^2} \\ &+ \rho\, c(V_t) \sqrt{V_t} \frac{\partial^2 C}{\partial S \partial V} \Bigg] dt = r\, C\, dt - \frac{\partial C}{\partial t}\, dt, \end{aligned} \tag{3.11}$$

the replacement of (3.11) in (3.10) leads to

$$dC = rC dt + \sqrt{V_t}\, S_t \frac{\partial C}{\partial S}\, d\tilde{W}_t^S + c(V_t) \frac{\partial C}{\partial V}\, d\tilde{W}_t^V . \tag{3.12}$$

Define the discounted value of the derivative as

$$\mathfrak{D} = \exp\{-rt\}\, C . \tag{3.13}$$

The evolution of the discounted value process is then given by

$$d\mathfrak{D} = \sqrt{V_t}\, S_t \frac{\partial \mathfrak{D}}{\partial S}\, d\tilde{W}_t^S + c(V_t) \frac{\partial \mathfrak{D}}{\partial V}\, d\tilde{W}_t^V . \tag{3.14}$$

[12] A derivative of European style can only be exercised at maturity. Contrary, American style derivatives can be exercised at any time between the actual date and maturity.

[13] This is a crucial, but common restriction. Cf. also Lewis (2000).

[14] The two-dimensional Itô formula is presented in Shreve (2004), p. 167.

[15] The generator of an Itô diffusion is defined in Øksendal (2000), p. 115.

By definition, a stochastic process which is driftless is a local martingale (but not necessarily a martingale).[16] Since (3.14) is driftless, this process is a local martingale under $\mathbb{Q}$. Provided that the technical conditions[17]

$$\mathbb{E}^{\mathbb{Q}}\left[\left(\int_0^T \left(\sqrt{V_t}\, S_t\, \frac{\partial C}{\partial S}\right)^2\right)^{\frac{1}{2}}\right] < \infty$$

$$\mathbb{E}^{\mathbb{Q}}\left[\left(\int_0^T \left(c(V_t)\, \frac{\partial C}{\partial V}\right)^2\right)^{\frac{1}{2}}\right] < \infty$$

hold, (3.14) is also a martingale under $\mathbb{Q}$.

As already mentioned above, the fact that the discounted derivative process is a martingale under the risk-neutral measure implies that the derivative's expected return net of opportunity costs is zero, i.e. buying and holding the derivative corresponds to the participation at a fair game. This does not mean that buying and holding is also a fair game under the real measure $\mathbb{P}$.

3.1.3 Change of Measure for Jump-Diffusion Processes

Now consider the case when the price process shows both continuous and jump components, as defined in (3.1). The aim of the change of measure is again to achieve the martingale property of the discounted derivative process. Let us focus only on the jump-diffusion process of the underlying which we recapitulate as given by

$$dS_t = a(S_t, \overline{V})\, S_t\, dt + \sqrt{\overline{V}}\, S_t\, dW_t^S + S_t\, dP_t^S\,, \tag{3.15}$$

where $\overline{V}$ denotes constant variance. Firstly, consider the jump part in (3.15). Every specification of jump components consists of a combination of a random variable with a Poisson process. This combination is often referred to as compound Poisson process (e.g. Shreve (2004). The Poisson process counts the number of jumps in the considered time interval and the random variable follows a certain distribution which specifies the amount of which the process jumps upward or downward. A Poisson process N_t is defined by

$$N_t = \sum_{n \geq 1} 1_{t \geq \sum_{k=1}^{n} \xi_k} \qquad \forall\, t \geq 0\,, \tag{3.16}$$

[16] This definition is given in Baxter and Rennie (1996). A more technical definition of local martingales can be found in Karatzas and Shreve (1991), p. 36.

[17] Cf. also Baxter and Rennie (1996).

where ξ_k is an independent and identically distributed (i.i.d.) sequence of exponential random variables with parameter λ.[18] The trajectories of N_t are right continuous with left limits, piecewise constant between the jump events and increase by jumps of size 1. The parameter λ is also called the intensity of the Poisson process.

To calculate the expected value of the increment dN_t, we can use the property that the probability of two or more simultaneous jumps is zero and the arrival of a jump is independent from previous jumps. The arrival of one jump in the next small time interval dt occurs with probability λdt. No jump will occur with probability $1 - \lambda dt$. Hence,

$$\mathbb{E}\big[dN_t\big] = 1\lambda dt + 0(1 - \lambda dt) = \lambda dt\,. \tag{3.17}$$

An interesting special case is the compensated Poisson process. It is defined by

$$dN_t^* = dN_t - \lambda dt\,.$$

The expected increment of N_t^* is zero, therefore the compensated Poisson process is a martingale. We make use of compensated processes while adding jump components to ensure the martingale property of the claim on X_t.

Zhu (2000) points out that in the presence of jumps, is not possible to construct a hedging portfolio which protects against any price changes at any time, but the martingale property of the price process ensures that the construction of a hedging portfolio "is a fair game over a long time in an expectation sense even when jumps happen" (Zhu, 2000).

N_t has independent increments and belongs therefore to the class of Markov processes. The characteristic function of a Poisson process with intensity λ is given by

$$\mathbb{E}\big[e^{i\phi N_t}\big] = \exp\big\{\lambda t(e^{i\phi} - 1)\big\}\,, \tag{3.18}$$

where ϕ is the Fourier parameter and i is the imaginary unit with $i^2 = -1$.[19] The compound Poisson process is given by

$$P_t^S = \sum_{k=1}^{N_t} J_k\,, \tag{3.19}$$

where N_t is a Poisson process with intensity λ^S defined by (3.16) and J_k denotes the jump size of the k-th jump. The jump sizes are i.i.d. with density function $\varphi(J_k)$.

[18] Cf. Cont and Tankov (2003), p. 48.

[19] The characteristic function is given by the Fourier transform of the density function. We address characteristic functions more detailed in Sect. 3.2.

Our listing of the properties of Poisson processes is not fully complete. Other less important technical properties of Poisson processes can be found in Cont and Tankov (2003) or Shreve (2004).

Let us now consider the change of measure. According to Girsanov's theorem as defined in the previous subsection, one replaces the Brownian motion in (3.15) as follows.

$$d W_t^S = d \tilde{W}_t^S - \frac{a(S_t, \overline{V}) - r}{\sqrt{\overline{V}}} \, dt \tag{3.20}$$

After the substitution in (3.20), the drift of the process is equal to $r \, S_t \, dt$. Hence, the discounted process defined in (3.13) is a local martingale if the jump process $\tilde{P}_t^S$ is a local martingale under $\mathbb{Q}$. In order to switch the Poisson process to the risk-neutral measure, both the intensity and the density function of the process are changed to $\tilde{\lambda}$ and $\tilde{\varphi}(J_k)$.

Equivalently to Girsanov's theorem in the continuous case, we have to show that $\tilde{P}_t^S$ is a Poisson process and $\tilde{W}_t^S$ is a Brownian motion under $\mathbb{Q}$. Shreve (2004) approaches the problem by showing that the two processes have the correct joint moment-generating function.

The Radon-Nikodym-derivative Z of the jump-diffusion process can be written as product of the diffusion and the jump component, since $d W_t^S$ and $d P_t^S$ are independent.

$$Z = \frac{d\mathbb{Q}}{d\mathbb{P}} = Z^D \, Z^J \,, \tag{3.21}$$

with[20]

$$\begin{aligned} Z^D &= \exp\left\{ - \int_0^T \frac{a(S_u, \overline{V}) - r}{\sqrt{\overline{V}}} \, du - \frac{1}{2} \int_0^T \left(\frac{a(S_u, \overline{V}) - r}{\sqrt{\overline{V}}} \right)^2 du \right\} \\ Z^J &= \exp\{(\lambda - \tilde{\lambda}) \, T\} \prod_{k=1}^{N_T} \frac{\tilde{\lambda} \tilde{\varphi}(J_k)}{\lambda \varphi(J_k)} \,, \end{aligned}$$

where Z^D and Z^J are the Radon-Nikodym-derivatives of the Brownian motion and the jump process, respectively. The joint moment-generating function of the two processes is given by

$$\mathbb{E}^{\mathbb{Q}}\big[\exp\{\phi_1 \tilde{W}_t^S + \phi_2 \tilde{P}_t^S\}\big] = \mathbb{E}^{\mathbb{P}}\big[\exp\{\phi_1 \tilde{W}_t^S\} Z^D\big] \cdot \mathbb{E}^{\mathbb{P}}\big[\exp\{\phi_2 \tilde{P}_t^S\} Z^J\big] \,. \tag{3.22}$$

Provided that Novikov's condition (3.6) holds, Girsanov's theorem assures that the first expectation on the right hand side in (3.22) is the moment-generating function

[20] For a detailed proof, see Shreve (2004).

of a normal random variable with mean zero and variance t, which corresponds to the Brownian motion $\tilde{W}_t^S$. The second expectation is given by[21]

$$\mathbb{E}^{\mathbb{P}}\left[\exp\{\phi_2 \tilde{P}_t^S\} Z^J\right] = \exp\left\{\tilde{\lambda} t \left(\tilde{\Upsilon}_J(\phi_2) - 1\right)\right\}, \tag{3.23}$$

where $\tilde{\Upsilon}_J(\phi_2)$ is the moment-generating function of the jump sizes under $\mathbb{Q}$ defined by

$$\tilde{\Upsilon}_J(\phi_2) = \mathbb{E}^{\mathbb{Q}}\left[\exp\{\phi_2 \hat{J}\}\right],$$

where the hat denotes the random variable property of $\hat{J}$.

Equation (3.18) provides that (3.23) is the moment-generating function of a Poisson process and finally that (3.22) is the joint moment-generating function of a Wiener process and a Poisson process under $\mathbb{Q}$.[22] Hence, if $\tilde{P}_t^S$ is a local martingale, the discounted derivative process is also a local martingale.[23] These findings can be generalized to vector processes which incorporate the subordinated variance process.

3.1.4 Change of Measure if the Underlying is not a Traded Asset

Now consider a commodity as underlying for the price process S_t. For commodities with high storing and holding costs of the good, the risk-neutral hedging argument does not apply.[24] Additionally, prices are influenced by production and consumption of the good.[25] As prices increase, production will grow and consumption will decline, therefore putting a downward pressure on prices. This argument holds also vice versa. Hence, the price process of a consumption good is to a lesser extent influenced by hedging with the physical commodity and to a larger extent governed by supply and demand.

In this case, the adjustment of the price process to the risk-neutral measure as in (3.4) does not require that (3.5) holds. The expected return of S under the risk-neutral measure may be different from r and we have

[21] The proof of this finding is not supplied in short. Again, we refer to Shreve (2004).

[22] The characteristic function $\Phi(\phi) = \mathbb{E}^{\mathbb{Q}}\left[e^{i\phi\hat{J}}\right]$ is linked to the moment-generating function Υ via $\Phi(-i\phi) = \Upsilon(\phi) = \mathbb{E}^{\mathbb{Q}}\left[e^{\phi\hat{J}}\right], \phi \in \mathbb{N}$.

[23] The jump processes of the underlying in Chap. 5 are defined as compensated processes and therefore fulfill the martingale property.

[24] Ross (1997) works with a mean-reverting price process without stochastic volatility and jumps based on this argument.

[25] Cf. also Schwartz (1997).

$$
\begin{aligned}
dS_t &= \tilde{a}(S_t, V_t)\, S_t\, dt + \sqrt{V_t}\, S_t\, d\tilde{W}_t^S + S_t\, d\tilde{P}_t^S \\
dV_t &= \tilde{b}(V_t)\, dt + c(V_t)\, d\tilde{W}_t^V + d\tilde{P}_t^V\,,
\end{aligned} \tag{3.24}
$$

where

$$
\begin{aligned}
\tilde{a}(S_t, V_t) &= a(S_t, V_t) - \chi_t^S(S_t, V_t)\, \sqrt{V_t} \\
\tilde{b}(V_t) &= b(V_t) - \chi_t^V(V_t)\, c(V_t)\,.
\end{aligned} \tag{3.25}
$$

In our model specifications in the following chapters, we deal with mean reverting log-price processes under the risk-neutral measure $\mathbb{Q}$. The application of Itô's lemma leads to the dynamics of the log-price process $dX_t = d(\ln S_t)$.[26]

$$
\begin{aligned}
dX_t &= \left(\tilde{a}(X_t, V_t) - \frac{1}{2}\, V_t\right) dt + \sqrt{V_t}\, d\tilde{W}_t^X + d\tilde{P}_t^X \\
dV_t &= \tilde{b}(V_t)\, dt + c(V_t)\, d\tilde{W}_t^V + d\tilde{P}_t^V\,,
\end{aligned} \tag{3.26}
$$

where

$$
\begin{aligned}
d\tilde{W}_t^X &= d\tilde{W}_t^S\,, \\
d\tilde{P}_t^X &= dN_t\left\{\ln\left(S_t(1+\hat{J})\right) - \ln\left(S_t\right)\right\} = dN_t \ln\left((1+\hat{J})\right).
\end{aligned}
$$

As shown in (3.24) – (3.26), the risk premiums are already incorporated in the drift term of the underlying and the subordinated process, respectively. Therefore, these processes are formulated under the risk-neutral measure. The jump process $\tilde{P}_t^S$ is defined as compensated process.[27] For notational convenience in this chapter, the drift term adaption of the compensated jump process is incorporated in the parameter $a(X_t, V_t)$. In Chap. 5, we explicitly work with the drift term adaption.

3.2 Characteristic Functions

In the previous section, the risk-neutral dynamics of the underlying were developed. Together with the actual price (and other parameter values), the SDE system determines the risk-neutral distribution of the underlying at time T, i.e. the maturity of the derivative security. The distribution function of S_T (the price at time T) is needed to solve for the value of the derivative as specified in (3.9). The characteristic function is the Fourier transform of the density function. Hence, distribution function, density

[26] The one-dimensional Itô formula is defined in Malliaris and Brock (1991), p. 81.

[27] A compensated jump process has a drift term adaption which ensures the martingale property, i.e. that the expected increment of the process is zero.

function (the derivative of the distribution function) and characteristic function (the Fourier transform of the density function) are completely interchangeable.[28]

The use of characteristic functions in finance became popular with the introduction of the Fourier inversion approach for option pricing by Heston (1993). A clear advantage of the Fourier inversion approach is the fact that it involves only one integration of the Fourier integral, even when more than one stochastic factor are involved (e.g. stock price and volatility). The integration methods for characteristic functions are much faster concerning computation time than other solution methods for differential equations such as finite difference or Monte Carlo methods. Due to computation speed, the Fourier inversion approach is often referred to as closed-form solution though it involves the (numerical) solution of the Fourier integral. Following Heston (1993), many authors adopted this solution method, among them are Bates (1996b), Scott (1997), Bakshi et al. (1997), Schöbel and Zhu (1999), Bakshi and Madan (2000), Duffie et al. (2000), Zhu (2000), Kispert (2005) and Repplinger (2008).[29]

The Fourier inversion approach based on characteristic functions allows for a rich spectrum of process specifications. It is even applicable when the density function is intractable, provided that the characteristic function has a closed-form solution.[30] Furthermore, the use of numerical integration algorithms leads to applicability of the Fourier inversion approach even when no closed-form solution for the characteristic function exists.[31]

We define the characteristic function of the state variable X_T (the log-price at time T) as

$$\Phi(t, T, \phi) = \mathbb{E}_t^{\mathbb{Q}}\left[e^{i\,\phi\,X_T}\right], \tag{3.27}$$

where i denotes the imaginary unit which is defined by $i^2 = -1$ and ϕ is the Fourier parameter.

The characteristic function is linked to the moment-generating function Υ via

$$\Phi(t, T, -i\,\phi) = \Upsilon(t, T, \phi) = \mathbb{E}_t^{\mathbb{Q}}\left[e^{\phi\,X_T}\right], \quad \phi \in \mathbb{N}, \tag{3.28}$$

provided that the moment-generating function exists, which is equivalent to the statement

$$\mathbb{E}_t^{\mathbb{Q}}\left[e^{\phi\,X_T}\right] < \infty \quad \forall\,\phi \in \mathbb{N}. \tag{3.29}$$

[28] The so-called spanning property of characteristic functions is addressed in Bakshi and Madan (2000).

[29] This list is far from being complete. Nevertheless, these papers already involve different problem specifications, e.g. diffusion processes with stochastic volatility and stochastic interest rates as well as jump-diffusion processes.

[30] An example for this case is the Variance Gamma model of Madan and Seneta (1990) and Madan et al. (1998).

[31] See Sect. 3.6.

The characteristic function Φ always exists, even when (3.29) is not fulfilled and therefore the moment-generating function does not exist.[32] This property is an advantage of handling with characteristic functions instead of moment-generating functions.[33]

3.3 Fundamental Partial Differential Equation

In order to compute the characteristic function, we need to solve the expectation in (3.27), which in case of (3.26) is a function of X_t, V_t and time t: $\Phi(t, X_t, V_t)$. The theorem of Feynman and Kac provides the link between stochastic differential equations and partial differential equations (PDEs). It also assures that solving the expectation in (3.27) is equivalent to solving the corresponding PDE.

Suppose that the system of SDEs as given in (3.26) describes the log-price dynamics. The integral representation of the dynamics of the characteristic function is given by[34]:

$$\begin{aligned}\Phi(T, X_T, V_T) = \Phi(t, X_t, V_t) &+ \int_t^T \frac{\partial \Phi}{\partial t}\, ds + \int_t^T \frac{\partial \Phi}{\partial X}\, dX_s + \frac{1}{2}\int_t^T \frac{\partial^2 \Phi}{\partial X^2}\, dX_s^2 \\ &+ \int_t^T \frac{\partial \Phi}{\partial V}\, dV_s + \frac{1}{2}\int_t^T \frac{\partial^2 \Phi}{\partial V^2}\, dV_s^2 + \int_t^T \frac{\partial^2 \Phi}{\partial X \partial V}\, dX_s\, dV_s \\ &+ \sum_{t<s\le T} [\Phi(s, X_s, V_s) - \Phi(s, X_{s-}, V_s)] \\ &+ \sum_{t<s\le T} [\Phi(s, X_s, V_s) - \Phi(s, X_s, V_{s-})]\,, \end{aligned} \tag{3.30}$$

where the jump of the log-underlying (respectively the variance jump) at time s is given by $J^X = X_s - X_{s-}$ (respectively $J^V = V_s - V_{s-}$). Replacing the process specifications as given in (3.26) and (3.30) and simplifying leads to

$$\Phi(T, X_T, V_T) = \Phi(t, X_t, V_t) + \int_t^T \left(\frac{\partial \Phi}{\partial t} + \tilde{A}\Phi\right) ds + \int_t^T \sqrt{V_s}\, \frac{\partial \Phi}{\partial X}\, d\tilde{W}_s^X$$

[32] A proof of this property can be found in Schaich and Münnich (2001), p. 134.

[33] However, it is possible that the characteristic function exhibits no closed-form representation, e.g. for the lognormal distribution.

[34] The Itô formula for two-dimensional jump-diffusion processes is given in Shreve (2004), p. 489. The necessary integrability conditions for jump-diffusions can be found in Duffie et al. (2000).

$$+\int_t^T c(V_s)\,\frac{\partial\Phi}{\partial V}\,d\tilde{W}_s^V+\sum_{t<s\le T}\left[\Phi(s,X_s,V_s)-\Phi(s,X_{s-},V_s)\right]$$

$$+\sum_{t<s\le T}\left[\Phi(s,X_s,V_s)-\Phi(s,X_s,V_{s-})\right], \tag{3.31}$$

where

$$\tilde{A}\Phi=\left(\tilde{a}(X_t,V_t)-\frac{1}{2}V_t\right)\frac{\partial\Phi}{\partial X}+\tilde{b}(V_t)\frac{\partial\Phi}{\partial V}+\frac{1}{2}\,V_t\,\frac{\partial^2\Phi}{\partial X^2}+\frac{1}{2}\,c^2(V_t)\,\frac{\partial^2\Phi}{\partial V^2}$$

$$+\rho\,\sqrt{V_t}\,c(V_t)\,\frac{\partial^2\Phi}{\partial X\,\partial V} \tag{3.32}$$

is the risk-neutral generator of the continuous process.[35]

Suppose that $\Phi(t,X_t,V_t)$ solves the PDE

$$\frac{\partial\Phi}{\partial t}+\tilde{A}\,\Phi+\lambda^X\int_{\mathbb{R}}\left[(\Phi(t,X_t+J^X,V_t)-\Phi(t,X_t,V_t))\right]d\varphi(J^X)$$

$$+\lambda^V\int_{\mathbb{R}}\left[(\Phi(t,X_t,V_t+J^V)-\Phi(t,X_t,V_t))\right]d\varphi(J^V)=0, \tag{3.33}$$

where λ^X, λ^V are the jump intensities of the two jump processes and J^X and J^V are assumed to be distributed with density $\varphi(J^X)$ and $\varphi(J^V)$. The boundary condition is given by $\Phi(T,X_T,V_T)=f(X_T,V_T)$. Under this assumption, (3.31) changes to

$$f(X_T,V_T)=\Phi(t,X_t,V_t)+\int_t^T\sqrt{V_s}\,\frac{\partial\Phi}{\partial X}\,d\tilde{W}_s^X+\int_t^T c(V_s)\,\frac{\partial\Phi}{\partial V}\,d\tilde{W}_s^V\,. \tag{3.34}$$

Now take expectation to obtain

$$\Phi(t,X_t,V_t)=\mathbb{E}_t^{\mathbb{Q}}\left[f(X_T,V_T)\middle|X_t=X_0,V_t=V_0\right], \tag{3.35}$$

where X_0 and V_0 are the initial values for X and V, respectively.

Hence, solving (3.27) and the PDE (3.33) is equivalent. Note that if (3.33) holds, the corresponding SDE to (3.34) is a local martingale.[36] Furthermore, one has to

[35] As mentioned earlier, the generator of an Itô diffusion is defined in Øksendal (2000), p. 115.

[36] A driftless stochastic process is a local martingale (Baxter and Rennie (1996)). Note that as a result of this, the futures price is also driftless under the martingale measure ($\mathbb{E}[dF]=0$). This is true since $F(t,T)=\Phi(t,T,\phi\,|\,\phi=-i)$ and $\mathbb{E}[dF]=\mathbb{E}[d\Phi\,|\,\phi=-i]$ (See (3.38) and (3.41) in Sect. 3.4.1). This finding is in line with Ross (1997), p. 392.

ensure that the process (3.34) has bounded variance:

$$\mathbb{E}^{\mathbb{Q}}\left[\left(\int_0^T \left(\sqrt{V_t}\,\frac{\partial \Phi}{\partial X}\right)^2\right)^{\frac{1}{2}}\right] < \infty$$

$$\mathbb{E}^{\mathbb{Q}}\left[\left(\int_0^T \left(c(V_t)\,\frac{\partial \Phi}{\partial V}\right)^2\right)^{\frac{1}{2}}\right] < \infty\,.$$

If (3.34) has bounded variance and no drift term, it corresponds to a global martingale process and the price of the claim on X is given by the discounted expectation under $\mathbb{Q}$.[37]

Equations (3.33) and (3.32) determine the fundamental partial differential equation (FPDE):

$$\begin{aligned}\frac{\partial \Phi}{\partial t} + \left(\tilde{a}(X_t, V_t) - \frac{1}{2}V_t\right)\frac{\partial \Phi}{\partial X} + \tilde{b}(V_t)\frac{\partial \Phi}{\partial V} + \frac{1}{2}\,V_t\,\frac{\partial^2 \Phi}{\partial X^2} + \frac{1}{2}\,c^2(V_t)\,\frac{\partial^2 \Phi}{\partial V^2}\\ +\rho\,\sqrt{V_t}\,c(V_t)\,\frac{\partial^2 \Phi}{\partial X\,\partial V} + \lambda^X\,\mathbb{E}^{\mathbb{Q}}[(\Phi(t, X_t + J^X, V_t) - \Phi(t, X_t, V_t))]\\ +\lambda^V\,\mathbb{E}^{\mathbb{Q}}[(\Phi(t, X_t, V_t + J^V) - \Phi(t, X_t, V_t))] = 0\end{aligned} \tag{3.36}$$

The FPDE can be transformed in a set of ordinary differential equations (ODEs) with an exponential guess for Φ. The structure of the guess depends on the system of SDEs in (3.26). For a SDE system with two state variables X and V, the guess is exponential affine[38]:

$$\Phi(t, X_t, V_t) = \exp\{i\phi A(\tau)X_t + B(\tau)V_t + C(\tau)\}\,, \tag{3.37}$$

where $\tau = T - t$. The replacement of the corresponding derivatives of (3.37) in (3.36) and collecting terms with X_t, V_t and constants leads to a system of ODEs. The ODE system can be solved subject to boundary conditions of the auxiliary functions $A(\tau)$, $B(\tau)$ and $C(\tau)$ providing that (3.27) holds at maturity of the derivative security.

Since the further proceeding is model dependent, we address the application of the exponential guess and the solution of the resulting ODE system in the following chapters.

---

[37] Cf. Lewis (2000).

[38] For the success of an exponential affine guess, it is necessary that the FPDE incorporates only terms with X_t, V_t or constants. Cf. Heston (1993).

3.4 European Style Derivatives

Armed with the FPDE and an exponential guess for Φ, we obtain a system of ODEs which can be solved analytically – if possible – or via Runge–Kutta methods as described in Sect. 3.6 in the appendix of this chapter. By this means, we can provide a solution for the characteristic function contingent on the SDE system. The characteristic function itself is necessary for the pricing of derivative instruments such as forwards and futures or European options. The pricing equation for these derivatives can be expressed in terms of characteristic functions.

3.4.1 Forwards and Futures

Forwards and futures are the simplest derivative instruments. All contract specifications (e.g. underlying, delivery price, maturity, contract size) are fixed when the contract is written, but the physical completion of the contract, i.e. payment and delivery, is deferred to the maturity date. Hence, a forward (futures) contract can be seen as a bet on the spot price at maturity.

Since no cash flows occur when the contract is written, the futures price is the price which makes the contract valueless. It is defined by[39]

$$F(t,T) = \mathbb{E}_t^{\mathbb{Q}}\big[S_T\big] = \mathbb{E}_t^{\mathbb{Q}}\big[\exp\{X_T\}\big], \tag{3.38}$$

where t is the actual date, T is the maturity date, r is the risk-free interest rate and S (respectively X) denotes the price (respectively log-price) of the underlying. The forward price is given by

$$FW(t,T) = \mathbb{E}_t^{\mathbb{Q}}\big[\exp\{\int_t^T r_s ds\}\big]S_t = \mathbb{E}_t^{\mathbb{Q}}\big[\exp\{\int_t^T r_s ds\}\big]\exp\{X_t\}\,. \tag{3.39}$$

Since a futures contract is settled at the end of each trading day in contrast to forward contracts, where the only cashflow is paid on the maturity date, the sum of the payments of a futures contract matches the payment of a forward contract, merely the timing of the cashflows is different. Consequently, an equality of the forward and futures price is given when interest rates are deterministic besides the assumption of the absence of market frictions, e.g. no transaction costs and taxes, perfect divisibility of futures contracts and lending and borrowing at the same rate. A nonrandom interest rate results in a zero covariance of the discount process $D(t,T) = \exp\{-\int_t^T r_s ds\}$ and the underlying process. When interest rates are stochastic, the difference Δ is given by[40]

[39] This finding traces back to Cox et al. (1981).

[40] See also Shreve (2004) or Miltersen and Schwartz (1998).

$$\Delta = FW(t,T) - F(t,T) = \frac{1}{\mathbb{E}_t^{\mathbb{Q}}\big[D(t,T)\big]}\, cov^{\mathbb{Q}}\big(D(t,T), S(T)\big)\,. \tag{3.40}$$

In our framework, we apply constant and therefore non-stochastic interest rates. In the following, we work with futures prices keeping in mind that the futures price equals the forward price under the above assumptions.[41]

The futures price in (3.38) is given by the first moment of the distribution of S_T. We do not need to apply Fourier transformation theory to calculate (3.38). Hence, the characteristic function as defined in (3.27) is not needed, but can be useful anyway since it determines the moments of the distribution of X_T via (3.28).

The first moment is required for the computation of the futures price. Therefore, the futures price is given by the characteristic function with a frequency of $-i$:

$$F(t,T) = \Phi(t,T,-i) = \Upsilon(t,T,1)\,. \tag{3.41}$$

3.4.2 European Options

Another class of standard derivative instruments are European call and put options, which give its holder the right, but not the obligation, to buy (respectively sell, in case of a put option) the underlying for a prespecified price at maturity. In contrast to futures and forwards, an option contract always has a nonnegative value for the holder of the option.[42]

It is important to note that most of the options in the commodity derivatives market are American style options on futures. European options on futures can be covered within our framework, when the (log-) spot price is replaced by the (log-) futures price. The price of the American option is the price of the equivalent European option plus an early exercise premium. The early exercise premium of the American option has to be estimated with an adequate method, e.g. the trinomial lattice model in Broadie and Detemple (1996) as mentioned in Richter and Sørensen (2002).[43]

---

[41] For a more detailed discussion of the differences between forward and futures prices, see e.g. French (1983) or Jarrow and Oldfield (1981).

[42] Contrarily, the option writer commits himself to deliver the underlying (respectively buy, in case of a put option) at the strike price. Hence, the possible loss of the deal is unlimited for the call option writer (and limited to the exercise price less the received option premium for the put option writer, respectively). The option premium received from the holder of the option is a compensation for the takeover of this risk.

[43] Another approximation method for the early exercise premium is described in Barone-Adesi and Whaley (1987).

In line with the definition given in (3.9) at the beginning of this chapter, the value of a European call option at time t with expiration date T is

$$C_t = \mathbb{E}_t^{\mathbb{Q}}\left[\exp(-\int_t^T r_s \,\mathrm{d}s)\,(S_T - K)^+\right] \tag{3.42}$$

$$= \int_k^\infty \exp(-\int_t^T r_s \,\mathrm{d}s)\,(e^{X_T} - K)\,\varphi(X_T)\,\mathrm{d}X_T\,. \tag{3.43}$$

The corresponding put option can be priced using put-call-parity. X_T and k are the log-transformations of the price S_T of the underlying and the strike price K. $\varphi(X_T)$ is the risk-neutral probability density function of the log-price at time T.

We present two ways of solving the expectation in (3.42): The traditional two-integral approach and the one-integral approach of Carr and Madan (1999) or Lewis (2000, 2001). Both approaches have their advantages: In the traditional approach, one directly calculates the risk-neutral probabilities which are useful for hedge ratios or the knowledge of the risk-neutral probability of ending up in the money. As a drawback of this approach, the calculation of two integrals can be a slow algorithm in case of numerical computation of the characteristic function. On the other hand, as discussed in Lee (2004), the one-integral approach is superior with respect to error management and faster in the calculation if one does not need the risk-neutral probabilities. The drawback of this approach is obviously that one forgoes the delta and the risk-neutral exercise probability of the option. As is the previous sections, we will assume constant interest rates in the following.

Traditional Approach

In this paragraph, we demonstrate the traditional approach for option pricing which was adopted by Heston (1993), Scott (1997), Bakshi and Madan (2000) and Zhu (2000), among others. The splitting of the maximum function in (3.42) in two parts and simplifying leads to

$$C_t = \mathbb{E}_t^{\mathbb{Q}}\left[\exp(-\int_t^T r_s \,\mathrm{d}s)\,S_T \mathbb{1}_{X_T > k}\right] - K\,\mathbb{E}_t^{\mathbb{Q}}\left[\exp(-\int_t^T r_s \,\mathrm{d}s)\,\mathbb{1}_{X_T > k}\right], \tag{3.44}$$

where $\mathbb{1}_{X_T > k}$ denotes the indicator function under the appropriate probability measure.

In order to simplify calculations, the measure is changed in both expectations from $\mathbb{Q}$ to $\mathbb{Q}_1$ and $\mathbb{Q}_2$, respectively.[44] $\mathbb{Q}_1$ is the measure with the underlying as

[44] An excellent reading for the change of numéraire in option pricing theory is the work of Geman et al. (1995).

numéraire. Under this measure, all assets are quoted in terms of the underlying, and the price of the underlying is therefore 1. Equivalently, $\mathbb{Q}_2$ is the measure with a zero bond $B(t,T)$ with time to maturity $T-t$ and a face value of 1 as numéraire. Hence, $\mathbb{Q}_2$ is also called the T-forward measure.

The equivalent martingale measures $\mathbb{Q}_1$ and $\mathbb{Q}_2$ are characterized via their Radon-Nikodym derivatives with respect to $\mathbb{Q}$[45]

$$Z_1 = \frac{d\,\mathbb{Q}_1}{d\,\mathbb{Q}} = \frac{\exp(-\int_t^T r_s\,\mathrm{d}s)\exp(X_T)}{\mathbb{E}^{\mathbb{Q}}\big[\exp(-\int_t^T r_s\,\mathrm{d}s)\exp(X_T)\big]} \tag{3.45}$$

$$Z_2 = \frac{d\,\mathbb{Q}_2}{d\,\mathbb{Q}} = \exp(-\int_t^T r_s\,\mathrm{d}s)\frac{1}{B(t,T)}\,. \tag{3.46}$$

Note that in case of non-mean-reverting assets, the denominator in (3.45) is just S_t since the underlying is expected to grow with rate r under $\mathbb{Q}$ and therefore, the Radon-Nikodym derivative is $Z_1 = \exp(-\int_t^T r_s\,\mathrm{d}s)S_T/S_t$. This simplification is not valid if one assumes mean-reversion under $\mathbb{Q}$. But, in the case of deterministic interest rates, the first Radon-Nikodym derivative can be simplified to $Z_1 = \exp(X_T)/\mathbb{E}^{\mathbb{Q}}\big[\exp(X_T)\big]$. Equivalently, we have $B(t,T) = \exp(-\int_t^T r_s\,\mathrm{d}s)$ and the second Radon-Nikodym derivative in (3.46) is $Z_2 = 1$. Therefore, the two measures $\mathbb{Q}$ and $\mathbb{Q}_2$ are identical.

Now change numéraire according to[46]

$$\begin{aligned} C_t &= e^{-r(T-t)}\cdot\left(\mathbb{E}^{\mathbb{Q}}\big[\exp(X_T)\big]\mathbb{E}^{\mathbb{Q}}\Big[Z_1\,\mathbb{1}_{X_T>k}\Big] - K\,\mathbb{E}^{\mathbb{Q}_2}\Big[\mathbb{1}_{X_T>k}\Big]\right) \\ &= e^{-r(T-t)}\cdot\left(\mathbb{E}^{\mathbb{Q}}\big[\exp(X_T)\big]\mathbb{E}^{\mathbb{Q}_1}\Big[\mathbb{1}_{X_T>k}\Big] - K\,\mathbb{E}^{\mathbb{Q}_2}\Big[\mathbb{1}_{X_T>k}\Big]\right). \end{aligned} \tag{3.47}$$

The expected value of $\exp(X_T)$ under $\mathbb{Q}$ corresponds to the characteristic function with a frequency of $-i$ and the two expectations of the indicator function are denoted by Π_1 and Π_2.[47] We obtain

$$C_t = e^{-r(T-t)}\cdot\big[\Phi(t,T,-i)\cdot\Pi_1 - K\cdot\Pi_2\big]. \tag{3.48}$$

[45] Cf. also Bakshi and Madan (2000), p. 214 or the remarks to Girsanov's theorem in Sect. 3.1.1 in this chapter.

[46] The change of measure is done according to $\mathbb{E}^{\mathbb{Q}_1}[\hat{Y}] = \mathbb{E}^{\mathbb{Q}}[Z_1\,\hat{Y}]$, where $\hat{Y}$ is a substitutional random variable. See also Geman et al. (1995).

[47] The characteristic function with a frequency of $-i$ is the futures price $F(t,T)$ (See also Sect. 3.4.1).

Π_2 is the risk-neutral probability of ending up in the money. Π_1 is the delta of the option. Both values can be expressed in terms of the characteristic function. Firstly, consider Π_2. The risk-neutral density function $\varphi(X_T)$ is linked to its characteristic function $\Phi(t,T,\phi)$ via the Fourier inversion theorem[48]:

$$\begin{aligned}\varphi(X_T) &= \frac{1}{2\pi}\int_0^\infty \left[e^{i\phi X_T}\Phi(t,T,-\phi) + e^{-i\phi X_T}\Phi(t,T,\phi)\right]\mathrm{d}\phi \\ &= \frac{1}{\pi}\int_0^\infty Re\left[e^{-i\phi X_T}\Phi(t,T,\phi)\right]\mathrm{d}\phi \end{aligned} \tag{3.49}$$

For the computation of the risk-neutral exercise probability, one needs the distribution function of X_T. Integration of (3.49) leads to

$$\Pi'(k) = \frac{1}{2} - \frac{1}{\pi}\int_0^\infty Re\left[\frac{e^{-i\phi k}\Phi(t,T,\phi)}{i\phi}\right]\mathrm{d}\phi\,.$$

$\Pi'(k)$ denotes the probability that $X_T < k$ (or, equivalently, that $S_T < K$). For a call option, one needs the inverse probability[49]

$$\Pi_2(K) = 1 - \Pi'(K) = \frac{1}{2} + \frac{1}{\pi}\int_0^\infty Re\left[\frac{K^{-i\phi}\Phi(t,T,\phi)}{i\phi}\right]\mathrm{d}\phi\,. \tag{3.50}$$

For the calculation of Π_1, the same steps can be done with a slightly different characteristic function $\Phi_1(t,T,\phi) = \mathbb{E}_t^{\mathbb{Q}}\left[e^{(1+i\phi)X_T}\right]$ and we obtain[50]

$$\Pi_1(K) = 1 - \Pi_1'(K) = \frac{1}{2} + \frac{1}{\pi}\int_0^\infty Re\left[\frac{K^{-i\phi}\Phi_1(t,T,\phi)}{i\phi}\right]\mathrm{d}\phi\,. \tag{3.51}$$

Armed with the option pricing (3.48) and the formulas for the delta (3.51) and the risk-neutral exercise probability (3.50), one can calculate the option price by calling the characteristic functions Φ_1 and Φ. However, Bakshi and Madan (2000) demonstrate that both characteristic functions can analytically be expressed in terms of the characteristic function of the state price density. Hence, Π_1 can be computed

[48] The Fourier inversion theorem is discussed in Bronstein et al. (2001), p. 746. The second equality in (3.49) is obtained by the following considerations: The complex number $\bar{\mathcal{Z}} = Re[\mathcal{Z}] - i\cdot Im[\mathcal{Z}] = e^{i\phi X_T}\Phi(t,T,-\phi)$ is the complex conjugate of $\mathcal{Z} = Re[\mathcal{Z}] + i\cdot Im[\mathcal{Z}] = e^{-i\phi X_T}\Phi(t,T,\phi)$, where $Re[\mathcal{Z}]$ denotes the real part and $Im[\mathcal{Z}]$ denotes the imaginary part of $\mathcal{Z}$. Therefore, $\bar{\mathcal{Z}} + \mathcal{Z} = Re[\mathcal{Z}] - i\cdot Im[\mathcal{Z}] + Re[\mathcal{Z}] + i\cdot Im[\mathcal{Z}] = 2Re[\mathcal{Z}]$.

[49] The probability that $S_T > K$ is the exercise probability of the call option. Remember that this probability is taken under the risk-neutral measure and is not the exercise probability under the real measure $\mathbb{P}$.

[50] Remember that $\Phi_2 = \Phi$ because the measures $\mathbb{Q}_2$ and $\mathbb{Q}$ are identical, which is due to the non-randomness of interest rates. For a detailed discussion of this approach, see Zhu (2000).

by calling the very same characteristic function Φ via[51]

$$\Pi_1(K) = \frac{1}{2} + \frac{1}{\pi} \int_0^\infty Re\left[\frac{K^{-i\phi}\, \Phi(t, T, \phi - i)}{i\phi\, \Phi(t, T, -i)} \right] \mathrm{d}\phi \,. \tag{3.52}$$

This definition of Π_1 seems more tractable since one has only to deal with one characteristic function when computing an option price.

Now consider the calculation of the integrals in (3.50) and (3.52). At first sight, the integration is not straightforward because both integrands have a pole at $\phi = 0$. However, the integrals can be recovered via Gauss-Laguerre quadrature (see Sect. 3.6), which does not require the evaluation of the integrands at $\phi = 0$.

Carr–Madan Approach

Conversely, the pole at $\phi = 0$ affects the application of Fast Fourier Transformation techniques of the following Sect. 3.5 since the integration node at $\phi = 0$ is needed for this integration algorithm. Following Carr and Madan (1999), a dampening parameter δ is introduced to eliminate the pole in both equations. Starting from (3.43), we get a dampened option price

$$C_t^\delta = e^{\delta k} \int_k^\infty e^{-r(T-t)} \left(e^{X_T} - e^k\right) \varphi(X_T)\, \mathrm{d}X_T \,. \tag{3.53}$$

The Fourier transform of the dampened option price is

$$\Psi(t, T, \phi) = \int_{-\infty}^\infty e^{i\phi k} e^{\delta k} \int_k^\infty e^{-r(T-t)} \left(e^{X_T} - e^k\right) \varphi(X_T)\, \mathrm{d}X_T\, \mathrm{d}k \,. \tag{3.54}$$

Changing the order of integration according to Fubini's theorem, solving the integral over k and splitting the remaining integral in two parts leads to[52]

$$\begin{aligned} \Psi(t, T, \phi) = {} & e^{-r(T-t)} \int_{-\infty}^\infty \varphi(X_T) \frac{1}{\delta + i\phi}\, e^{X_T \cdot (1+\delta+i\phi)}\, \mathrm{d}X_T \\ & - e^{-r(T-t)} \int_{-\infty}^\infty \varphi(X_T) \frac{1}{1 + \delta + i\phi}\, e^{X_T \cdot (1+\delta+i\phi)}\, \mathrm{d}X_T . \end{aligned} \tag{3.55}$$

The option price is recovered by Fourier inversion and multiplication with factor $e^{-\delta k}$.

[51] See Bakshi and Madan (2000), case 2 on p. 218.

[52] See e.g. Björk (2005), p. 414.

$$C_t = \frac{e^{-r(T-t)}\, e^{-\delta k}}{2\pi} \cdot \left\{ \int_{-\infty}^{\infty} e^{-i\phi k} \cdot \frac{\Phi(t,T,\phi - i(\delta+1))}{\delta + i\phi}\, \mathrm{d}\phi \right.$$
$$\left. - \int_{-\infty}^{\infty} e^{-i\phi k} \cdot \frac{\Phi(t,T,\phi - i(\delta+1))}{1+\delta + i\phi}\, \mathrm{d}\phi \right\}$$
$$C_t = \frac{e^{-r(T-t)}\, K^{-\delta}}{\pi} \cdot \left\{ \int_{0}^{\infty} Re\left[\frac{K^{-i\phi}\, \Phi(t,T,\phi - i(\delta+1))}{\delta + i\phi} \right] \mathrm{d}\phi \right.$$
$$\left. - \int_{0}^{\infty} Re\left[\frac{K^{-i\phi}\, \Phi(t,T,\phi - i(\delta+1))}{1+\delta + i\phi} \right] \mathrm{d}\phi \right\} \tag{3.56}$$

The one-integral approach of Carr and Madan is analogous to (3.53) – (3.56) in the previous subsection except for the splitting of the integral. The Fourier transform of the dampened option price is

$$\Psi(t,T,\phi) = \int_{-\infty}^{\infty} e^{-r(T-t)} e^{(\delta+1+i\phi)X_T} \left(\frac{1}{\delta + i\phi} - \frac{1}{1+\delta+i\phi} \right) \varphi(X_T)\, \mathrm{d}X_T$$
$$= e^{-r(T-t)} \frac{\Phi(t,T,\phi - i(\delta+1))}{\delta^2 + \delta - \phi^2 + i\phi(2\delta+1)}.$$

The option price is again obtained by Fourier inversion and undampening with factor $e^{-\delta k}$.

$$C_t = \frac{e^{-r(T-t)}\, K^{-\delta}}{\pi} \cdot \int_{0}^{\infty} Re\left[\frac{K^{-i\phi}\, \Phi(t,T,\phi - i(\delta+1))}{\delta^2 + \delta - \phi^2 + i\phi(2\delta+1)} \right] \mathrm{d}\phi \tag{3.57}$$

The valuation equation for the call option price in (3.57) is perfect for the application of fast algorithms which are described in the next section, since only one integral has to be solved for each moneyness. If one needs the delta and the risk-neutral exercise probability, (3.56) is the appropriate equation for the fast algorithms.

3.5 Fast Fourier Algorithms

3.5.1 Fast Fourier Transformation

The use of Fast Fourier Transformation (FFT) algorithms in option pricing is adequate if we want to price options for multiple strikes. The idea to use FFT for this purpose traces back to Carr and Madan (1999). FFT delivers a vector of all option prices simultaneously and significantly speeds up the computation compared to the repeated calculation of single option values. However, FFT has a crucial disadvantage: the algorithm requires a circular convolution property of the transform vector.

The resulting restrictions are the following: Firstly, the number of strikes has to equal the number of nodes of the integral over ϕ and secondly, the distance of the nodes over the ϕ-axis and the strike axis cannot be chosen independently.

FFT is the corresponding fast algorithm of the discrete Fourier transform (DFT). The DFT F_m of a vector f_n is defined as follows[53]:

$$F_m = \sum_{n=0}^{N-1} f_n \, \exp\left(-\frac{2\,\pi\, i\, m\, n}{N}\right) \tag{3.58}$$

To map the complete vector f_n into its DFT F_m, we have to perform the summation in (3.58) N times for $m = 0, .., N-1$. Consequently, both vectors F_m and f_n contain N elements. Each element of the sum in (3.58) can be interpreted as polar coordinate of a complex number where $\frac{2\,\pi\, m\, n}{N}$ denotes the angle and f_n is the radius. For $n = N$, we have performed a full circle and obtain the same result as for $n = 0$. Due to this circular convolution property, we have also $F_{-n} = F_{N-n}$. Each element $\exp(\frac{2\,\pi\, i\, m\, n}{N})$ is used N times and can therefore be stored to speed up the computation.

Now apply (3.58) to our integration problem. Consider again (3.57). The continuous inverse Fourier transformation can be approximated by its discrete counterpart via

$$\begin{aligned} C_t(k_m) &= \frac{e^{-k_m \delta}}{\pi} \cdot \int_0^{\infty} Re\left[e^{-i\, k_m \phi}\, \Psi(t, T, \phi)\right] \mathrm{d}\phi \\ &\approx \frac{e^{-k_m \delta}}{\pi} \cdot \sum_{n=0}^{N-1} Re\left[e^{-i\, k_m \phi_n}\, \Psi(t, T, \phi_n)\right] w_n\, \Delta_\phi\,. \end{aligned} \tag{3.59}$$

w_n is some weighting function determined by the trapezoidal or Simpson's rule, it can also be unity.[54] Note that both indices n (which determines the value of the integration parameter ϕ) and m (which determines the strike of the call option) take N values from zero to $N-1$. To discretize the integral, it is truncated at some large value $\phi_{\max}$, for which the function value of the integrand is satisfactorily small, say 10^{-6}. Subsequently, the size of Δ_ϕ is fixed. Depending on accuracy, the value of Δ_ϕ is located in the interval $[0.1, 0.25]$.[55] With Δ_ϕ given, we adjust $\phi_{\max}$ upwards so that the number of nodes is a power of 2. $N \in 2^x \,\forall\, x \in \mathbb{N}$ is convenient for the Fast Fourier algorithm. The result is $\phi_n = \Delta_\phi \cdot n$, for $n = 0, .., N-1$.

Starting from this setting for ϕ_n, there is only one degree of freedom left for the log-strike axis k_m. The smallest log-strike k_0 can be chosen freely. The number of

[53] See Bronstein et al. (2001).

[54] The trapezoidal and Simpson's rule are illustrated in Bronstein et al. (2001), p. 922 and p. 923.

[55] Of course, smaller or larger values for Δ_ϕ are possible. However, the location of Δ_ϕ in the specified interval is a convenient trade-off between accuracy and computation time.

strikes is already fixed at N. The m-th element of the log-strike vector is defined by $k_m = k_0 + \Delta_k \cdot m$, for $m = 0, .., N-1$. Plugging these results in (3.59), we have

$$\begin{aligned} C_t(k_m) &\approx \frac{e^{-(k_0+\Delta_k m)\delta}}{\pi} \sum_{n=0}^{N-1} Re\left[e^{-i\,\Delta_k m \Delta_\phi n}\, e^{-ik_0\Delta_\phi n}\, \Psi(t,T,\Delta_\phi n)\right] w_n\, \Delta_\phi \\ &\approx \frac{e^{-(k_0+\Delta_k m)\delta}}{\pi} \Delta_\phi \sum_{n=0}^{N-1} Re\left[e^{-i\,\Delta_k m \Delta_\phi n}\, f_n\right]. \end{aligned} \tag{3.60}$$

A comparison with (3.58) reveals the restriction on Δ_k so that (3.60) is a DFT:

$$\Delta_k \cdot \Delta_\phi = \frac{2\pi}{N} \tag{3.61}$$

A small value of Δ_ϕ leads to a coarser grid over the strike axis and vice versa. High accuracy can be achieved with small values of Δ_ϕ. Unfortunately, increasing the accuracy leads to calculation of option prices which are not needed because of unrealistic strikes.

The DFT as described in (3.58) or (3.60) requires N^2 computations. The corresponding fast algorithm uses the fact that N is a power of 2 and divides the sum stepwise into sums with even and odd elements[56]:

$$\begin{aligned} &\sum_{n=0}^{N-1} Re\left[e^{-i\,\frac{2\pi}{N}nm}\, f_n\right] \\ &= \underbrace{\sum_{n=0}^{N/2-1} Re\left[e^{-i\,\frac{2\pi}{N/2}nm}\, f_{2n}\right]}_{even\ (e)} + \underbrace{e^{-i\,\frac{2\pi}{N}m} \sum_{n=0}^{N/2-1} Re\left[e^{-i\,\frac{2\pi}{N/2}nm}\, f_{2n+1}\right]}_{odd\ (o)} \\ &= \underbrace{\sum_{n=0}^{N/4-1} Re\left[e^{-i\,\frac{2\pi}{N/4}nm}\, f_{4n}\right]}_{ee} + \underbrace{e^{-i\,\frac{2\pi}{N}2m} \sum_{n=0}^{N/4-1} Re\left[e^{-i\,\frac{2\pi}{N/4}nm}\, f_{4n+2}\right]}_{eo} \\ &+ \underbrace{e^{-i\,\frac{2\pi}{N}m} \sum_{n=0}^{N/4-1} Re\left[e^{-i\,\frac{2\pi}{N/4}nm}\, f_{4n+1}\right]}_{oe} + \underbrace{e^{-i\,\frac{2\pi}{N}3m} \sum_{n=0}^{N/4-1} Re\left[e^{-i\,\frac{2\pi}{N/4}nm}\, f_{4n+3}\right]}_{oo} \\ &\ldots \end{aligned}$$

This procedure can be repeated $\log_2 N$ times until there is a sum of N single elements and no longer a sum of sums on the right hand side. For example, the

[56] See also Press et al. (1997).

single Fourier transforms of a vector f with eight elements 0, 1, 2, 3, 4, 5, 6, 7 are arranged after three steps in order 0, 4, 2, 6, 1, 5, 3, 7. If we express the elements in binary code, we observe a change from 000, 001, 010, 011, 100, 101, 110, 111 to 000, 100, 010, 110, 001, 101, 011, 111. A closer look at the binary codes reveals that the rearranging is obtained by reverting the binary code for each element. The fast algorithm consists of rearranging the Fourier transforms of single elements of f according to the reversion of their binary codes and then performing the $\log_2 N$ steps of merging adjacent elements until the sum over all elements is obtained. The resulting length of the algorithm is reduced from order N^2 to order $N \log_2 N$.

This procedure works also for other prime factors, e.g. 3, 5, 7 etc. The Matlab® function fft does not require N to be a power of 2 and uses the smallest prime factors of N. If a decomposition of N into small prime factors is not possible, the resulting FFT is not very fast. The worst case scenario is for N being a prime number, where we obtain no speedup in the computation. It is then convenient to increase N to a well-factorized number by padding the vector with zeros. For further reading of this topic, we suggest Cerny Cerny (2004), who provides a short overview of computation speeds for different values of N.

3.5.2 Fractional Fast Fourier Transformation

The Fractional Fast Fourier Transformation (FRFT) remedies the deficiencies of the FFT algorithm. The number and the spacing of the nodes over the strike axis can be chosen independently. The structure of FRFT can be found in Bailey and Swartztrauber (1991).[57] Chourdakis (2004) was first in adopting FRFT in finance, he uses a normalized characteristic function with an asset price of unity (and therefore a log-price of zero) to improve accuracy. The option prices are finally obtained by multiplication with the real asset price. If we want to apply the normalization of the characteristic function on mean-reverting assets, we do not only have to adjust the asset price and the strike, but also the mean-reversion level.[58] In this chapter, we do not work with normalized characteristic functions. Since the loss of accuracy is marginal, we apply the original characteristic function and use log-strikes rather than log-moneyness as transform variable.

The FRFT of a vector f with fractional parameter α according to Bailey and Swartztrauber (1991) is defined as:

[57] The definition of FRFT according to Bailey and Swartztrauber (1991) virtually is another name for a z-transform which corresponds to a DFT. There exists a rival definition for FRFT, which is short for Fractional Fourier Transform and denotes the n-th power of a Fourier transform where n is not required to be an integer (see e.g. Namias (1980)). Following Chourdakis (2004), we refer to the z-transform as FRFT.

[58] The long-term equilibrium level corresponds to the parameter $\overline{X}$ in (4.1) or (4.18), for example. The linear homogeneity property (Merton (1973)) of option prices in the case of mean-reverting asset prices is also discussed in Sect. 4.1.

$$G_m = \sum_{n=0}^{N-1} f_n e^{-2\pi i m n \alpha} \tag{3.62}$$

Following Chourdakis (2004), we show that this transform can be expressed in terms of conventional FFTs.

Consider again (3.60) as discretized integral under account. Note that it is no longer necessary that the number of strikes M equals the number of nodes N for each integral. This property accounts for the superiority of the FRFT algorithm over the FFT approach in the previous subsection. Following Carr and Madan (1999) and Chourdakis (2004), we calculate option prices for the log-moneyness range $[-b, +b]$. Therefore, we have a log-strike range from $k_0 = -b + \ln(S)$ to $k_{M-1} = +b + \ln(S)$. The number of strikes M is only required to be smaller or equal N. This condition for M is not a crucial restriction, since high accuracy requires a sizeable N. The maximal number of strikes grows with increasing accuracy, smaller values are possible. With M given, the value of Δ_k results in $\Delta_k = 2b/(M-1)$.
Setting

$$\alpha = \frac{\Delta_\phi \, \Delta_k}{2\pi} = \frac{\Delta_\phi \, b}{\pi \, (M-1)}, \tag{3.63}$$

we obtain

$$C_t(k_m) \approx \frac{e^{-k_m \delta}}{\pi} \Delta_\phi \sum_{n=0}^{N-1} Re\left[e^{-2\pi i n m \alpha} \, f_n\right]. \tag{3.64}$$

Using $2nm = n^2 + m^2 - (m-n)^2$, we have

$$C_t(k_m) \approx \frac{e^{-k_m \delta}}{\pi} \Delta_\phi \, Re\left[e^{-\pi i m^2 \alpha} \sum_{n=0}^{N-1} e^{-\pi i n^2 \alpha} \, e^{\pi i (m-n)^2 \alpha} \, f_n\right]. \tag{3.65}$$

Substitution of

$$f_n e^{-\pi i n^2 \alpha} = f_j e^{-\pi i j^2 \alpha} = y_j$$

and

$$e^{\pi i (m-n)^2 \alpha} = e^{\pi i j^2 \alpha} = z_j$$

leads to

$$C_t(k_m) \approx \frac{e^{-k_m \delta}}{\pi} \Delta_\phi \, Re\left[e^{-\pi i m^2 \alpha} \sum_{n=0}^{N-1} y_n z_{m-n}\right]. \tag{3.66}$$

We notice that the index of z depends on both n and m and becomes negative for $n > m$. The value of the sum over all elements of z does not depend on m if z shows circular convolution, but this property is not yet fulfilled since $z_{m-n} \neq z_{m-n+N}$. Following this objective, the length of the sequences y and z is doubled; the second N elements are defined as $y_j = 0$ and $z_j = e^{\pi i (j-2N)^2 \alpha}$ for $j = N, N+1, .., 2N-1$. With this setting for z, a circular convolution of length $2N$ is obtained, i.e. $z_{j+2N} = z_{j-2N} = z_j$.

$$C_t(k_m) \approx \frac{e^{-k_m\delta}}{\pi}\Delta_\phi \, Re\Big[e^{-\pi i m^2\alpha} \sum_{n=0}^{2N-1} y_n z_{m-n}\Big] \tag{3.67}$$

Performing an identity operation by Fourier transform and inverse Fourier transform leads to

$$C_t(k_m) \approx \frac{e^{-k_m\delta}}{\pi}\Delta_\phi \cdot \\ \cdot Re\Bigg[e^{-\pi i m^2\alpha}\,\frac{1}{2N}\sum_{j=0}^{2N-1}\sum_{l=0}^{2N-1}\sum_{n=0}^{2N-1} y_n z_{l-n}\exp\Big(-\frac{i\pi jl}{N}\Big)\exp\Big(\frac{i\pi jm}{N}\Big)\Bigg]. \tag{3.68}$$

Split the exponential function of the Fourier transform and change the order of summation:

$$C_t(k_m) \approx \frac{e^{-k_m\delta}}{\pi}\,\Delta_\phi \, Re\Bigg[\frac{e^{-\pi i m^2\alpha}}{2N}\sum_{j=0}^{2N-1}\sum_{n=0}^{2N-1} y_n \exp\Big(-\frac{i\pi jn}{N}\Big)\cdot \\ \cdot \sum_{l=0}^{2N-1} z_{l-n}\exp\Big(-\frac{i\pi j(l-n)}{N}\Big)\exp\Big(\frac{i\pi jm}{N}\Big)\Bigg]. \tag{3.69}$$

Now consider the third sum which is the DFT of z. Due to circular convolution, it is extraneous at which element the summation starts and $DFT(z_{l-n})$ can be simplified to $DFT(z_l)$. We identify the two DFT's and the inverse DFT, replace them with their corresponding fast algorithms and obtain

$$C_t(k_m) \approx \frac{e^{-k_m\delta}}{\pi}\Delta_\phi Re\big[e^{-\pi i m^2\alpha}\, IFFT\{FFT(y)\odot FFT(z)\}\big], \tag{3.70}$$

where $\odot$ denotes element-by-element vector multiplication and IFFT is the inverse FFT. This approximation is only valid for $m = 0, 1, .., M-1$. All FFT's are of length $0, 1, .., 2N-1$, the first M elements are used and the remaining elements are discarded.

3.6 Recovering Single Option Prices with Gauss-Laguerre Quadrature

The FFT algorithms described in the previous section are convenient if multiple option prices for different strikes are needed. Especially when the characteristic function is calculated numerically, the calculation process can become

very time-consuming. Hence, an integration routine for single option prices saves computation time if one does not need option prices for multiple strikes.

It is necessary to calculate integrals of the type

$$\int_0^\infty Re[f(\phi)]\,\mathrm{d}\phi \tag{3.71}$$

to recover the risk-neutral probabilities ((3.50) and (3.52)) and the option price. The integrand is an oscillating function which decays as ϕ approaches infinity. An integration of (3.71) with standard quadrature routines such as the trapezoidal or Simpson's rule is suboptimal, especially when the function values are not given in closed form and time-consuming numerical procedures are applied.[59]

A fast and accurate way to calculate integrals in the interval $[0, \infty)$ is the use of Gauss-Laguerre quadrature, since less function calls of the characteristic function are required.[60] As in every quadrature routine, the integral is approximated via a sum.

$$\int_0^\infty w(\phi) \cdot g(\phi)\,\mathrm{d}\phi = \sum_{k=1}^{n} w_k(\phi_k) \cdot g(\phi_k) + E_n \tag{3.72}$$

$w(\phi)$ is the weighting function and the ϕ_k are the nodes of the quadrature formula. The nodes of Gauss formulae are not required to be equidistant. The possibility to choose the coefficients w_k and also the nodes ϕ_k leads to additional degrees of freedom in the quadrature rule which can be used to approximate the integrand by polynomials of higher degree. The maximum degree for a formula with n points is $2n - 1$. The quadrature rule has small approximation errors if the integrand is a continuous and differentiable function. In the case of indefinite integrals in the interval $[0, \infty)$, we also have a truncation error. E_n in (3.72) denotes the summarized error. The weighting function is only required to be nonnegative; it can also be unity. Other weighting functions are used when the approximation works better for the product of weighting function and modified integrand than for the original integrand. In the case of Gauss-Laguerre quadrature we have $w(\phi) = \exp(-\phi)$. In order to apply the quadrature routine, the weighting function is plugged into the Integral (3.71).

$$\int_0^\infty w(\phi)\ \exp(\phi)\ Re[f(\phi)]\,\mathrm{d}\phi = \sum_{k=1}^{n} w_k(\phi_k)\ \exp(\phi_k)\ Re[f(\phi_k)] + E_n \tag{3.73}$$

[59] We used Runge–Kutta and predictor-corrector algorithms as described in Sect. 3.6 in the appendix of this chapter. A discussion of Runge–Kutta computation time is provided in Sect. 4.2.3 in the appendix Chap. 4. For a discussion of the trapezoidal and Simpon's rule, see Bronstein et al. (2001), p. 922 and p. 923.

[60] See also Tahani (2004).

The function $f(\phi)$ has to be computed only at n points. The choice of n determines the size of the error: A large n uses more function calls and results in a small error and vice versa.

The nodes ϕ_k are the zeros of a special polynomial $L_n(\phi)$ which is orthonormal to the weighting function. Orthonormality in this respect means that

$$\int_0^\infty w(\phi)\, L_n(\phi)\, P_m(\phi)\, \mathrm{d}\phi = 1 \quad \text{for} \quad m = n$$

$$\int_0^\infty w(\phi)\, L_n(\phi)\, P_m(\phi)\, \mathrm{d}\phi = 0 \quad \text{for} \quad m \neq n$$

holds for any polynomial $P_m(\phi)$ with $m = n$ and $m \neq n$, respectively. It can be shown that the orthonormal polynomial always exists and is unique.[61] In the case of the interval $[0, \infty)$ with the weighting function $w(\phi) = \exp(-\phi)$, the orthonormal polynomial is a Laguerre polynomial L_n. The zeros of Laguerre polynomials and the corresponding weights are tabulated in Abramowitz and Stegun (1970) for $n \leq 15$. For higher orders, the nodes can be found by solving an eigenvalue problem for the tridiagonal matrix

$$\mathbf{T} = \begin{pmatrix} 1 & -1 & 0 & 0 & \dots & 0 \\ -1 & 3 & -2 & 0 & \dots & 0 \\ 0 & -2 & 5 & -3 & \ddots & \vdots \\ 0 & 0 & -3 & 7 & \ddots & 0 \\ \vdots & \vdots & \ddots & \ddots & \ddots & -(n-1) \\ 0 & 0 & \dots & 0 & -(n-1) & 2n-1 \end{pmatrix}.$$

The eigenvalues of $\mathbf{T}$ are the nodes of the Gauss-Laguerre quadrature rule of order n. The weights $w_k(\phi_k)$ are acquired by squaring the first element of the corresponding eigenvector.[62]

For any n, the nodes lay in the interval $(0, \infty)$. This property has the advantage that the function $f(\phi)$ does not have to be calculated at $\phi = 0$, which is a pole. Hence, we can apply Gauss Laguerre quadrature directly without using a dampening parameter as described in Sect. 3.4.2.

[61] See Stroud (1974) for a proof of this finding.

[62] The proofs of these properties are given in Golub and Welsch (1969).

Appendix

The Hedging Portfolio in the Stochastic Volatility Framework

In this section, we demonstrate according to Lewis (2000) the construction of a hedging portfolio out of n_C call options and n_S shares of the underlying:

$$\mathfrak{W} = n_C\, C + n_S\, S\,, \tag{3.74}$$

where $\mathfrak{W}$ denotes the portfolio wealth. Lewis adopts a stochastic volatility framework without jumps and constructs a hedging portfolio which is uncorrelated with the underlying, i.e. if $d\mathfrak{W}\, dS = 0$ holds, the portfolio is hedged against price changes of the underlying for an infinitesimal time segment dt (though it is not hedged against changes of variance). We obtain

$$\begin{aligned} d\mathfrak{W}\, dS = \Bigg\{ & n_C \Bigg[\frac{\partial C}{\partial t} + a(X_t, V_t)\, S_t\, \frac{\partial C}{\partial S} + \frac{1}{2}\, V_t\, S_t^2\, \frac{\partial^2 C}{\partial S^2} + b(V_t)\, \frac{\partial C}{\partial V} \\ & + \frac{1}{2}\, c^2(V_t) \frac{\partial^2 C}{\partial V^2} + \rho\, c(V_t)\, \sqrt{V_t}\, \frac{\partial^2 C}{\partial S \partial V} + n_S\, a(X_t, V_t)\, S_t \Bigg] dt \\ & + \sqrt{V_t}\, S_t \left[n_C\, \frac{\partial C}{\partial S} + n_S \right] dW_t^X + n_C\, c(V_t)\, \frac{\partial C}{\partial V}\, dW_t^V \Bigg\} \\ & \times \left\{ a(X_t, V_t)\, S_t\, dt + \sqrt{V_t} S_t\, dW_t^X \right\} = 0\,. \end{aligned} \tag{3.75}$$

Using

$$\begin{aligned} dt^2 = dt\, dW_t^X = dt\, dW_t^V &= 0 \\ (dW_t^X)^2 &= dt \\ dW_t^X\, dW_t^V &= \rho\, dt\,, \end{aligned}$$

(3.75) simplifies to

$$\sqrt{V_t}\, S_t \left[n_C \left(\sqrt{V_t}\, S_t \frac{\partial C}{\partial S} + \rho\, c(V_t)\, \frac{\partial C}{\partial V} \right) + \sqrt{V_t}\, S_t\, n_S \right] = 0\,. \tag{3.76}$$

(3.76) holds for

$$n_S = -n_C \left(\frac{\partial C}{\partial S} + \frac{\rho\, c(V_t)}{\sqrt{V_t}\, S_t}\, \frac{\partial C}{\partial V} \right). \tag{3.77}$$

Substitute n_S via (3.77) and set $n_C = 1$ to obtain for the dynamics of the portfolio wealth[63]

$$d\mathfrak{W} = \left[\frac{\partial C}{\partial t} + \frac{1}{2} V_t S_t^2 \frac{\partial^2 C}{\partial S^2} + \frac{\partial C}{\partial V}\left(b(V_t) - \frac{\rho\, c(V_t)\, a(X_t, V_t)}{\sqrt{V_t}}\right) + \frac{1}{2} c^2(V_t) \frac{\partial^2 C}{\partial V^2} + \rho\, c(V_t) \sqrt{V_t} \frac{\partial^2 C}{\partial S \partial V}\right] dt + c(V_t) \frac{\partial C}{\partial V}\left[dW_t^V - \rho\, dW_t^X\right]. \tag{3.78}$$

To switch to the risk-adjusted dynamics, one defines the risk premium of the hedging portfolio as

$$\chi_t^P = \frac{a_t^P - r}{\sigma_t^P}, \tag{3.79}$$

where $a_t^P \mathfrak{W}$ refers to the drift of $d\mathfrak{W}$ via

$$a_t^P \mathfrak{W} = \frac{\partial C}{\partial t} + \frac{1}{2} V_t S_t^2 \frac{\partial^2 C}{\partial S^2} + \frac{\partial C}{\partial V}\left(b(V_t) - \frac{\rho\, c(V_t)\, a(X_t, V_t)}{\sqrt{V_t}}\right) + \frac{1}{2} c^2(V_t) \frac{\partial^2 C}{\partial V^2} + \rho\, c(V_t) \sqrt{V_t} \frac{\partial^2 C}{\partial S \partial V}, \tag{3.80}$$

and σ_t^P is given by

$$(\sigma_t^P \mathfrak{W})^2 = c^2(V_t)\left(\frac{\partial C}{\partial V}\right)^2 (1 - \rho^2). \tag{3.81}$$

Plug (3.80) and (3.81) in (3.79). Together with (3.74) and (3.77), one arrives at the following relation:

$$\frac{\partial C}{\partial t} + \frac{1}{2} V_t S_t^2 \frac{\partial^2 C}{\partial S^2} + \frac{\partial C}{\partial V} \tilde{b}(V_t) + \frac{1}{2} c^2(V_t) \frac{\partial^2 C}{\partial V^2} + \rho\, c(V_t) \sqrt{V_t} \frac{\partial^2 C}{\partial S \partial V} - r\, C + r\, S \frac{\partial C}{\partial S} = 0. \tag{3.82}$$

$\tilde{b}(V_t)$ in (3.82) is the risk-adjusted volatility parameter which is given by

$$\tilde{b}(V_t) = b(V_t) - c(V_t)\left(\rho\, \chi_t^S \pm \sqrt{1 - \rho^2}\, \chi_t^P\right), \tag{3.83}$$

[63] The volume of the hedge portfolio is extraneous. If the parameter is not replaced, it is canceled in the result anyway (Lewis (2000)).

where the $\pm$ sign in (3.83) depends on the nonnegativity condition for σ_t^P. Hence, the risk premium for the variance process is

$$\chi_t^V = \rho\,\chi_t^S \pm \sqrt{1-\rho^2}\,\chi_t^P\,. \tag{3.84}$$

The variance risk premium which is used in the Girsanov transformation in (3.4) and (3.8) has to fulfill the condition in (3.84).

Numerical Integration of ODE Systems

When the system of ODEs does not have an analytic solution or the analytic solution is difficult to compute, it can be solved numerically. Matlab® provides different integration algorithms in its ODE suite. We will focus on the ode45-routine which is based on the Dormand and Prince (1980) 4-5-pair of embedded Runge–Kutta-formulae.

A Question of Computational Efficiency: Explicit or Implicit Schemes?

The integration routines of the Matlab® ODE suite extrapolate the value of a scalar or vector $y(t)$ stepwise when an initial condition $y(0)$ is known and a (system of) ODE(s) describes the dynamics of $y(t)$[64]:

$$y'(t) = f(y(t), t)\,. \tag{3.85}$$

The different integration methods can be classified coarsely in explicit and implicit schemes. Explicit schemes have a lower computational cost per integration step than implicit ones. Hence, explicit schemes are usually applied. However, when the ODE system exhibits stiffness, an explicit integration scheme is forced to reduce the stepsize dramatically to maintain the stability of the solution. The drawback of this pattern is twofold: Firstly, the overall computation time is highly increased and secondly, there is more machine roundoff error accumulated.[65] Since the stability of implicit schemes is not affected by stiffness or non-stiffness, implicit schemes prove to be much more effective in the case of heavy stiffness. When only mild stiffness is involved, the decision is more challenging since it is questionable whether the lesser number of time steps compensates for the higher computational effort per time step or not.

The choice of the appropriate ODE solver therefore depends on the stiffness of (3.85). A definition of this concept is required. However, the definition of stiffness in the literature is not clear-cut. Ekeland et al. (1998) provide a short overview of

[64] In our case, the initial condition is the boundary condition at maturity of the derivative security.

[65] An example for the integration of a stiff ODE system with explicit schemes is given in Huang and Yu (2007).

the various definitions. Huang and Yu (2007) discuss stiffness in affine asset pricing models based on the following definition: "Stiff differential equations are differential equations with greatly differing time constants (i.e., rates of decay)." According to Ekeland et al. as well as Huang and Yu, we choose the eigenvalues of the Jacobian of (3.85) as indicator for stiffness. Ekeland et al. point out that "an eigenvalue with a large negative real part can be an indication of stiffness." The authors also assert that stiffness properties may change as the integration proceeds. Huang and Yu use a similar approach based on the ratio of the largest absolute value and the smallest absolute value of the real parts of the eigenvalues. The larger the value of the ratio, the larger is the stiffness of the underlying ODE system.

Huang and Yu (2007) study the performance of explicit (ode45, ode23) and implicit (ode23s, ode15s) Matlab® solvers. In the Huang and Yu paper, the implicit schemes prove to be superior for all problems under account since all ODE systems exhibit mild or heavy stiffness.

The results are not that clear for the integration problems arising in our model settings which are discussed in the following chapters. Explicit integration schemes prove to be (slightly) faster than implicit routines since the ODE systems are non-stiff (respectively moderately stiff) for reasonable parameter values. Take the ODE system of the square-root stochastic volatility model (4.7) as an example:

$$\begin{aligned}\frac{\mathrm{d}B(\tau)}{\mathrm{d}\tau} &= -\frac{1}{2}i\phi e^{-\eta\tau} + \frac{1}{2}(i\phi)^2 e^{-2\eta\tau} - \kappa B(\tau) + \frac{1}{2}\zeta^2 B^2(\tau) + \rho\zeta i\phi e^{-\eta\tau} B(\tau)\\ \frac{\mathrm{d}C(\tau)}{\mathrm{d}\tau} &= \eta\overline{X} i\phi e^{-\eta\tau} + \kappa\theta B(\tau)\,.\end{aligned}$$

The Jacobian for this integration problem is given by

$$\mathbf{J} = \begin{pmatrix} \zeta^2 B(\tau) + \rho\zeta i\phi e^{-\eta\tau} - \kappa & 0 \\ \kappa\theta & 0 \end{pmatrix},$$

with eigenvalues

$$\lambda(\mathbf{J}) = \begin{pmatrix} \zeta^2 B(\tau) + \rho\zeta i\phi e^{-\eta\tau} - \kappa \\ 0 \end{pmatrix}.$$

An examination of the nonzero eigenvalue reveals the following properties of its constituents: $B(\tau)$ is a complex number whereas the parameter values and the integration variable τ are constrained to real numbers.[66] The restrictions are

[66] An exception is $\phi = -i$ which corresponds to the calculation of futures prices (See Sect. 3.4.1). When $\phi = -i$ holds, the term $\rho\zeta i\phi e^{-\eta\tau}$ is a real (and depending on the sign of ρ a positive or negative) number. However, due to parameter restrictions, the term is small and therefore does not have a large impact on the absolute value of the real part of the eigenvalue. Secondly, $B(\tau)$ is also a real number when $\phi = -i$ holds. The impact of $B(\tau)$ on the eigenvalue increases as the integration proceeds.

$\kappa, \zeta, \eta, \phi > 0$, $\tau \geq 0$ and $\rho \in [-1, 1]$.[67] The boundary condition defines $\tau = 0$ and $B(0) = 0$ as the starting values of the integration scheme. If we firstly restrict our view to the start of the integration, a large negative real part of the eigenvalue is only obtained when κ is large. Small values of κ are equivalent to a nonstiff ODE system. Secondly, the stiffness of the system will increase (decrease) as the integration proceeds when $B(\tau)$ exhibits a negative (positive) real part. These considerations are confirmed by our tests. We tested the ode45 and the ode15s scheme since these two routines involve the highest accuracy among the explicit and implicit schemes, respectively.[68] Small values of κ involve superiority of the explicit scheme and vice versa. The real part of $B(\tau)$ turns out to be negative; the larger the value of ϕ, the larger is the absolute value of the real part of $B(\tau)$ and the higher is the stiffness of the ODE system. Hence, both ϕ and κ influence stiffness and the choice of the fastest ODE solver.

The computation time of the explicit ode45 scheme with respect to ϕ and κ is displayed in the upper left subfigure of Fig. 3.1.[69] The other parameters are set to $\rho = -0.5$, $\zeta = 0.2$, $\eta = 1$, $\tau = 0.5$. The efficiency of the implicit ode15s scheme is shown in the second row on the left, and the upper right subfigure contains the computational advantage of the explicit scheme compared with ode15s. Since all values of the difference matrix are positive, the explicit ode45 integration procedure is superior with respect to the implicit scheme for all shown values of ϕ and κ. All schemes show minimal computation time for ϕ and κ close to zero. For larger values of the two parameters, computation time for the implicit ode15s scheme is nearly constant at ≈ 0.7 s per function call. Since the computation time for the explicit scheme increases with both parameters, the implicit scheme will be more efficient for very large values of ϕ and κ. However, values of ϕ larger than 100 are seldom used in the quadrature scheme and large values of the variance mean reversion parameter κ seem unrealistic.[70]

The third integration routine under account is ode113. Huang and Yu (2007) did not examine the performance of this solver because it is not applicable for stiff problems. This integration scheme is based on the Adams-Bashforth-Moulton

[67] κ, ζ, η are constant model parameters as explained in Sect. 4.1, ϕ is the Fourier parameter and τ denotes time to maturity. ρ is also a model parameter which determines the correlation between asset price variations and volatility variations. For financial assets, a negative value of ρ is appropriate (This pattern is called leverage effect). In the case of commodities, both positive and negative correlations are realistic.

[68] The implicit ode23s scheme does not apply to the problem (see Shampine and Reichelt (1997) for the requirements of this function). Furthermore, the explicit ode23 routine is slightly faster than ode45, but associated with a larger error.

[69] The displayed computation time refers to the average time of 25 replications of the calculation. The calculations were done on a 2×2.8 GHz Pentium® Dual Core workstation.

[70] When κ is very large, the impact of the Brownian motion term in (4.1) on variance behavior vanishes. In this case, a stochastic volatility model seems to be inappropriate since variance could as well be modeled deterministic.

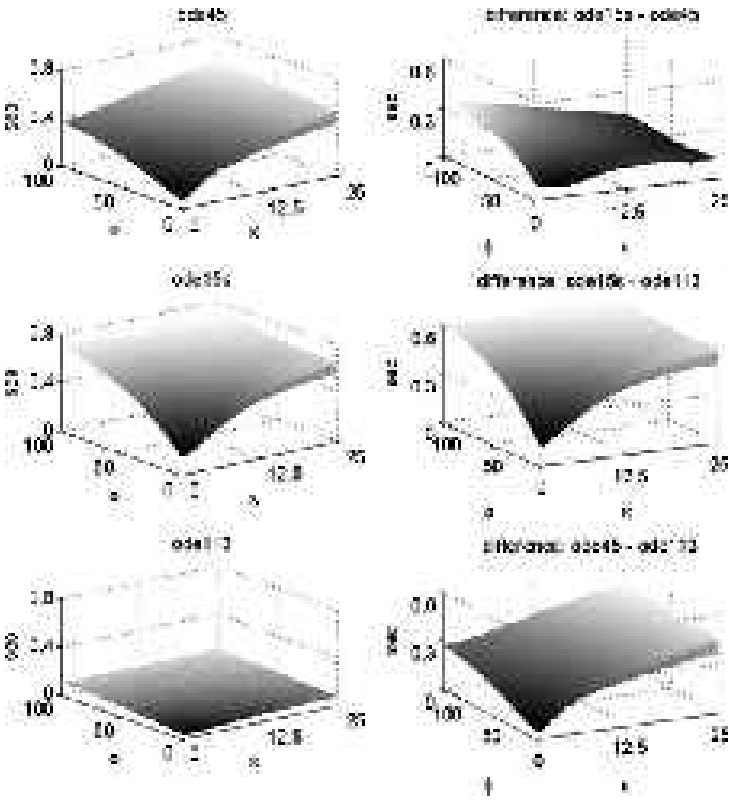

Fig. 3.1 Performance of Matlab® ODE solvers for the square-root stochastic volatility model

predictor-corrector method. It is a linear multistep PECE solver.[71] Since the multistep solver requires multiple starting values to proceed, but only one initial value is known, the necessary starting values are extrapolated with an explicit Runge–Kutta scheme (see the illustration of the ode45 integration routine in the next subsection).

The low computational cost per iteration is its greatest advantage. For each iteration, only one function value has to be estimated based on data which is available from the preceding steps. This efficiency can be seen in the lower left subfigure. The computation time differences with respect to the two other schemes are displayed

[71] PECE stands for predict, evaluate, correct, evaluate. The explicit predictor method yields a value $y^p(t+h)$ of the integrated function y for the new time step $t+h$. The predicted value $y^p(t+h)$ is plugged in the implicit corrector method which yields a corrected value $y^c(t+h)$. This procedure is repeated until the predetermined error tolerance is achieved. More information about the Matlab® ODE solvers is given in Shampine and Reichelt (1997).

in the second and third row on the right. For the given parameter setting and the square-root stochastic volatility ODE system, the computation time of the multistep solver turns out to be six to seven times faster than ode45 and ode15s, respectively. The accuracy of ode113 is similar to the other two solvers. The same findings are obtained when integrating the ODE set (4.20) for the Ornstein–Uhlenbeck stochastic volatility model in Sect. 4.2.2.

An example of superiority of the implicit ode15s solver with respect to the explicit ode45 solver, can be obtained with the ODE set defined by (6.3) and (6.16) in Sect. 6.2.1.

$$\frac{\mathrm{d}C(\tau)}{\mathrm{d}\tau} = -\frac{1}{2}\,i\phi e^{-\eta\tau} + \frac{1}{2}\,(i\phi)^2 e^{-2\eta\tau} + \frac{1}{2}\sigma_{\mathfrak{X}}^2 B^2(\tau) + \rho_{\mathfrak{X}}\sigma_{\mathfrak{X}} i\phi e^{-\eta\tau} B(\tau)$$
$$+ \left[\rho\zeta i\phi e^{-\eta\tau} - \kappa + \rho_{\mathfrak{X}V}\zeta\sigma_{\mathfrak{X}} B(\tau)\right] C(\tau) + \frac{1}{2}\,\zeta^2 C^2(\tau)$$

$$\frac{\mathrm{d}D(\tau)}{\mathrm{d}\tau} = \kappa\theta C(\tau) + \kappa_{\mathfrak{X}}\theta_{\mathfrak{X}} B(\tau)\,,$$

where

$$B(\tau) = \frac{\eta i\phi}{\eta - \kappa_{\mathfrak{X}}}\left(e^{-\kappa_{\mathfrak{X}}\tau} - e^{-\eta\tau}\right) \quad \text{for} \quad \eta \neq \kappa_{\mathfrak{X}}\,.$$

This model setting incorporates a mean reverting (log-)price process with mean reverting stochastic equilibrium level and square-root stochastic volatility. For $\kappa_{\mathfrak{X}}$ large (say 50) and κ small (say 0.5) and vice versa, the implicit solver turns out to be slightly faster (around 20%) than ode45.[72] Again, the predictor-corrector method ode113 turns out to be the fastest ($\approx$80% faster than ode45). All solvers are comparable concerning accuracy.

Therefore, implicit schemes seem to be in an inferior position for reasonable parameter values in our model settings. Albeit the ode113 solver performed best for our tests, the standard ode45 Runge–Kutta integration scheme still is a maintainable choice. However, if computation time is crucial (e.g. due to numerous replications of the integration), our tests support the choice of ode113. In the following chapters, we refer generally to Runge–Kutta-solutions meaning that either ode45 or ode113 were applied. In case of ode113, the term Runge–Kutta-solution is strictly speaking not correct, but is used anyway since the solution for the two solvers is identical and the ode45 solver is the standard method.

[72] $\kappa_{\mathfrak{X}}$ is the adjustment speed parameter of the stochastic equilibrium level process and κ is the adjustment speed of the square-root stochastic volatility process.

The Ode45 Integration Scheme

The easiest method to solve for (3.85) is known as the Euler method where the differential coefficient is approximated by the difference coefficient $\frac{y(t+h)-y(t)}{h}$. The result for the estimate after a small time step h is

$$y(t+h) = y(t) + hf(y(t),t) + \mathcal{O}(h^2)\,.$$

The disadvantage of this algorithm is that the Taylor series expansion is already truncated after the first derivative and the error is of order h^2 and therefore relatively large. To compensate for the large error term, one has to choose a very small stepsize to achieve reliable results. By this means, the procedure becomes either very time-consuming or inexact, or both.

Hence, algorithms with an error term of higher order are required. Runge–Kutta-formulae do not only use the slope at t, but also at $t+h$ and within the stepsize interval. These slopes are extrapolated from the known values at time t. The general form of a Runge–Kutta-formula of order n is

$$y(t+h) = y(t) + h\big[\mathcal{A}_1 k_1 + \mathcal{A}_2 k_2 + \cdots + \mathcal{A}_n k_n\big]\,, \tag{3.86}$$

where

$$\begin{aligned} k_1 &= f(y(t),t) \\ k_2 &= f(y(t+\varpi_{2,1}k_1), t+\varsigma_2 h) \\ &\vdots \\ k_n &= f(y(t+\varpi_{n,1}k_1 + \cdots + \varpi_{n,n-1}k_{n-1}), t+\varsigma_n h)\,. \end{aligned} \tag{3.87}$$

For $n=1$, the Runge–Kutta-scheme matches the Euler method. For larger n and $i>1$, the coefficients k_i are the additional slopes which are extrapolated via

$$\begin{aligned} k_i = f(y(t),t) &+ \varsigma_i h \frac{\partial}{\partial t} f(y(t),t) + \cdots + \frac{(\varsigma_i\, h)^{n-1}}{(n-1)!}\frac{\partial^{n-1}}{\partial t^{n-1}} f(y(t),t) \\ &+ hf(y(t),t)\frac{\partial}{\partial y(t)}\big[\varpi_{i,1}k_1 + \cdots + \varpi_{i,i-1}k_{i-1}\big]\,. \end{aligned} \tag{3.88}$$

The approximations of the k_i according to (3.88) with the unknowns $\varpi_{i,j}$ and ς_i are set in (3.86). Keeping in mind that $f(y(t),t)$ is the first derivative of $y(t)$, one asserts that (3.86) is a sum which contains derivatives of $y(t)$ up to order n. This sum has to take the form of the Taylor series expansion of order n:

$$y(t+h) = y(t) + hy'(t) + \frac{h^2}{2}y^{(2)}(t) + \cdots + \frac{h^n}{n!}y^{(n)}(t) + \mathcal{O}(h^{n+1})\,. \tag{3.89}$$

Equation (3.89) reveals that the error term is one order smaller than the order of the Runge–Kutta-algorithm. The required matching of (3.86) with (3.89) determines the constants $\mathcal{A}_i$, $\varpi_{i,j}$ and ς_i. There are less equations than unknowns so that there are one or more degrees of freedom which lead to multiple Runge–Kutta-schemes for the same order.

The most commonly used Runge–Kutta formula is of order 4. The Matlab® function ode45 incorporates the Dormand and Prince (1980) pair of embedded Runge–Kutta formulae. In this coherence, embedded means that the same function evaluations which are calculated for a Runge–Kutta step of order 4 are used for a step of order 5 in parallel. Both results together are used for an error estimate. The error estimate is needed for an adaptive stepsize algorithm which repeats the step with a smaller stepsize when the predetermined error is exceeded or enlarges the stepsize for the next iteration if the estimate is in favor of a smooth interval of the extrapolated function. Due to the adaptive stepsize, the numerical integration is still acceptably fast.[73]

[73] For a discussion of the computation time of the ode45 Runge–Kutta algorithm compared with other calculation methods, we refer the reader to Sect. 4.2.3 in the appendix of Chap. 4.

Chapter 4
Stochastic Volatility Models

So far, the characteristic function of the log-price at maturity was used without further specifications. In the following chapters, we derive characteristic functions for different settings. Once the characteristic function is obtained, it can be applied in the pricing equations as presented in Chap. 3.

We will focus on the pricing of commodity contingent claims. Applications of mean-reverting OU processes for commodity prices were done by Schwartz (1997) and Ross (1997), among others. In both papers, futures prices and hedge ratios are derived, but no stochastic volatility is incorporated. Schwartz (1997) also provides an empirical survey for the proposed models. The commodities involved are crude oil, copper, and gold.

Longstaff and Schwartz (1995) apply an Ornstein–Uhlenbeck (OU) model without stochastic volatility to price credit spread options. Following Zhu (2000), Tahani (2004) extends their proposal by incorporation of square-root and OU-stochastic volatility, respectively. In our stochastic volatility models, we will refer to the results and interpretations of Tahani.

In our framework, all models exhibit mean reversion of the underlying under the risk-neutral measure $\mathbb{Q}$ and can therefore represent price processes with this feature, e.g. log-commodity price processes or log-credit spread processes.

4.1 Square-Root Stochastic Volatility

The process of X_t is modeled as an Ornstein–Uhlenbeck process with long-term equilibrium level $\overline{X}$ and adjustment speed parameter η. The variance V_t follows a square-root process first introduced in finance by Cox et al. (CIR 1985). ζ, κ and θ are positive constants where ζ denotes the volatility of volatility, θ is the attractor and κ the adjustment speed of the variance process. Hence, both processes are mean-reverting.

$$\begin{aligned} dX_t &= \left(\eta\{\overline{X} - X_t\} - \frac{1}{2}V_t\right)dt + \sqrt{V_t}\,dW_t^X \\ dV_t &= \kappa(\theta - V_t)dt + \zeta\sqrt{V_t}\,dW_t^V \end{aligned} \tag{4.1}$$

B. Lutz, *Pricing of Derivatives on Mean-Reverting Assets*,
Lecture Notes in Economics and Mathematical Systems,
DOI 10.1007/978-3-642-02909-7_4, © Springer-Verlag Berlin Heidelberg 2010

The processes in (4.1) are already formulated under the measure $\mathbb{Q}$. For notational convenience, we omit in this chapter and the following chapters the tilde which denotes risk adjustment. Note that we do not develop a full general equilibrium model, instead of this we assume that the market prices of risk premiums of the underlying and volatility risk are already included in the risk-adjusted parameters $\overline{X}$ and θ, respectively. This assumption is valid for all models we derive.

The standard reference for the application of the CIR process as subordinated variance process is Heston (1993). Among the stochastic volatility models, it is quite popular in practice due to nonnegativity and analytical tractability. The variance process described by (4.1) is ensured to be nonnegative, because if V_t ever becomes zero, the diffusion term will vanish and the drift term will push the process back to the positive mean. For $\zeta^2 \leq \kappa\theta$, the process never reaches zero because the drift term always has a stronger impact than the diffusion term. If $\zeta^2 > \kappa\theta$, $V_t = 0$ is possible as a reflecting barrier.[1] Another appealing property of the assumption of the square-root process for instantaneous variance is the fact that it leads in many cases of interest to closed-form or semi closed-form solutions for the characteristic function. We are also able to derive a closed-form solution based on hypergeometric functions when the underlying follows a mean-reverting process.[2]

4.1.1 Comparison with the Tahani Square-Root Model

The specification in (4.1) is similar to the square-root mean-reverting model of Tahani (2004):

$$\begin{aligned} dX_t &= (\mu - \eta X_t)\, dt + \sqrt{V_t}\, dW_t^X \\ dV_t &= \kappa(\theta - V_t)dt + \zeta \sqrt{V_t}\, dW_t^V \end{aligned} \tag{4.2}$$

Tahani applies the mean reverting framework to price credit spread options following Longstaff and Schwartz (1995), who do not incorporate stochastic volatility in their model.[3] The author points out that the process specifications in (4.2) can also be applied to price derivatives on commodities which show a mean reversion property.

Tahani reports a strong impact of even weak mean reversion on credit spread option prices. He calculates call option prices for small adjustment speed parameters $\eta = 0.01$, 0.02 and 0.03 and gets relative differences of the prices between 4% and 56% (depending on η and maturity) compared to the reference value with no mean reversion for $\eta = 0$. This comparison seems questionable since μ does either

[1] A proof for nonnegativity can be found in Feller (1951).

[2] See Sect. 4.1.2.

[3] The log-process of the underlying in Longstaff and Schwartz (1995) is also of the form $dX_t = (a - bX_t)dt + \sigma dW_t$. Contrary to Tahani (2004), they do not report any parameter values and resulting option prices.

determine the mean reversion level (together with η, as we shall see) or the drift of the process when there is no mean reversion. Typically, the drift is expressed in percentage terms and the mean reversion level in absolute terms. Consequently, the two values have different dimensions.

This could be a reason for the fact that the only call prices provided by the author are for relatively small values of the underlying and the strike, i.e. $S = K = 0.02$. S is interpreted as credit spread and can therefore be expressed in percentage terms. The maturity is set to 3, 6, 9 and 12 months.

Unfortunately, the reason for the major effect is not the mean reversion itself, but rather a misunderstanding of the process parameters and as a result of this, the unrealistic parameter settings. One can easily see this by adapting equation (4.1) to the setting of Tahani. To recover the results of Tahani, we change the first equation in (4.1) to

$$dX_t = \eta\{\overline{X} - X_t\}\, dt + \sqrt{V_t}\, dW_t^X\,, \tag{4.3}$$

which is equivalent to incorporating a term $+0.5\, V_t\, dt$ in the process of S_t via Itô's lemma. Obviously, this adaption results in slightly higher option values. Which process assumption is chosen is a matter of taste, but when starting from the price of the underlying, (4.1) for the log-process seems more reasonable.

However, this is not the reason for the unrealistic behavior of the price process. Regarding (4.2), the author sets $\mu = 0.03$. The other parameters are set to $S = K = 0.02$, $T - t = 0.5$, $\zeta = 0.2$, $\sqrt{V} = 0.2$, $\kappa = 1$, $r = 0.05$, $\rho = -0.5$, $\theta = 0.05$. η takes the values 0.01, 0.02 and 0.03. Hence, the three values for the adjustment speed are very small and one would expect at most marginal differences in the process behavior. The behavior of the Tahani and our OU model for the parameter setting of Tahani is plotted in Fig. 4.1. All six trajectories correspond to

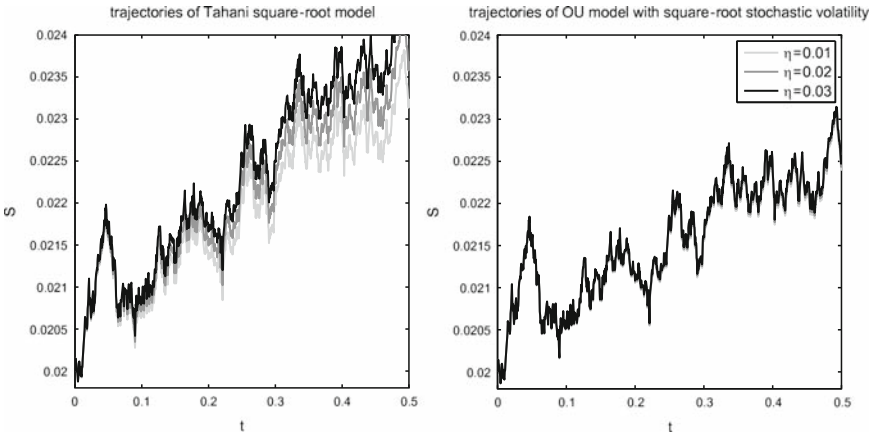

Fig. 4.1 Trajectories for Tahani and our OU processes with square-root stochastic volatility for the parameter settings of Tahani

the same set of random numbers to point up the effects of the different processes and values of η, respectively. We observe that the marginal differences can only be seen in the right figure for our modified OU model (4.3). The impact of η in the Tahani model is quite larger, and the process is driven at a faster speed away from the initial value. The reason for the large impact of η in the Tahani model is that the long-term equilibrium level of the log-process dX_t is not μ, but rather μ/η. Comparing (4.2) and (4.3), we obtain the same processes for $\overline{S} = \exp(\overline{X}) = \exp(\mu/\eta)$. This means that the equilibrium level of the underlying $\overline{S}$ is exp(3) (exp(1.5), exp(1), respectively, depending on the value of η). Therefore, the process is driven to a level which lies by a factor of 1004 (224, 136, respectively) above the initial value of $S = 0.02$. Not surprisingly, even very small adjustment speeds have a substantial effect on call values when combined with a very large equilibrium level. Due to the coupling of $\overline{X}$ and η in one parameter μ, the real equilibrium level $\overline{X}$ increases as η decreases, and one observes a crucial effect of mean reversion.

The shortcoming gets even more obvious if ceteris paribus the values of S, K and the would-be equilibrium level μ are expressed in absolute terms, i.e. $S = K = 2$, $\mu = 3$, $\eta = 0.03$, $T - t = 0.5$, $\zeta = 0.2$, $\sqrt{V} = 0.2$, $\kappa = 1$, $r = 0.05$, $\rho = -0.5$, $\theta = 0.05$. One would expect that the call value is not affected by the change from percentage to absolute terms and therefore also increases by a factor of 100, i.e. $C = 0.2220$.[4] Secondary, if one wants to apply the model for commodity price processes, this value of S seems much more realistic.

A trajectory of this setting is plotted in Fig. 4.2. For $\eta = 0.03$ and the Tahani model, both the delta and the risk-neutral probability of ending up in the money are unity and the call price is $C = 6.6929$ (see also Table 4.1). The call is more

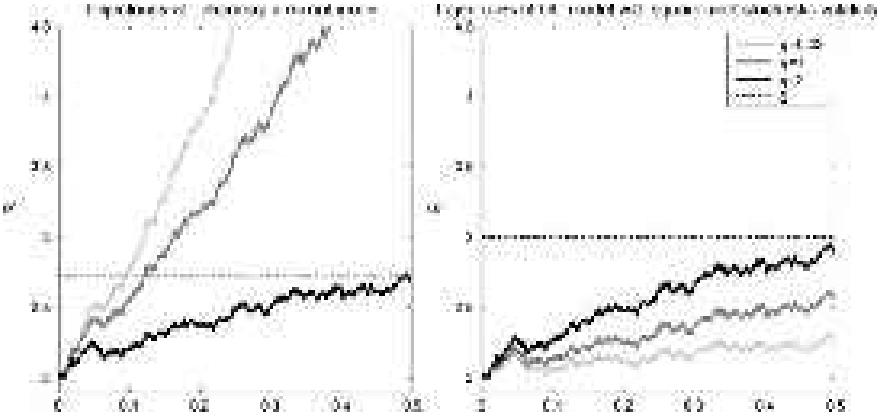

Fig. 4.2 Trajectories for Tahani and our OU processes with square-root stochastic volatility with increased parameter values

[4] This property is independent from the distribution of the underlying and known as linear homogeneity (Merton 1973)

Table 4.1 Tahani square-root call prices

	percentage terms $S = K = 0.02$ $\mu = 0.03$			absolute terms $S = K = 2$ $\mu = 3$		
η	C	Exercise prob.	$\overline{S}$	C	Exercise prob.	$\overline{S}$
0.01	0.00165	0.6232	20.09	6.81832	1.0000	$1.94 \cdot 10^{130}$
0.02	0.00192	0.6721	4.48	6.75523	1.0000	$1.39 \cdot 10^{65}$
0.03	0.00222	0.7172	2.72	6.69285	1.0000	$2.69 \cdot 10^{43}$
1	0.07310	1.0000	1.03	2.91608	1.0000	20.09
3	0.39265	1.0000	1.01	0.53406	0.9924	2.72

Table 4.2 Modified OU model call prices

	percentage terms $S = K = 0.02$			absolute terms $S = K = 2$		
η	C	Exercise prob.	$\overline{S}$	C	Exercise prob.	$\overline{S}$
0.01	0.00123	0.5351	0.03	0.12323	0.5351	3
0.02	0.00125	0.5409	0.03	0.12527	0.5409	3
0.03	0.00127	0.5465	0.03	0.12732	0.5465	3
1	0.00364	0.9102	0.03	0.36422	0.9102	3
3	0.00731	0.9987	0.03	0.73132	0.9987	3
3				0.53406	0.9924	2.72

than three times more expensive than the asset. Of course, this unrealistic result is due to the equilibrium level of the price process which is $\overline{S} = 2.69 \cdot 10^{43}$. We also implemented trajectories for more realistic adjustment speeds, i.e. $\eta \in \{1; 3\}$, where one can also see the inverse relationship of the mean reversion level and the adjustment speed for the model of Tahani. The dotted line in this figure displays the attractor $\overline{S} = \exp(1)$ which corresponds to $\eta = 3$.

In the right figure, which corresponds to our modified OU process as described in (4.3), we observe for all values of η an adjustment to the mean reversion level $\overline{S} = 3$. The call prices in this model increased by a factor of 100, as expected (see Table 4.2).

Hence, the claim of Tahani that even weak mean reversion has a strong impact on option prices is not correct. In our OU model, where the equilibrium level is independent from the adjustment speed, the influence of the drift term is marginal for small adjustment speeds. Due to the independence of the parameters, our model also fulfills the linear homogeneity condition of call prices in contrast to the Tahani model which fails.

Another interesting property of European in-the-money call prices written on mean reverting assets is reported by Longstaff and Schwartz (1995). When the long-term equilibrium level $\overline{S}$ is smaller than the actual price of the underlying, a European in-the-money call has a price which is smaller than its intrinsic value. This finding is plausible since the price of the underlying is expected to fall and therefore, the immediate exercise of the option would be optimal. For small values of the adjustment speed parameter, this case is unlikely to occur in the Tahani setting

since it is improbable that the real equilibrium level is smaller than the actual price of the underlying.

4.1.2 Solution for the Characteristic Function

Consider again the dynamics as described in (4.1). According to the general form of the FPDE, we set the corresponding process parameters of (4.1) in (3.36) and obtain

$$\frac{\partial \Phi}{\partial t} + \left(\eta\{\overline{X} - X_t\} - \frac{1}{2}V_t\right)\frac{\partial \Phi}{\partial X} + \kappa(\theta - V_t)\frac{\partial \Phi}{\partial V} + \frac{1}{2}V_t\frac{\partial^2 \Phi}{\partial X^2} + \frac{1}{2}\zeta^2 V_t\frac{\partial^2 \Phi}{\partial V^2} + \rho V_t \zeta \frac{\partial^2 \Phi}{\partial X\,\partial V} = 0\,. \tag{4.4}$$

We notice that the FPDE depends on terms with the state variables X_t and V_t and terms with constant parameters. Therefore, our exponential affine guess takes the form

$$\Phi(t, X_t, V_t) = \exp\{i\,\phi\,A(\tau)\,X_t + B(\tau)\,V_t + C(\tau)\}\,, \tag{4.5}$$

where $\tau = T - t$. The boundary conditions at maturity are $A(0) = 1$, $B(0) = 0$, $C(0) = 0$. Setting the partial derivatives in (4.4) and collecting the terms with X_t, V_t and constants, we obtain the following set of ODEs:

$$\begin{aligned}
\frac{\mathrm{d}A(\tau)}{\mathrm{d}\tau} &= -\eta A(\tau) \\
\frac{\mathrm{d}B(\tau)}{\mathrm{d}\tau} &= -\frac{1}{2}i\phi A(\tau) + \frac{1}{2}(i\phi)^2 A^2(\tau) - \kappa B(\tau) + \frac{1}{2}\zeta^2 B^2(\tau) + \rho\zeta i\phi A(\tau) B(\tau) \\
\frac{\mathrm{d}C(\tau)}{\mathrm{d}\tau} &= \eta\overline{X} i\phi A(\tau) + \kappa\theta B(\tau)
\end{aligned} \tag{4.6}$$

The solution of the first ODE is given by

$$A(\tau) = e^{-\eta\,\tau}\,,$$

leading us to a system of two ODEs with boundary conditions $B(0) = C(0) = 0$:

$$\begin{aligned}
\frac{\mathrm{d}B(\tau)}{\mathrm{d}\tau} &= -\frac{1}{2}i\phi e^{-\eta\tau} + \frac{1}{2}(i\phi)^2 e^{-2\eta\tau} - \kappa B(\tau) + \frac{1}{2}\zeta^2 B^2(\tau) + \rho\zeta i\phi e^{-\eta\tau} B(\tau) \\
\frac{\mathrm{d}C(\tau)}{\mathrm{d}\tau} &= \eta\overline{X} i\phi e^{-\eta\tau} + \kappa\theta B(\tau)
\end{aligned} \tag{4.7}$$

Tahani (2004) obtained a similar system of ODEs. However, the author only provided a very short derivation of the analytic solution based on Maple™ software. The

Maple™ solution for the Tahani square-root model is given in terms of Whittaker functions. Since the integration constants are not defined, the analytic solutions of Tahani are rather cumbersome to reproduce. We present a detailed derivation including integration constants which are determined by the boundary conditions. We further show that the structure of the solution, which is either in terms of Kummer or in terms of Bessel functions, depends crucially on the parameter values.

Firstly, we consider the ODE for $B(\tau)$ in (4.7) and make the standard substitution for Riccati equations. Substitute

$$G(\tau) = \exp\{-\int \frac{1}{2}\zeta^2 B(\tau)\mathrm{d}\tau\}$$

to transform the Riccati equation in a second order linear homogenous equation (Polyanin and Zaitsev 2003, p. 8)

$$\frac{\mathrm{d}^2 G(\tau)}{\mathrm{d}\tau^2} - \rho i\phi e^{-\eta\tau}\frac{\mathrm{d}G(\tau)}{\mathrm{d}\tau} + \kappa\frac{\mathrm{d}G(\tau)}{\mathrm{d}\tau} + \frac{1}{4}\zeta^2(i\phi)^2 e^{-2\eta\tau}G(\tau) - \frac{1}{4}\zeta^2 i\phi e^{-\eta\tau}G(\tau) = 0\,. \tag{4.8}$$

Repplinger (2008) ends up at a similar equation involving exponential functions of the time variable in an unspanned stochastic volatility framework following Collin-Dufresne and Goldstein (2002) and Heath et al. (1992). We make a similar substitution and change the time variable to $\upsilon = i\phi e^{-\eta\tau}$ to arrive at the following equation:

$$\upsilon\frac{\mathrm{d}^2 G(\upsilon)}{\mathrm{d}\upsilon^2} + \frac{\mathrm{d}G(\upsilon)}{\mathrm{d}\upsilon}\left[1 + \frac{\rho\zeta}{\eta}\upsilon - \frac{\kappa}{\eta}\right] + \frac{1}{4}\frac{\zeta^2}{\eta^2}G(\upsilon)[\upsilon - 1] = 0\,. \tag{4.9}$$

The solution of this second order linear homogenous (4.9) depends on the parameters ρ, κ and η. We begin with the most general case. Under the constraints that firstly, $\rho \neq \pm 1$ (i.e. the Brownian motions of the underlying and variance processes are not perfectly correlated) and secondly, the quotient κ/η is not a positive integer, the solution of the function $G(\upsilon)$ is given by[5]

$$G(\upsilon) = \exp\left\{\frac{\zeta}{2\eta}(\sqrt{\rho^2-1} - \rho)\,\upsilon\right\}\cdot\left[\mathcal{C}_1\cdot M\left(a, b, -\upsilon\cdot\frac{\zeta\sqrt{\rho^2-1}}{\eta}\right) + \mathcal{C}_2\cdot U\left(a, b, -\upsilon\cdot\frac{\zeta\sqrt{\rho^2-1}}{\eta}\right)\right], \tag{4.10}$$

[5] Solutions for second order linear homogenous equations of the general form $(a_2x + b_2)\frac{\mathrm{d}^2y}{\mathrm{d}x^2} + (a_1x + b_1)\frac{\mathrm{d}y}{\mathrm{d}x} + (a_0x + b_0)y = 0$ can be found in Polyanin and Zaitsev (2003), Table 15.

with

$$a = \frac{(1-\frac{\kappa}{\eta})(\sqrt{\rho^2-1}-\rho)-\frac{1}{2}\frac{\zeta}{\eta}}{2\sqrt{\rho^2-1}}$$
$$b = 1-\frac{\kappa}{\eta}$$

and $\mathcal{C}_1, \mathcal{C}_2$ being the integration constants which are determined by the boundary condition $B(0) = 0$. M and U are the Kummer functions of the first and second kind, respectively.

We make the inverse transformations to obtain the solutions for the functions B and C[6]:

$$B(\tau) = \frac{c(\tau)}{\zeta}\Bigg[\frac{\rho}{\sqrt{\rho^2-1}} - 1 + 2a \cdot \frac{\mathcal{C}\, b^{-1} M(1+a,1+b,c(\tau)\frac{\zeta}{\eta}) - U(1+a,1+b,c(\tau)\frac{\zeta}{\eta})}{\mathcal{C}M(a,b,c(\tau)\frac{\zeta}{\eta}) + U(a,b,c(\tau)\frac{\zeta}{\eta})}\Bigg] \tag{4.11}$$

$$C(\tau) = \big[c(\tau)-c(0)\big]\cdot\left[\frac{\overline{X}}{\sqrt{\rho^2-1}} + \frac{\kappa\theta}{\zeta\eta}\left(1-\frac{\rho}{\sqrt{\rho^2-1}}\right)\right] - \frac{2\kappa\theta}{\zeta^2}\ln\left[\frac{\mathcal{C}M(a,b,c(\tau)\frac{\zeta}{\eta}) + U(a,b,c(\tau)\frac{\zeta}{\eta})}{\mathcal{C}M(a,b,c(0)\frac{\zeta}{\eta}) + U(a,b,c(0)\frac{\zeta}{\eta})}\right], \tag{4.12}$$

with

$$\mathcal{C} = \frac{\mathcal{C}_1}{\mathcal{C}_2} = \frac{2aU\big(1+a,1+b,c(0)\frac{\zeta}{\eta}\big) + \left(1-\frac{\rho}{\sqrt{\rho^2-1}}\right)U\big(a,b,c(0)\frac{\zeta}{\eta}\big)}{\frac{2a}{b}M\big(1+a,1+b,c(0)\frac{\zeta}{\eta}\big) - \left(1-\frac{\rho}{\sqrt{\rho^2-1}}\right)M\big(a,b,c(0)\frac{\zeta}{\eta}\big)},$$
$$c(\tau) = -i\phi e^{-\eta\tau}\sqrt{\rho^2-1}\,.$$

Special Case 1

If $\rho \neq \pm 1$ and $(\kappa/\eta) \in \mathbb{N}$, the solution for $G(\upsilon)$ is given by (see case 2 in section "Case 2: κ/η is a Positive Integer" in the appendix)[7]:

[6] For a more detailed derivation, see case 1 in section "Solution for B and C in the Square-Root Stochastic Volatility Framework with Imperfectly Correlated Brownian Motions".

[7] Polyanin and Zaitsev (2003), p. 222.

$$G(\upsilon) = \exp\left\{\frac{\zeta}{2\eta}(\sqrt{\rho^2-1}-\rho)\upsilon\right\}\cdot\left(-\upsilon\frac{\zeta\sqrt{\rho^2-1}}{\eta}\right)^{1-b}$$
$$\cdot\left[\mathcal{C}_1^* M\left(a-b+1,2-b,-\upsilon\frac{\zeta\sqrt{\rho^2-1}}{\eta}\right)\right.$$
$$\left.+\mathcal{C}_2^* U\left(a-b+1,2-b,-\upsilon\frac{\zeta\sqrt{\rho^2-1}}{\eta}\right)\right].$$

After making the inverse transformations, one obtains the solutions for $B(\tau)$ and $C(\tau)$ as follows:

$$B(\tau) = \frac{c(\tau)}{\zeta}\left(\frac{\rho}{\sqrt{\rho^2-1}}-1\right)+\frac{2\kappa}{\zeta^2}+\frac{2c(\tau)(a-b+1)}{\zeta}$$
$$\cdot\frac{\mathcal{C}^*(2-b)^{-1}M(a-b+2,3-b,c(\tau)\frac{\zeta}{\eta})-U(a-b+2,3-b,c(\tau)\frac{\zeta}{\eta})}{\mathcal{C}^*M(a-b+1,2-b,c(\tau)\frac{\zeta}{\eta})+U(a-b+1,2-b,c(\tau)\frac{\zeta}{\eta})}, \tag{4.13}$$

$$C(\tau) = \left[c(\tau)-c(0)\right]\cdot\left\{\frac{\overline{X}}{\sqrt{\rho^2-1}}+\frac{\kappa\theta}{\zeta\eta}\left(1-\frac{\rho}{\sqrt{\rho^2-1}}\right)\right\}+\frac{2\kappa^2\theta\tau}{\zeta^2}$$
$$-\frac{2\kappa\theta}{\zeta^2}\ln\left[\frac{\mathcal{C}^*M(a-b+1,2-b,c(\tau)\frac{\zeta}{\eta})+U(a-b+1,2-b,c(\tau)\frac{\zeta}{\eta})}{\mathcal{C}^*M(a-b+1,2-b,c(0)\frac{\zeta}{\eta})+U(a-b+1,2-b,c(0)\frac{\zeta}{\eta})}\right], \tag{4.14}$$

with

$$\mathcal{C}^* = \frac{2(a-b+1)U(a-b+2,3-b,c(0)\frac{\zeta}{\eta})+d\cdot U(a-b+1,2-b,c(0)\frac{\zeta}{\eta})}{2\cdot\frac{a-b+1}{2-b}M(a-b+2,3-b,c(0)\frac{\zeta}{\eta})-d\cdot M(a-b+1,2-b,c(0)\frac{\zeta}{\eta})},$$
$$d = 1-\frac{\rho}{\sqrt{\rho^2-1}}-\frac{2\kappa}{\zeta c(0)}.$$

Special Case 2

Let us now consider the special case of assuming perfect correlation between the Brownian motions of the underlying and variance processes (i.e. $\rho = \pm 1$). We obtain the solution of (4.9) in terms of Bessel functions (see section "Solution for B and C in the Square-Root Stochastic Volatility Framework with Perfectly Correlated Brownian Motions" in the appendix). The solutions for the functions $G(\upsilon)$, $B(\tau)$ and $C(\tau)$ are[8]

[8] Polyanin and Zaitsev (2003), Table 15.

$$G(\upsilon) = \exp\left\{-\frac{\rho\,\zeta}{2\eta}\,\upsilon\right\}\,\upsilon^{\left(\frac{\kappa}{2\eta}\right)}\left[\widetilde{\mathcal{C}}_1 J_{\frac{\kappa}{\eta}}\left(\frac{\zeta}{\eta}\sqrt{\upsilon\left\{\frac{2\kappa\rho}{\zeta}-\frac{2\eta\rho}{\zeta}-1\right\}}\right)\right.$$
$$\left.+\,\widetilde{\mathcal{C}}_2 Y_{\frac{\kappa}{\eta}}\left(\frac{\zeta}{\eta}\sqrt{\upsilon\left\{\frac{2\kappa\rho}{\zeta}-\frac{2\eta\rho}{\zeta}-1\right\}}\right)\right],$$
$$B(\tau) = -\frac{\rho i\phi}{\zeta}\,e^{-\eta\tau}+\frac{\eta}{\zeta^2}\,g(\tau)\,\frac{\widetilde{\mathcal{C}}J_{\frac{\kappa}{\eta}-1}\big(g(\tau)\big)+Y_{\frac{\kappa}{\eta}-1}\big(g(\tau)\big)}{\widetilde{\mathcal{C}}J_{\frac{\kappa}{\eta}}\big(g(\tau)\big)+Y_{\frac{\kappa}{\eta}}\big(g(\tau)\big)}, \tag{4.15}$$

and

$$C(\tau) = \big(e^{-\eta\tau}-1\big)\left(\frac{\kappa\theta i\phi}{\eta\zeta}-\overline{X}i\phi\right)+\frac{\kappa^2\theta\tau}{\zeta^2}$$
$$-\,\frac{2\kappa\theta}{\zeta^2}\ln\left[\frac{\widetilde{\mathcal{C}}J_{\frac{\kappa}{\eta}}\big(g(\tau)\big)+Y_{\frac{\kappa}{\eta}}\big(g(\tau)\big)}{\widetilde{\mathcal{C}}J_{\frac{\kappa}{\eta}}\big(g(0)\big)+Y_{\frac{\kappa}{\eta}}\big(g(0)\big)}\right], \tag{4.16}$$

with

$$g(\tau) = \frac{\zeta}{\eta}\sqrt{i\phi\,e^{-\eta\tau}\left(\frac{2\rho}{\zeta}(\kappa-\eta)-1\right)}.$$

J and Y denote the Bessel functions of the first and second kind, respectively. The boundary condition $C(0) = 0$ determines the constant

$$\widetilde{\mathcal{C}} = \frac{\widetilde{\mathcal{C}}_1}{\widetilde{\mathcal{C}}_2} = \frac{\zeta\rho i\phi\,Y_{\frac{\kappa}{\eta}}\big(g(0)\big)-\eta\,g(0)\,Y_{\frac{\kappa}{\eta}-1}\big(g(0)\big)}{\eta\,g(0)\,J_{\frac{\kappa}{\eta}-1}\big(g(0)\big)-\zeta\rho i\phi\,J_{\frac{\kappa}{\eta}}\big(g(0)\big)}. \tag{4.17}$$

4.1.3 Comparison with the Monte-Carlo Solution

In this section, the accuracy of the analytic solution is tested by comparing it with the result of a Monte-Carlo (MC) simulation. We apply the solution of the characteristic function for the unmodified OU model with square-root stochastic volatility (4.1). The parameter values are set to $S = 80, \overline{S} = 85, \eta = 1, T-t = 0.5, \zeta = 0.2, \sqrt{V} = 0.2, \kappa = 1, \rho = -0.5, \theta = 0.05$, which corresponds to the special case 1 solution in the previous subsection ($\rho \neq \pm 1$ and $\kappa/\eta \in \mathbb{N}$).[9]

The MC simulation involves 1.5 million simulation paths, 375,000 of them are independent. Each path contains 2,500 time steps. A large number of paths accounts for a small confidence interval and a large number of time steps per path reduces the overall discretization error.

[9] With these parameter values, we try to provide a realistic model setup.

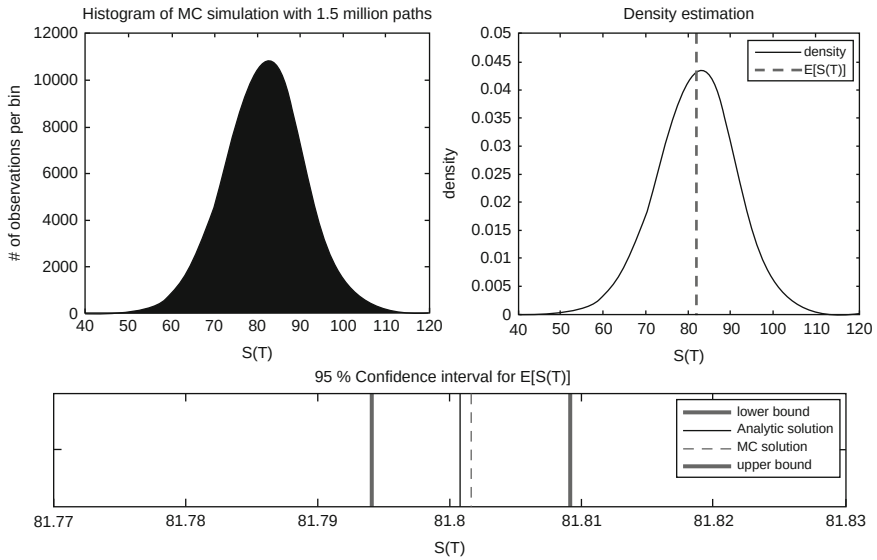

Fig. 4.3 Histogram, density function and confidence interval for the OU model with square-root stochastic volatility

Antithetic sampling as variance reduction technique has been applied.[10] Antithetic sampling makes use of the fact that for a given trajectory, its mirror image has equal probability. For the simulation of the process in (4.1), one set of random numbers $\tilde{z}_X$ is needed for the underlying process and another set $\tilde{z}_V$ for the subordinated process. While drawing one set of random numbers per Brownian motion, we get four simulation paths by using the corresponding mirror images according to $(+\tilde{z}_X, +\tilde{z}_V)$, $(+\tilde{z}_X, -\tilde{z}_V)$, $(-\tilde{z}_X, +\tilde{z}_V)$ and $(-\tilde{z}_X, -\tilde{z}_V)$.[11] The average of the four paths is used as individual sample. The advantage of antithetic sampling is a reduction of variance, and a correction of the first moment which is useful for the computation of futures prices.[12]

The results of the MC simulation are shown in Fig. 4.3. The histogram and the estimated density function of the spot price at time T are displayed.[13] The histogram

[10] The MC simulation setup with 1.5 million paths and 2,500 time steps per path is valid for all simulations in this thesis. However, antithetic sampling is only applied in the stochastic volatility framework, since the concept of mirror images is not applicable in the presence of asymmetric jumps.

[11] Of course, the random numbers are only pseudo-random. We applied the Matlab® pseudo-random number generator 'randn' for normally distributed random variables, which uses the ziggurat algorithm of Marsaglia and Tsang (2000) with a period of approximately 2^{64}.

[12] The correction of the first moment is mentioned in Jäckel (2002). More information about MC simulations in general and antithetic sampling in particular are given in Kloeden and Platen (1999) or Glasserman (2004).

[13] The density estimation is obtained with the Matlab® function ksdensity.

consists of 1,500 bins of equal length which are set in the interval of interest. The mean reversion in the drift term results in a distribution which is close to normal. The skewness of the distribution of S_T is -0.083 and the kurtosis is 3.173.[14]

In subfigure 3, the 95% confidence interval $[81.7941, 81.8090]$ for the spot price at time T includes the analytic solution

$$F = \exp\{e^{-\eta(T-t)}\, X_t + B(\tau)\, V_t + C(\tau)\} = 81.8008\,,$$

where $B(\tau)$ and $C(\tau)$ are given by (4.11) and (4.12) with $\phi = -i$. The analytic solution matches very well the MC Solution where $\mathbb{E}[S_T] = 81.8016$.

4.2 Ornstein–Uhlenbeck Stochastic Volatility

The system of SDEs is similar to the previous section, the only difference is included in the subordinated process. The OU process for the log-underlying remains unchanged, but volatility is also modeled as an Ornstein–Uhlenbeck process. Therefore, the process dynamics are the following:

$$\begin{aligned} dX_t &= (\eta\{\overline{X} - X_t\} - \frac{1}{2}\sigma_t^2)\, dt + \sigma_t\, dW_t^X \\ d\sigma_t &= \kappa(\theta - \sigma_t)dt + \zeta\, dW_t^\sigma \end{aligned} \tag{4.18}$$

Stein and Stein (1991) assumed an OU stochastic volatility process under the constraint that the two Brownian motions dW_t^X and dW_t^σ are uncorrelated. Schöbel and Zhu (1999) extend their proposal and allow for constant correlation. Tahani (2004) applies their model on mean-reverting assets (see also Sect. 4.2.1).

Schöbel and Zhu examine the behavior of OU-stochastic volatilities and point out that there exists no barrier (neither reflecting nor absorbing) for the volatility σ.[15] Volatility enters in the model not only as variance σ^2, but also as linear term. Consequently, the probability for negative volatilities is non-zero (though very small) and cannot be seen as being reflected at $\sigma = 0$.[16]

---

[14] Note that the skewness of the distribution of the log-price X_T is -0.477 and the kurtosis is 3.597. Hence, due to stochastic volatility, the price S_T is no longer lognormally distributed which would be the case if the log-price process is determined by the somewhat simpler constant volatility model 1 in Schwartz (1997) which is given by $dX_t = \eta(\overline{X} - X_t)dt + \sqrt{V_t}dW_t^X$. This simple process specification leads to a normal distribution of X_T with parameters $\mathbb{E}[X_T] = e^{-\eta\tau}X_t + (1-e^{-\eta\tau})\overline{X}$ and $var(X_T) = \frac{V_t}{2\eta}(1 - e^{-2\eta\tau})$.

[15] Schöbel and Zhu (1999) point out that the volatility σ_T conditional on an initial value σ_t is normally distributed. The parameters of the distribution are the mean $a = \theta + (\sigma_t - \theta)e^{-\kappa(T-t)}$ and the variance $b^2 = \frac{\zeta^2}{2\kappa}(1 - e^{-2\kappa(T-t)})$. The probability for negative volatilities σ_T is then given by $N(-a/b)$.

[16] Only for $\theta = 0$, the same results are obtained for positive and negative volatilities and the model can therefore be treated as if volatility is reflected at $\sigma = 0$ (Schöbel and Zhu 1999).

The possibility of negative volatilities can be seen as a drawback of the OU-stochastic volatility model. However, the probabilities for such an event are marginal when κ and θ are large enough and ζ is relatively small. For example, if $\kappa \geq 2, \theta \geq 0.2$ and $\zeta \leq 0.1$, the probability will be smaller or equal $8.48 \cdot 10^{-6}$, when the other parameters are set to $T - t = 0.5, \sigma = 0.2$. Of course, the squared volatility always remains positive.

An advantage of OU stochastic volatility compared with a subordinated CIR stochastic volatility process could be that this richer model setup is able to perform better when fitting the model at an observed volatility smile.

4.2.1 Comparison with the Tahani OU Model

The Ornstein–Uhlenbeck mean-reverting model of Tahani (2004) shows the same difficulties as in the previous section, since the shortcoming was due to the underlying and not due to the subordinated process. As in the previous section, the results of Tahani can be recovered by changing the process of the log-underlying to (4.3) and setting $\overline{S} = \exp(\mu/\eta)$.

4.2.2 Solution for the Characteristic Function

By setting the drift and volatility parameters in (3.36), we obtain the following FPDE:

$$\begin{aligned} &\frac{\partial \Phi}{\partial t} + \left(\eta\{\overline{X} - X_t\} - \frac{1}{2}\sigma_t^2\right)\frac{\partial \Phi}{\partial X} + \kappa(\theta - \sigma_t)\frac{\partial \Phi}{\partial \sigma} \\ &\quad + \frac{1}{2}\sigma_t^2\frac{\partial^2 \Phi}{\partial X^2} + \frac{1}{2}\zeta^2\frac{\partial^2 \Phi}{\partial \sigma^2} + \rho\sigma_t\zeta\frac{\partial^2 \Phi}{\partial X\,\partial \sigma} = 0 \end{aligned} \tag{4.19}$$

This FPDE consists of terms with X_t, terms containing volatility σ_t, terms with squared volatility σ_t^2 and terms with constant parameters. Hence, the guess for Φ is exponential linear-quadratic in σ_t and takes the form

$$\Phi(t, X_t, \sigma_t) = \exp\{i\,\phi\,A(\tau)\,X_t + B(\tau)\,\sigma_t^2 + C(\tau)\,\sigma_t + D(\tau)\}\,,$$

with boundary conditions $A(0) = 1$, $B(0) = C(0) = D(0) = 0$.

Again, we set the partial derivatives of the characteristic function in the FPDE (4.19) to obtain a system of ODEs as follows.

$$\begin{aligned} \frac{\mathrm{d}B(\tau)}{\mathrm{d}\tau} &= -\frac{1}{2}i\phi e^{-\eta\tau} + \frac{1}{2}(i\phi)^2 e^{-2\eta\tau} - 2\kappa B(\tau) + 2\zeta^2 B^2(\tau) + 2\rho\zeta i\phi e^{-\eta\tau} B(\tau) \\ \frac{\mathrm{d}C(\tau)}{\mathrm{d}\tau} &= 2\zeta^2 B(\tau)C(\tau) + 2\kappa\theta B(\tau) - \kappa C(\tau) + \rho\zeta i\phi e^{-\eta\tau} C(\tau) \end{aligned}$$

$$\frac{\mathrm{d}D(\tau)}{\mathrm{d}\tau} = \eta\overline{X}i\phi e^{-\eta\tau} + \kappa\theta C(\tau) + \zeta^2 B(\tau) + \frac{1}{2}\zeta^2 C^2(\tau)\,, \tag{4.20}$$

with $A(\tau) = e^{-\eta\tau}$ as in the square-root case (Sect. 4.1.2).

Consider the first equation in (4.20). The structure is almost identical to the first equation of the ODE system (4.7) in the square-root model. Therefore, we make the same substitutions (4.8) and (4.9) as in the previous section and obtain the following second order linear homogenous equation:

$$\upsilon\frac{\partial^2 G(\upsilon)}{\partial\upsilon^2} + \left[1 + \frac{2\rho\zeta}{\eta}\upsilon - \frac{2\kappa}{\eta}\right]\frac{\partial G(\upsilon)}{\partial\upsilon} + \frac{\zeta^2}{\eta^2}\big[\upsilon - 1\big]G(\upsilon) = 0\,. \tag{4.21}$$

Not surprisingly, the solution of (4.21) is given in terms of Kummer functions if we assume imperfect correlation of the Brownian motions or in terms of Bessel functions if we set $\rho = \pm 1$. Since the derivation of the solution for $B(\tau)$ is almost identical to the previous section, we want to refer the reader to the corresponding sections "Solution for B and C in the Square-Root Stochastic Volatility Framework with Imperfectly Correlated Brownian Motions" and "Solution for B and C in the Square-Root Stochastic Volatility Framework with Perfectly Correlated Brownian Motions" of the square-root stochastic volatility model for a more detailed derivation of the solutions.

General Case: $\rho \neq \pm 1$ and $(2\kappa/\eta) \notin \mathbb{N}$

Under the constraints that the Brownian motions W_t^X and W_t^σ are imperfectly correlated and the quotient $(2\kappa/\eta)$ is not a positive integer, the solution for $B(\tau)$ according to case 1 of section "Solution for B and C in the Square-Root Stochastic Volatility Framework with Imperfectly Correlated Brownian Motions" in the appendix is

$$B(\tau) = \frac{c(\tau)}{\zeta}\Bigg[\frac{\rho}{2\sqrt{\rho^2-1}} - \frac{1}{2} + a^* \cdot \frac{\mathcal{K}(b^*)^{-1}M\big(1+a^*, 1+b^*, 2c(\tau)\frac{\zeta}{\eta}\big) - U\big(1+a^*, 1+b^*, 2c(\tau)\frac{\zeta}{\eta}\big)}{\mathcal{K}M\big(a^*, b^*, 2c(\tau)\frac{\zeta}{\eta}\big) + U\big(a^*, b^*, 2c(\tau)\frac{\zeta}{\eta}\big)}\Bigg], \tag{4.22}$$

where

$$a^* = \frac{\big(1-\frac{2\kappa}{\eta}\big)\big(\sqrt{\rho^2-1}-\rho\big) - \frac{\zeta}{\eta}}{2\sqrt{\rho^2-1}}\,,$$

$$b^* = 1 - \frac{2\kappa}{\eta}\,,$$

$$\mathcal{K} = \frac{a^* U\left(1+a^*, 1+b^*, 2c(0)\frac{\zeta}{\eta}\right) + \frac{1}{2}\left(1 - \frac{\rho}{\sqrt{\rho^2-1}}\right) U\left(a^*, b^*, 2c(0)\frac{\zeta}{\eta}\right)}{\frac{a^*}{b^*} M\left(1+a^*, 1+b^*, 2c(0)\frac{\zeta}{\eta}\right) - \frac{1}{2}\left(1 - \frac{\rho}{\sqrt{\rho^2-1}}\right) M\left(a^*, b^*, 2c(0)\frac{\zeta}{\eta}\right)}.$$

Plug the result (4.22) in the ODE for $C(\tau)$ (see (4.20)) to arrive at the following ODE

$$\frac{\mathrm{d}C(\tau)}{\mathrm{d}\tau} = \left[\zeta\sqrt{\rho^2-1} i\phi e^{-\eta\tau} - \frac{\mathcal{K}M'\left(a^*, b^*, 2c(\tau)\frac{\zeta}{\eta}\right) + U'\left(a^*, b^*, 2c(\tau)\frac{\zeta}{\eta}\right)}{\mathcal{K}M\left(a^*, b^*, 2c(\tau)\frac{\zeta}{\eta}\right) + U\left(a^*, b^*, 2c(\tau)\frac{\zeta}{\eta}\right)} - \kappa\right]$$

$$\times C(\tau) + 2\kappa\theta B(\tau),$$

which takes therefore the form

$$\frac{\mathrm{d}C(\tau)}{\mathrm{d}\tau} = f_1(\tau)C(\tau) + f_0(\tau).$$

The solution of this linear ODE is

$$C(\tau) = \mathcal{D}\, e^{\int f_1(\tau)\mathrm{d}\tau} + e^{\int f_1(\tau)\mathrm{d}\tau} \int e^{-\int f_1(\tau)\mathrm{d}\tau} f_0(\tau)\mathrm{d}\tau, \tag{4.23}$$

where $\mathcal{D}$ is determined by the boundary condition $C(0) = 0$. The inner integral is given by

$$\int f_1(\tau)\mathrm{d}\tau = -\frac{\zeta}{\eta}\sqrt{\rho^2-1}\; i\phi\, e^{-\eta\tau}$$

$$- \ln\left[\mathcal{K}M\left(a^*, b^*, 2c(\tau)\frac{\zeta}{\eta}\right) + U\left(a^*, b^*, 2c(\tau)\frac{\zeta}{\eta}\right)\right] - \kappa\tau,$$

but the outer integral in (4.23) cannot be expressed in closed form. Therefore, we are also not able to provide an analytic solution for the function $D(\tau)$. Nevertheless, the characteristic function can be computed numerically with numerical integration methods which are specified in Sect. 3.6.

Special Case 1: $\rho \neq \pm 1$ and $(2\kappa/\eta) \in \mathbb{N}$

Now consider the special case of assuming imperfect correlation of the Brownian motions, but the quotient $(2\kappa/\eta)$ is a positive integer. The solution for $B(\tau)$ according to case 2 of section "Solution for B and C in the Square-Root Stochastic Volatility Framework with Imperfectly Correlated Brownian Motions" in the appendix is

$$B(\tau) = \frac{c(\tau)}{\zeta}\left(\frac{\rho}{2\sqrt{\rho^2-1}} - \frac{1}{2}\right) + \frac{\kappa}{\zeta^2} + \frac{c(\tau)(a^* - b^* + 1)}{\zeta}$$
$$\cdot \frac{\frac{\mathcal{K}^*}{2-b^*} M\left(a^* - b^* + 2, 3 - b^*, 2c(\tau)\frac{\zeta}{\eta}\right) - U\left(a^* - b^* + 2, 3 - b^*, 2c(\tau)\frac{\zeta}{\eta}\right)}{\mathcal{K}^* M\left(a^* - b^* + 1, 2 - b^*, 2c(\tau)\frac{\zeta}{\eta}\right) + U\left(a^* - b^* + 1, 2 - b^*, 2c(\tau)\frac{\zeta}{\eta}\right)}, \tag{4.24}$$

with the constants

$$\mathcal{K}^* = \frac{(a^* - b^* + 1)U\left(a^* - b^* + 2, 3 - b^*, 2c(0)\frac{\zeta}{\eta}\right) + d^* U\left(a^* - b^* + 1, 2 - b^*, 2c(0)\frac{\zeta}{\eta}\right)}{\frac{a^* - b^* + 1}{2 - b^*} M\left(a^* - b^* + 2, 3 - b^*, 2c(0)\frac{\zeta}{\eta}\right) - d^* M\left(a^* - b^* + 1, 2 - b^*, 2c(0)\frac{\zeta}{\eta}\right)},$$

$$d^* = \frac{1}{2} - \frac{\rho}{2\sqrt{\rho^2-1}} - \frac{\kappa}{\zeta c(0)}.$$

Apply the solution for $B(\tau)$ in the ODE for $C(\tau)$ to obtain

$$\frac{\mathrm{d}C(\tau)}{\mathrm{d}\tau} = 2\kappa\theta B(\tau) + \left[\zeta\sqrt{\rho^2-1} i\phi e^{-\eta\tau} + \kappa\right.$$
$$\left. - \frac{\mathcal{K}^* M'\left(a^* - b^* + 1, 2 - b^*, 2c(\tau)\frac{\zeta}{\eta}\right) + U'\left(a^* - b^* + 1, 2 - b^*, 2c(\tau)\frac{\zeta}{\eta}\right)}{\mathcal{K}^* M\left(a^* - b^* + 1, 2 - b^*, 2c(\tau)\frac{\zeta}{\eta}\right) + U\left(a^* - b^* + 1, 2 - b^*, 2c(\tau)\frac{\zeta}{\eta}\right)}\right] C(\tau),$$

which is of the same form (4.23) as in the general case.

Special Case 2: $\rho = \pm 1$

If we assume perfect correlation, the solution for $B(\tau)$ is given in terms of Bessel functions according to section "Solution for B and C in the Square-Root Stochastic Volatility Framework with Perfectly Correlated Brownian Motions" in the appendix.

$$B(\tau) = -\frac{\rho i\phi}{2\zeta} e^{-\eta\tau} + \frac{h(\tau)}{4\zeta^2} \frac{\widetilde{\mathcal{K}} J_{\frac{2\kappa}{\eta}-1}\left(h(\tau)\right) + Y_{\frac{2\kappa}{\eta}-1}\left(h(\tau)\right)}{\widetilde{\mathcal{K}} J_{\frac{2\kappa}{\eta}}\left(h(\tau)\right) + Y_{\frac{2\kappa}{\eta}}\left(h(\tau)\right)}, \tag{4.25}$$

where

$$h(\tau) = \frac{2\zeta}{\eta}\sqrt{i\phi e^{-\eta\tau}\left(\frac{2\kappa\rho}{\zeta} - \frac{\eta\rho}{\zeta} - 1\right)},$$

$$\widetilde{\mathcal{K}} = \frac{2\rho\zeta i\phi Y_{\frac{2\kappa}{\eta}}\left(h(0)\right) - h(0) Y_{\frac{2\kappa}{\eta}-1}\left(h(0)\right)}{h(0) J_{\frac{2\kappa}{\eta}-1}\left(h(0)\right) - 2\rho\zeta i\phi J_{\frac{2\kappa}{\eta}}\left(h(0)\right)}.$$

Plug the result for $B(\tau)$ in the ODE for $C(\tau)$. In this special case, we obtain a somewhat simpler expression

$$\frac{\mathrm{d}C(\tau)}{\mathrm{d}\tau} = -\frac{\widetilde{\mathcal{K}} J'_{\frac{2\kappa}{\eta}}\big(h(\tau)\big) + Y'_{\frac{2\kappa}{\eta}}\big(h(\tau)\big)}{\widetilde{\mathcal{K}} J_{\frac{2\kappa}{\eta}}\big(h(\tau)\big) + Y_{\frac{2\kappa}{\eta}}\big(h(\tau)\big)} C(\tau) + 2\kappa\theta B(\tau)\,.$$

The solution for this ODE is given by

$$C(\tau) = \frac{\int \big[\widetilde{\mathcal{K}} J_{\frac{2\kappa}{\eta}}\big(h(\tau)\big) + Y_{\frac{2\kappa}{\eta}}\big(h(\tau)\big)\big] 2\kappa\theta B(\tau)\,\mathrm{d}\tau + \mathcal{D}}{\widetilde{\mathcal{K}} J_{\frac{2\kappa}{\eta}}\big(h(\tau)\big) + Y_{\frac{2\kappa}{\eta}}\big(h(\tau)\big)}\,.$$

Again, the remaining integral cannot be solved and we are forced to apply numerical methods to compute the characteristic function.

4.2.3 Comparison with the Monte-Carlo Solution

As in the previous section, we test our Runge-Kutta solution (see Sect. 3.6) by performing a MC simulation with 1.5 million simulation paths from which 375,000 are independent due to antithetic sampling. Each path consists of 2,500 time steps. Contrary to square-root stochastic volatility, we embedded no boundary for the volatility σ within the simulation. The parameter values are $S = 80, \overline{S} = 85, \eta = 1, T - t = 0.5, \zeta = 0.1, \sigma = 0.2, \kappa = 2, \rho = -0.5, \theta = 0.22$. The probability for negative volatilities is therefore $2.40 \cdot 10^{-6}$.

The histogram, the estimated density function of the distribution of S_T and the 95% confidence interval for the futures price are displayed in Fig. 4.4. The Runge-Kutta solution $F = 81.7946$ lies within the confidence interval $[81.7874; 81.8028]$ of the MC simulation and matches very well the numerical solution of the MC simulation where $\mathbb{E}[S_T] = 81.7951$.

The adjustment speed κ of the volatility process has been raised to 2 to reduce the probability of negative volatilities. Due to this increased adjustment speed, very large volatilities also become less likely. Hence, the distribution is even closer to normal than in Sect. 4.1.3. The skewness is -0.010 and the kurtosis is 3.090.

Appendix

Solution for B and C in the Square-Root Stochastic Volatility Framework with Imperfectly Correlated Brownian Motions

Case 1: κ/η is an Arbitrary Noninteger

Consider the general case where $\rho \neq \pm 1$ and $(\kappa/\eta) \notin \mathbb{N}$. We get the solution for $G(\upsilon)$ after the transformations

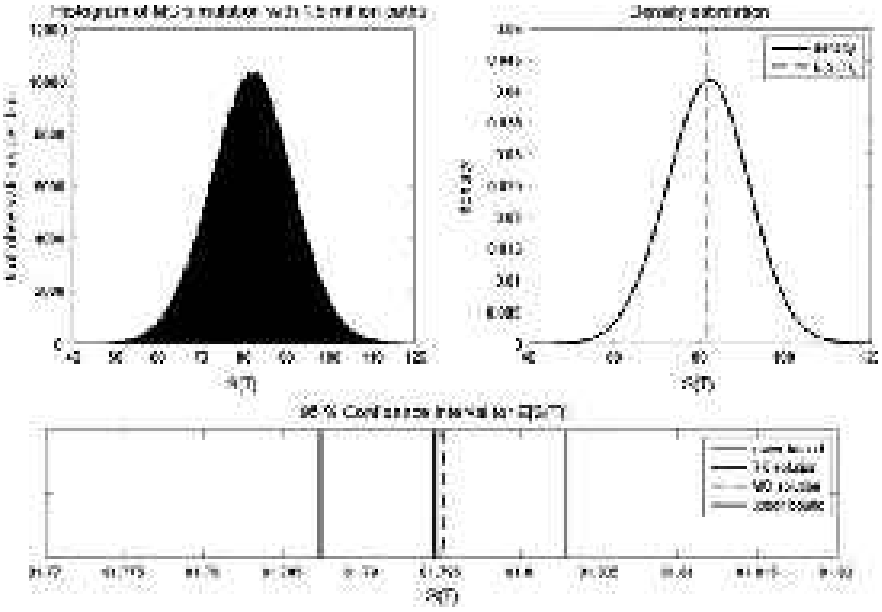

Fig. 4.4 Histogram, density function and confidence interval for the OU model with OU stochastic volatility

$$G(\tau) = \exp\{-\int \frac{1}{2}\zeta^2 B(\tau)\mathrm{d}\tau\}$$

and

$$\upsilon = i\phi e^{-\eta\tau}: \quad G(\upsilon) = \exp\left\{\frac{\zeta}{2\eta}(\sqrt{\rho^2-1}-\rho)\,\upsilon\right\}$$
$$\cdot\left[\mathcal{C}_1 \cdot M\left(a, b, -\upsilon\cdot\frac{\zeta\sqrt{\rho^2-1}}{\eta}\right) + \mathcal{C}_2 \cdot U\left(a, b, -\upsilon\cdot\frac{\zeta\sqrt{\rho^2-1}}{\eta}\right)\right],$$

with

$$a = \frac{(1-\frac{\kappa}{\eta})(\sqrt{\rho^2-1}-\rho) - \frac{1}{2}\frac{\zeta}{\eta}}{2\sqrt{\rho^2-1}}$$
$$b = 1 - \frac{\kappa}{\eta}$$

(see (4.10)).

$B(\tau)$ is recovered by the inverse relationship

$$B(\tau) = -\frac{2G'(\tau)}{\zeta^2 G(\tau)},$$

and we have

$$B(\tau) = -\frac{2}{\zeta^2}\left(\frac{\zeta c(\tau)}{2} + \frac{\zeta}{2} i\phi\rho e^{-\eta\tau} - \eta\frac{\mathcal{C}M'(a,b,c(\tau)\frac{\zeta}{\eta}) + U'(a,b,c(\tau)\frac{\zeta}{\eta})}{\mathcal{C}M(a,b,c(\tau)\frac{\zeta}{\eta}) + U(a,b,c(\tau)\frac{\zeta}{\eta})}\right)$$
$$= \frac{c(\tau)}{\zeta}\left(\frac{\rho}{\sqrt{\rho^2-1}} - 1\right) + \frac{2\eta}{\zeta^2}\frac{\mathcal{C}M'(a,b,c(\tau)\frac{\zeta}{\eta}) + U'(a,b,c(\tau)\frac{\zeta}{\eta})}{\mathcal{C}M(a,b,c(\tau)\frac{\zeta}{\eta}) + U(a,b,c(\tau)\frac{\zeta}{\eta})}, \tag{4.26}$$

with

$$c(\tau) = -i\phi e^{-\eta\tau}\sqrt{\rho^2-1}$$

and

$$\mathcal{C} = \frac{\mathcal{C}_1}{\mathcal{C}_2}.$$

The recurrence relations for the two Kummer functions are[17]

$$M'\left(a,b,c(\tau)\frac{\zeta}{\eta}\right) = \frac{a}{b}M\left(1+a,1+b,c(\tau)\frac{\zeta}{\eta}\right)\cdot\frac{\partial c(\tau)\frac{\zeta}{\eta}}{\partial\tau}$$
$$U'\left(a,b,c(\tau)\frac{\zeta}{\eta}\right) = -aU\left(1+a,1+b,c(\tau)\frac{\zeta}{\eta}\right)\cdot\frac{\partial c(\tau)\frac{\zeta}{\eta}}{\partial\tau}, \tag{4.27}$$

and we get

$$B(\tau) = \frac{c(\tau)}{\zeta}\left[\frac{\rho}{\sqrt{\rho^2-1}} - 1 \right.$$
$$\left. +2a\cdot\frac{\mathcal{C}b^{-1}M(1+a,1+b,c(\tau)\frac{\zeta}{\eta}) - U(1+a,1+b,c(\tau)\frac{\zeta}{\eta})}{\mathcal{C}M(a,b,c(\tau)\frac{\zeta}{\eta}) + U(a,b,c(\tau)\frac{\zeta}{\eta})}\right]. \tag{4.28}$$

Apply the boundary condition $B(0) = 0$ to solve for the constant

$$\mathcal{C} = \frac{2aU\left(1+a,1+b,c(0)\frac{\zeta}{\eta}\right) + \left(1-\frac{\rho}{\sqrt{\rho^2-1}}\right)U\left(a,b,c(0)\frac{\zeta}{\eta}\right)}{\frac{2a}{b}M\left(1+a,1+b,c(0)\frac{\zeta}{\eta}\right) - \left(1-\frac{\rho}{\sqrt{\rho^2-1}}\right)M\left(a,b,c(0)\frac{\zeta}{\eta}\right)}.$$

[17] Abramowitz and Stegun (1970), p. 507.

Going back to the ODE for $C(\tau)$ (see (4.7)), we obtain

$$\frac{\mathrm{d}C(\tau)}{\mathrm{d}\tau} = \eta\overline{X}i\phi e^{-\eta\tau} + \frac{\kappa\theta i\phi}{\zeta}e^{-\eta\tau}(\sqrt{\rho^2-1}-\rho) - \frac{2\kappa\theta}{\zeta^2}\frac{\mathcal{C}M'(a,b,c(\tau)\frac{\zeta}{\eta}) + U'(a,b,c(\tau)\frac{\zeta}{\eta})}{\mathcal{C}M(a,b,c(\tau)\frac{\zeta}{\eta}) + U(a,b,c(\tau)\frac{\zeta}{\eta})}. \tag{4.29}$$

The solution for this ODE is straightforward:

$$C(\tau) = \frac{c(\tau)\overline{X}}{\sqrt{\rho^2-1}} + \frac{\kappa\theta c(\tau)}{\zeta\eta}\left(1-\frac{\rho}{\sqrt{\rho^2-1}}\right) - \frac{2\kappa\theta}{\zeta^2}\ln\left[\mathcal{C}M\left(a,b,c(\tau)\frac{\zeta}{\eta}\right) + U\left(a,b,c(\tau)\frac{\zeta}{\eta}\right)\right] + \mathcal{D}, \tag{4.30}$$

where the integration constant $\mathcal{D}$ is determined by the boundary condition. Setting $C(0) = 0$, we obtain

$$\mathcal{D} = \frac{2\kappa\theta}{\zeta^2}\ln\left[\mathcal{C}M\left(a,b,c(0)\frac{\zeta}{\eta}\right) + U\left(a,b,c(0)\frac{\zeta}{\eta}\right)\right] - \frac{c(0)\overline{X}}{\sqrt{\rho^2-1}} - \frac{\kappa\theta c(0)}{\zeta\eta}\left(1-\frac{\rho}{\sqrt{\rho^2-1}}\right).$$

Plugging the solution for $\mathcal{D}$ in (4.30) and simplifying leads to

$$C(\tau) = \left[c(\tau)-c(0)\right]\cdot\left[\frac{\overline{X}}{\sqrt{\rho^2-1}} + \frac{\kappa\theta}{\zeta\eta}\left(1-\frac{\rho}{\sqrt{\rho^2-1}}\right)\right] - \frac{2\kappa\theta}{\zeta^2}\ln\left[\frac{\mathcal{C}M(a,b,c(\tau)\frac{\zeta}{\eta}) + U(a,b,c(\tau)\frac{\zeta}{\eta})}{\mathcal{C}M(a,b,c(0)\frac{\zeta}{\eta}) + U(a,b,c(0)\frac{\zeta}{\eta})}\right]. \tag{4.31}$$

Case 2: κ/η is a Positive Integer

Under the constraints that $\rho \neq \pm 1$ and $(\kappa/\eta) \in \mathbb{N}$, the solution after the two substitutions (4.8) and (4.9) is[18]:

$$G(\upsilon) = \exp\left\{\frac{\zeta}{2\eta}(\sqrt{\rho^2-1}-\rho)\upsilon\right\}\cdot\left(-\upsilon\frac{\zeta\sqrt{\rho^2-1}}{\eta}\right)^{1-b}$$

[18] Polyanin and Zaitsev (2003), p. 222.

$$\cdot\left[\mathcal{C}_1^* M\left(a-b+1,2-b,-\upsilon\frac{\zeta\sqrt{\rho^2-1}}{\eta}\right)\right.$$
$$\left.+\,\mathcal{C}_2^* U\left(a-b+1,2-b,-\upsilon\frac{\zeta\sqrt{\rho^2-1}}{\eta}\right)\right].$$

Hence, $B(\tau)$ is given by

$$B(\tau)=\frac{c(\tau)}{\zeta}\left(\frac{\rho}{\sqrt{\rho^2-1}}-1\right)+\frac{2(1-b)\eta}{\zeta^2}$$
$$+\frac{2}{\zeta^2}\frac{\mathcal{C}^* M'\left(a-b+1,2-b,c(\tau)\frac{\zeta}{\eta}\right)+U'\left(a-b+1,2-b,c(\tau)\frac{\zeta}{\eta}\right)}{\mathcal{C}^* M\left(a-b+1,2-b,c(\tau)\frac{\zeta}{\eta}\right)+U\left(a-b+1,2-b,c(\tau)\frac{\zeta}{\eta}\right)}.$$

Again, we apply the recurrence relations for Kummer functions in (4.27) and obtain

$$B(\tau)=\frac{c(\tau)}{\zeta}\left(\frac{\rho}{\sqrt{\rho^2-1}}-1\right)+\frac{2\kappa}{\zeta^2}+\frac{2c(\tau)(a-b+1)}{\zeta}$$
$$\cdot\frac{\mathcal{C}^*(2-b)^{-1}M\left(a-b+2,3-b,c(\tau)\frac{\zeta}{\eta}\right)-U\left(a-b+2,3-b,c(\tau)\frac{\zeta}{\eta}\right)}{\mathcal{C}^* M\left(a-b+1,2-b,c(\tau)\frac{\zeta}{\eta}\right)+U\left(a-b+1,2-b,c(\tau)\frac{\zeta}{\eta}\right)},\tag{4.32}$$

with

$$\mathcal{C}^*=\frac{\mathcal{C}_1^*}{\mathcal{C}_2^*}$$
$$=\frac{2(a-b+1)U\left(a-b+2,3-b,c(0)\frac{\zeta}{\eta}\right)+d\cdot U\left(a-b+1,2-b,c(0)\frac{\zeta}{\eta}\right)}{2\cdot\frac{a-b+1}{2-b}M\left(a-b+2,3-b,c(0)\frac{\zeta}{\eta}\right)-d\cdot M\left(a-b+1,2-b,c(0)\frac{\zeta}{\eta}\right)},$$
$$d=1-\frac{\rho}{\sqrt{\rho^2-1}}-\frac{2\kappa}{\zeta c(0)}.$$

We set the solution for $B(\tau)$ in (4.7) and get the following ODE for $C(\tau)$:

$$\frac{\mathrm{d}C(\tau)}{\mathrm{d}\tau}=\eta\overline{X}i\phi e^{-\eta\tau}+\frac{\kappa\theta i\phi}{\zeta}e^{-\eta\tau}(\sqrt{\rho^2-1}-\rho)+\frac{2\kappa^2\theta}{\zeta^2}$$
$$-\frac{2\kappa\theta}{\zeta^2}\frac{\mathcal{C}^* M'(a-b+1,2-b,c(\tau)\frac{\zeta}{\eta})+U'(a-b+1,2-b,c(\tau)\frac{\zeta}{\eta})}{\mathcal{C}^* M(a-b+1,2-b,c(\tau)\frac{\zeta}{\eta})+U(a-b+1,2-b,c(\tau)\frac{\zeta}{\eta})}.$$

(4.33)

The solution of this ODE under consideration of the boundary condition $C(0) = 0$ is

$$C(\tau) = \big[c(\tau) - c(0)\big] \cdot \left\{ \frac{\overline{X}}{\sqrt{\rho^2 - 1}} + \frac{\kappa\theta}{\zeta\eta}\left(1 - \frac{\rho}{\sqrt{\rho^2 - 1}}\right)\right\} + \frac{2\kappa^2\theta\tau}{\zeta^2} - \frac{2\kappa\theta}{\zeta^2} \ln\left[\frac{\mathcal{C}^* M(a-b+1, 2-b, c(\tau)\frac{\zeta}{\eta}) + U(a-b+1, 2-b, c(\tau)\frac{\zeta}{\eta})}{\mathcal{C}^* M(a-b+1, 2-b, c(0)\frac{\zeta}{\eta}) + U(a-b+1, 2-b, c(0)\frac{\zeta}{\eta})}\right]. \tag{4.34}$$

Solution for B and C in the Square-Root Stochastic Volatility Framework with Perfectly Correlated Brownian Motions

If we have perfectly correlated Brownian motions of the underlying and variance processes (i.e. $\rho = \pm 1$), the solution of (4.9) is given in terms of Bessel functions.[19]

$$G(\upsilon) = \exp\left\{-\frac{\rho\,\zeta}{2\eta}\,\upsilon\right\}\, \upsilon^{\left(\frac{\kappa}{2\eta}\right)} \left[\widetilde{\mathcal{C}}_1 J_{\frac{\kappa}{\eta}}\left(\frac{\zeta}{\eta}\sqrt{\upsilon\left\{\frac{2\kappa\rho}{\zeta} - \frac{2\eta\rho}{\zeta} - 1\right\}}\right) + \widetilde{\mathcal{C}}_2 Y_{\frac{\kappa}{\eta}}\left(\frac{\zeta}{\eta}\sqrt{\upsilon\left\{\frac{2\kappa\rho}{\zeta} - \frac{2\eta\rho}{\zeta} - 1\right\}}\right)\right], \tag{4.35}$$

where J and Y are the bessel functions of the first and second kind, respectively. We make the backward substitutions as in section "Solution for B and C in the Square-Root Stochastic Volatility Framework with Imperfectly Correlated Brownian Motions" and obtain the wanted function

$$B(\tau) = -\frac{\rho i\phi}{\zeta}\, e^{-\eta\tau} + \frac{\kappa}{\zeta^2} - \frac{2}{\zeta^2}\frac{\widetilde{\mathcal{C}} J'_{\frac{\kappa}{\eta}}\big(g(\tau)\big) + Y'_{\frac{\kappa}{\eta}}\big(g(\tau)\big)}{\widetilde{\mathcal{C}} J_{\frac{\kappa}{\eta}}\big(g(\tau)\big) + Y_{\frac{\kappa}{\eta}}\big(g(\tau)\big)}, \tag{4.36}$$

with

$$g(\tau) = \frac{\zeta}{\eta}\sqrt{i\phi\, e^{-\eta\tau}\left(\frac{2\kappa\rho}{\zeta} - \frac{2\eta\rho}{\zeta} - 1\right)}.$$

The recurrence relations for the two Bessel functions are[20]

$$J'_{\frac{\kappa}{\eta}}\big(g(\tau)\big) = \left(J_{\frac{\kappa}{\eta}-1}\big(g(\tau)\big) - \frac{\kappa}{\eta g(\tau)} J_{\frac{\kappa}{\eta}}\big(g(\tau)\big)\right)\frac{\partial g(\tau)}{\partial\tau},$$

[19] Polyanin and Zaitsev (2003), Table 15.

[20] Abramowitz and Stegun (1970), p. 361

$$Y'_{\frac{\kappa}{\eta}}\big(g(\tau)\big) = \left(Y_{\frac{\kappa}{\eta}-1}\big(g(\tau)\big) - \frac{\kappa}{\eta g(\tau)} Y_{\frac{\kappa}{\eta}}\big(g(\tau)\big)\right)\frac{\partial g(\tau)}{\partial \tau}.$$

Plugging the recurrence relations in (4.36) and simplifying leads to

$$B(\tau) = -\frac{\rho i\phi}{\zeta}\, e^{-\eta\tau} + \frac{\eta}{\zeta^2}\, g(\tau)\, \frac{\widetilde{\mathcal{C}} J_{\frac{\kappa}{\eta}-1}\big(g(\tau)\big) + Y_{\frac{\kappa}{\eta}-1}\big(g(\tau)\big)}{\widetilde{\mathcal{C}} J_{\frac{\kappa}{\eta}}\big(g(\tau)\big) + Y_{\frac{\kappa}{\eta}}\big(g(\tau)\big)}, \tag{4.37}$$

with

$$\widetilde{\mathcal{C}} = \frac{\widetilde{\mathcal{C}}_1}{\widetilde{\mathcal{C}}_2} = \frac{\zeta\rho i\phi\, Y_{\frac{\kappa}{\eta}}\big(g(0)\big) - \eta\, g(0)\, Y_{\frac{\kappa}{\eta}-1}\big(g(0)\big)}{\eta\, g(0)\, J_{\frac{\kappa}{\eta}-1}\big(g(0)\big) - \zeta\rho i\phi\, J_{\frac{\kappa}{\eta}}\big(g(0)\big)}.$$

The ODE for $C(\tau)$ (4.7) together with the solution for $B(\tau)$ (4.36) is

$$\frac{\mathrm{d}C(\tau)}{\mathrm{d}\tau} = \eta\overline{X}\, i\phi\, e^{-\eta\tau} - \frac{\rho\kappa\theta i\phi}{\zeta}\, e^{-\eta\tau} + \frac{\kappa^2\theta}{\zeta^2} - \frac{2\kappa\theta}{\zeta^2}\frac{\widetilde{\mathcal{C}} J'_{\frac{\kappa}{\eta}}\big(g(\tau)\big) + Y'_{\frac{\kappa}{\eta}}\big(g(\tau)\big)}{\widetilde{\mathcal{C}} J_{\frac{\kappa}{\eta}}\big(g(\tau)\big) + Y_{\frac{\kappa}{\eta}}\big(g(\tau)\big)}. \tag{4.38}$$

The solution of this ODE with respect to the boundary condition is straightforward:

$$C(\tau) = \big(e^{-\eta\tau} - 1\big)\left(\frac{\kappa\theta i\phi}{\eta\zeta} - \overline{X} i\phi\right) + \frac{\kappa^2\theta\tau}{\zeta^2} - \frac{2\kappa\theta}{\zeta^2}\ln\left[\frac{\widetilde{\mathcal{C}} J_{\frac{\kappa}{\eta}}\big(g(\tau)\big) + Y_{\frac{\kappa}{\eta}}\big(g(\tau)\big)}{\widetilde{\mathcal{C}} J_{\frac{\kappa}{\eta}}\big(g(0)\big) + Y_{\frac{\kappa}{\eta}}\big(g(0)\big)}\right]. \tag{4.39}$$

Comparison of Computation Time Using Runge-Kutta Algorithms and Hypergeometric Functions with Gauss Laguerre Quadrature

In the square-root stochastic volatility model (see Sect. 4.1), we have the possibility to calculate the characteristic function either with Kummer or Bessel functions or numerically with solvers from the Matlab® ODE suite. As explained in Sect. 3.6, ode45 (a Runge-Kutta solver) and ode113 (a predictor-corrector method) turn out to be superior with respect to computation time and accuracy. Among these two solvers, ode113 proved to be faster for our tested ODE systems and parameter settings. Nevertheless, we decided to compare the computation time of the hypergeometric functions with the ode45 Runge-Kutta solver, because it is the method which is mainly used in the literature.

The calculation with Bessel functions in Matlab® is straightforward and fast, while the calculation using Kummer functions is not. The type of hypergeometric function which is appropriate depends on the parameter settings (see Sect. 4.1.2).

In case of Bessel functions, the average computation time for one integration node of a Gauss-Laguerre quadrature (see Sect. 3.6) with overall 50 nodes on a 2x 2.8 GHz Pentium® Dual Core workstation are the following (while the results are virtually identical): 0.29 seconds for a Runge-Kutta calculation compared to 0.01 seconds for the calculation with Bessel functions.[21] This is a sizeable speedup of computation, but unfortunately, the use of Bessel functions refers to the special case while the need for Kummer functions applies to the standard case.

For the calculation with Kummer functions, we use the Matlab® translation of a fortran77 source code for the calculation of the generalized hypergeometric function. The original fortran77 code has been written by W.F. Perger from the Michigan Technological University. B. Barrowes from the MIT translated the code and made the Matlab® code available via the Matlab® Central File Exchange (Barrowes 2004). To adapt the code to our problem, we additionally implemented a Maple™ call for the calculation of the Kummer function of the second kind $U(a, b, z)$ for integer values of b.

The average computation time for one integration node is the following (again, the results are virtually identical): 0.28 seconds for a Runge-Kutta calculation compared to 1.89 seconds for the calculation with the generalized hypergeometric function. The computation time subject to different values of ϕ is displayed in Fig. 4.5 and Fig. 4.6. Each experiment has been repeated 25 times and the average time of the replications entered the graphs in the two figures. The parameter values are identical with the setting of the Monte Carlo simulation in Sect. 4.1.3 of

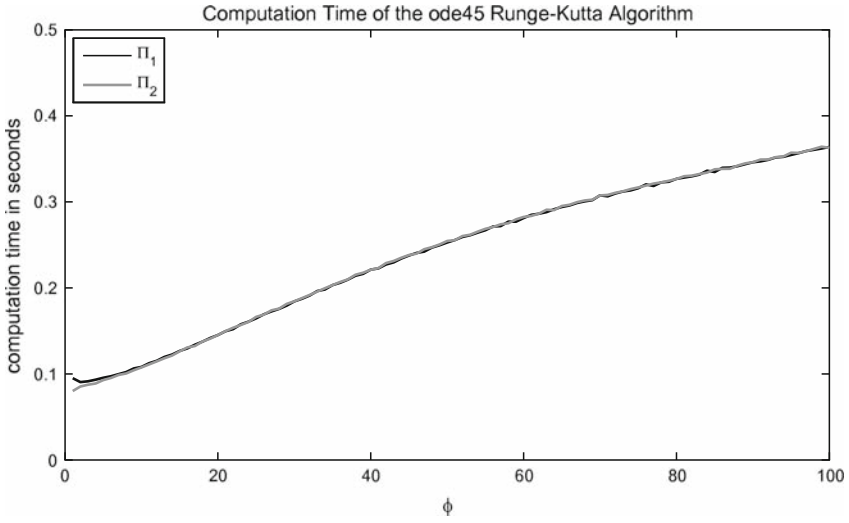

Fig. 4.5 Computation time per integration node of the ode45 Runge-Kutta algorithm

[21] Remember that the integration nodes of a Gauss Laguerre quadrature are not equidistant. The concentration of the nodes decreases with ϕ. Since the computation time per node increases with ϕ, the arrangement of the integration nodes is an advantage regarding the overall computation time.

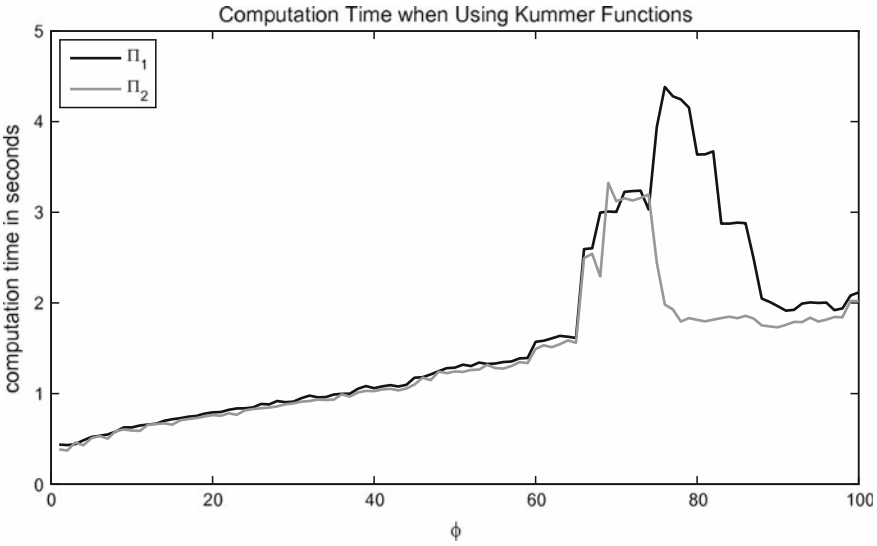

Fig. 4.6 Computation time per integration node when using Kummer functions

the following chapter: $S = 80, \overline{S} = 85, \eta = 1, T - t = 0.5, \zeta = 0.2, \sqrt{V} = 0.2, \kappa = 1, \rho = -0.5, \theta = 0.05$. This setting refers to the special case 1 solution of Sect. 4.1.2. The computation time of the general case solution and the special case 1 solution is very similar. The two plots Π_1 and Π_2 refer to calculations of (3.52) and (3.50), respectively.

Note that the Runge-Kutta calculation time is virtually identical for the general case and the two special cases. When using hypergeometric functions, a special case solution is based on Bessel functions. The calculation with Bessel functions is so fast that the differences of the computation time subject to ϕ are so small that they can be neglected. Hence, we did not implement a graph which compares the computation time for the special case 2 solution.

A comparison of Fig. 4.5 and Fig. 4.6 shows that the calculation with Runge-Kutta algorithms is up to ten times faster compared with Kummer functions. The exact reason for the sharp increase of computation time for $\phi \approx 66$ in Fig. 4.6 could not be resolved, it seems to be due to convergence difficulties in the 'hyper' subroutine of the translated fortran code.

Barrowes reports that for the Kummer function, a considerable speedup of computation with a factor of approximately 85 can be achieved when using the original fortran source code. This would lead to an average calculation time for one integration node of 0.02 seconds. We did not test the original code since this would require the installation of fortran on a linux machine, which was beyond the scope of this work. It should be expected that the use of Runge-Kutta fortran code would also lead to a speedup compared to Runge-Kutta Matlab® code. Hence, when the solution for the characteristic function involves Kummer functions, we basically used numerical ODE solvers (ode45 and ode113) for the calculation of option and futures prices.

Chapter 5
Integration of Jump Components

Jumps are a feature which may occur both in the underlying and in the subordinated processes. They show typically negative correlation, i.e., a downward jump in the underlying process is associated with an upward jump in the variance process. The negative correlation of Brownian motions in the stochastic volatility case or of jumps in the case of pure jump or jump-diffusion models is known as leverage effect.[1]

The first approach of incorporating jumps in derivative pricing models traces back to Merton (1976), though he did not work with any form of a subordinated volatility process. Bates (1996b) makes use of the characteristic function approach of Heston (1993) and adds lognormal jumps to a CIR stochastic volatility model. Bakshi, Cao and Chen (1997) allow for jumps in the (log-)underlying process, for stochastic volatility and stochastic interest rates. They provide an empirical analysis of jump-diffusion option pricing models without mean reversion of the underlying. Bates (2000) also tests his jump-diffusion model in an empirical survey.[2] The authors point out that the incorporation of jumps is especially important for the correct valuation of short-term options, since they can explain the non-zero prices of options which are out of the money and have only a few days left to maturity. The drawback of continuous diffusion processes in this context is that they have too little time to come back in the money and therefore result in an exercise probability which is virtually zero. In contrast to pure diffusion processes, a jump-diffusion process exhibits a non-zero probability for a jump event even in a small time interval so that the model matches the empirical observation of option prices. The importance of jump components in the valuation model weakens with increasing maturity since in the long run, the jump-diffusion and the pure diffusion model with stochastic volatility both generate a skewed probability distribution of X_t with fat

[1] The leverage effect is especially important for financial assets. When dealing with commodity price processes, a price increase may also lead to an increase in volatility.

[2] BCC (1997) and Bates (2000) applied their analysis on non-mean-reverting assets. Mean reversion in the assumed model causes a distribution which is closer to normal since the pressure to come back to the mean inhibits both fat tails and a large skewness.

B. Lutz, *Pricing of Derivatives on Mean-Reverting Assets*,
Lecture Notes in Economics and Mathematical Systems,
DOI 10.1007/978-3-642-02909-7_5,

tails.[3] Hilliard and Reis (1998, 1999) apply the framework of Bates (1996a, 1996b) on the valuation of commodity futures and options. However, the commodity price processes in Hilliard and Reis are not mean-reverting.

Duffie, Pan and Singleton (2000) generalize the approach of BCC (1997) and define the class of affine jump-diffusions. They allow for normally distributed jumps in the log-underlying process, exponentially distributed jumps in the variance process and for correlation between these two jump components under the restriction that both jumps occur simultaneously. It is also possible to incorporate Γ-distributed jumps in the variance process, which can be seen as a generalization of exponential distributed jumps. For the insertion of Γ-distributed jumps, we refer to Kispert (2005).

DPS (2000) did not incorporate mean reversion in the (log-)underlying process. Following Kamat and Oren (2002) and Kispert (2005), we apply the framework of Duffie et al. (2000) on mean-reverting assets. However, the authors combined jumps with mean reversion or jumps with stochastic volatility, but did not associate mean reversion with stochastic volatility. Due to the use of Runge-Kutta-algorithms, we are able to solve for characteristic functions which incorporate mean reversion of the underlying, stochastic volatility, and jumps in the underlying and volatility processes. In the context of commodity derivative pricing, the combination of these three features is new in this study, at least to our knowledge.

A recent work in this context is provided by Geman and Roncoroni (2006) who incorporate jumps in a mean-reverting electricity price process. The corresponding jump process is regime-shifting, which covers quite well the empirical properties of the electricity price process, but inhibits closed-form or semi-closed form solutions. We do not apply regime-shifting jump processes since the regime shift inhibits the solution by means of ODE integration. Furthermore, the authors did not implement a subordinated stochastic volatility process.

For the specification and technical properties of Poisson processes, we refer to the second paragraph in Sect. 3.1.1.

5.1 Simulation of Poisson Processes

We tested our Runge-Kutta solutions of the following subsections with Monte-Carlo simulations of the SDE systems. In the following, we illustrate shortly the simulation of distributions for jump-diffusion processes.

Let us suppose a compound Poisson process with intensity $\lambda = 5$ in the time interval $T - t = 0.5$. The expected number of jumps according to (3.17) is therefore 2.5. The number of jumps per trajectory is taken from a pseudo random number

[3] To generate comparable results, the volatility in the pure diffusion model will be larger than in the jump-diffusion model to compensate for the absence of jumps. The shape of the empirical distribution of returns depends on the time scale over which returns are calculated. For large time scales, the empirical distribution of returns approaches a normal distribution (Cont 2001).

generator for a Poisson distribution with parameter $\lambda(T-t)$.[4] For the simulation of jumps in the log-underlying process with mean reversion of the underlying (see Sect. 5.2.2), it is important to know where exactly in the time interval the process jumps since the jump affects the subsequent behavior of the drift term because of the existence of autocorrelation when assuming an OU-process.

For non-mean-reverting processes as in Bates (1996) or DPS (2000), one could continue by identifying the amount of each jump. One is not interested in the exact simulation of the time of a jump event since it does neither affect the drift term nor the Brownian motion.

The same considerations are valid when we simulate jumps in the subordinated variance process (see Sects. 5.3 and 5.4). One has to determine the exact jump time because the jump in the variance process affects the subsequent behavior of the log-underlying process.

With the number of jumps given, one can now identify the time of each jump by another pseudo random number which is uniformly distributed in the considered time interval $(0; T]$. Since the appropriate Matlab® random number generator 'rand' simulates a uniformly distributed random variable in the interval $(0; 1]$, the adaption is simply done by multiplication of the results with T. A jump at time 0 is not allowed, but this realization is excluded by the random number generator. Some trajectories for a Poisson process according to (3.16) with the above parameter settings are plotted in Fig. 5.1.

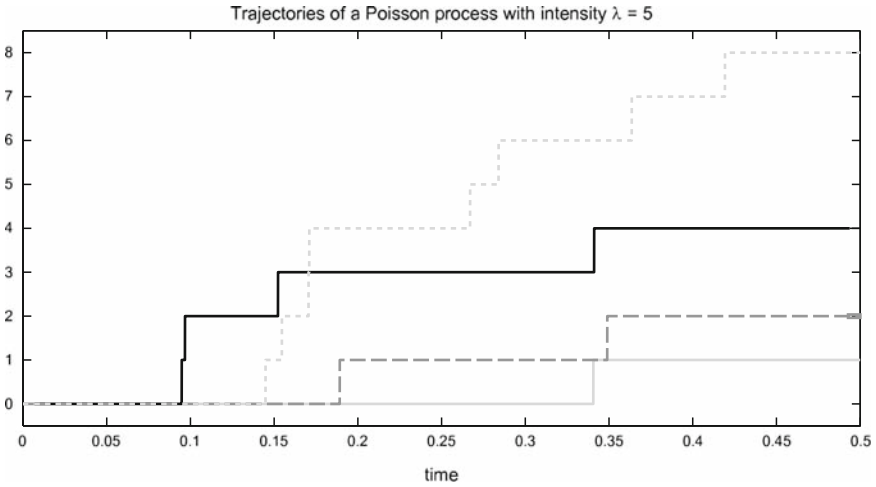

Fig. 5.1 Trajectories of a poisson process with intensity $\lambda = 5$

[4] It is also possible to simulate the number of jumps by a pseudo random number generator for a Binomial distribution with parameters n_t and $\lambda(T-t)/n_t$ (where n_t denotes the number of time steps per path). The Binomial distribution can be applied since for each small time step, there occurs either one jump or no jump. For large n_t, the Binomial distribution approaches the Poisson distribution (cf. Bronstein et al. (2001), p. 778). With 2,500 time steps, the results for the two alternatives are virtually identical.

Monte-Carlo simulations of processes where the jumps have an impact on the subsequent behavior are quite vulnerable to an imprecise specification of the time discretization scheme. Therefore, we applied the derivative-free jump-adapted discretization scheme of Bruti-Liberati and Platen (2006).[5] We need the criterion of weak convergence since we are interested in an approximation of the density function at maturity and not in a pathwise approximation which would be useful for hedging simulations or the valuation of path-dependent derivatives such as American options.

As in the continuous case, the jump-adapted scheme is based on an equidistant discretization of the time interval. Contrary to the simulation of continuous processes, the jump times are additionally inserted in the scheme which leads to the following modifications: First, the time steps before and at the jump interval are smaller than the other time steps, and second, the number of time steps for a simulated path is no longer constant but depends on the number of jump events. By this means, the process can only jump at a discretization time and not between the time steps. The order of a discretization scheme can be improved by a Taylor series expansion of the SDE under account. The fact that the discretized process in the jump-adapted scheme exhibits only jumps at a discretization time allows a negligence of the jump term in the Taylor series expansion. The insertion of a jump step is shown in Fig. 5.2.

Let us consider the following SDE as being discretized (cf. also (3.26)):

$$dX_t = \left(a(X_t, V) - \frac{1}{2}V\right) dt + \sqrt{V}\, dW_t^X + dP_t^X .$$

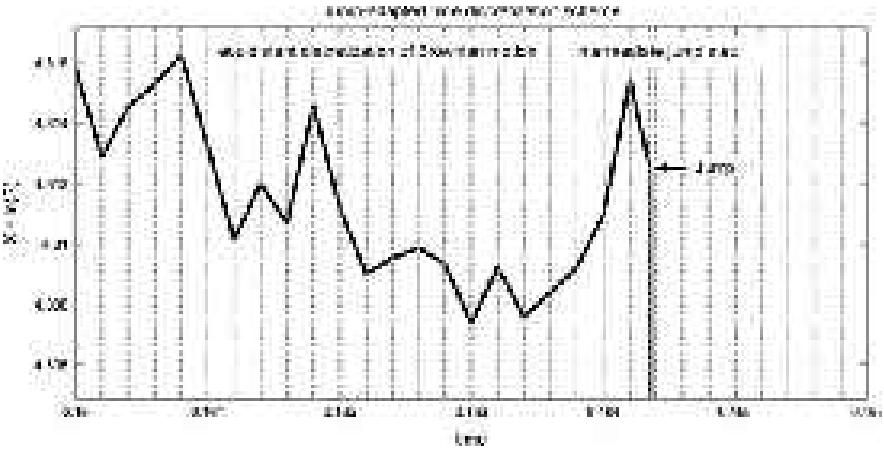

Fig. 5.2 Jump-adapted time discretization scheme

[5] Note that the simulation paths in Figs. 5.1 and 5.3 are obtained with the Euler scheme which is both of strong and weak order 1.

The jump-adapted Euler scheme for this SDE is given by

$$X_{t_{k+1-}} = X_{t_k} + \left(a(X_{t_k}, V) - \frac{1}{2} V \right) \Delta_{t_k} + \sqrt{V}\, \Delta W_{t_k}^X \tag{5.1}$$

$$X_{t_{k+1}} = X_{t_{k+1-}} + P_{t_{k+1}}^X - P_{t_{k+1-}}^X , \tag{5.2}$$

with $\Delta_{t_k} = t_{k+1} - t_k, k = 0, 1, .., n+n_J, \Delta W_{t_k}^X \sim N(0, \Delta_{t_k})$, where n is the number of basis time steps and n_J is the number of jumps in the simulated trajectory.[6] When no jumps occurs at time t_{k+1}, then we have $X_{t_{k+1}} = X_{t_{k+1-}}$.

The discretization scheme described by (5.1) and (5.2) achieves an order of convergence of 1. Although this is sufficient for a fast test of the results, one can increase the order of convergence by applying the jump-adapted order 2 derivative-free scheme.[7]

The usage of weak Taylor schemes with equidistant time steps and an incorporation of the jump in the Taylor series expansion as shown in another section in Bruti-Liberati and Platen (2006) is also possible but much more complex.[8] The jump-adapted order 2 derivative-free scheme of the authors also achieves an order of convergence of 2. Hence, the cost of weak Taylor schemes seems not to be covered by its benefit.

Finally, one has to identify the amount of which the process jumps upwards or downwards. In Fig. 5.3, we plotted trajectories for lognormal distributed jumps as

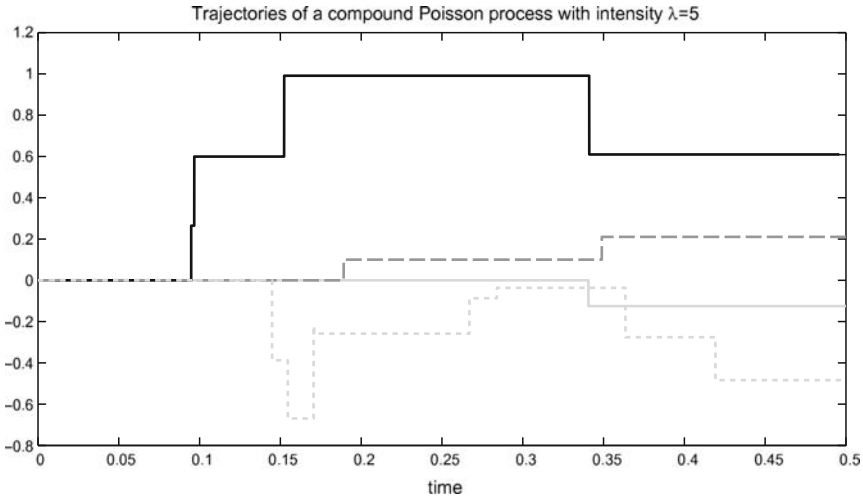

Fig. 5.3 Trajectories of a compound poisson process with intensity $\lambda = 5$

[6] As already discussed in Chap. 4, the number of basis time steps is 2,500.

[7] Cf. Bruti-Liberati and Platen (2006), p. 14.

[8] This alternative scheme is not jump-adapted.

in (5.5) with the same jump times as in Fig. 5.1 and parameters $\lambda = 5, T - t = 0.5, \mu_J = 0.1$ and $\sigma_J = 0.4$. The jump sizes are determined by draws from a pseudo random number generator for standard normal random variables $\tilde{z}$, keeping in mind that a normally distributed random variable with arbitrary mean μ_J and variance σ_J is acquired by $\mu_J + \sigma_J \cdot \tilde{z}$.[9]

5.2 Lognormal Jumps of the Underlying

5.2.1 Non-Mean-Reverting Assets

Firstly, let us illustrate shortly the simple case of independent jumps in the underlying when the asset shows no mean reversion. To keep things simple, we take the Black and Scholes (1973) price process of the underlying under the risk-neutral measure $\mathbb{Q}$

$$dS_t = r\, S_t\, dt + \sigma\, S_t\, dW_t^S + S_t\, dP_t^S\,, \tag{5.3}$$

where r denotes the return of the risk-free bond and the jump component is defined as compensated process

$$P_t^S = \sum_{k=1}^{N_t} J_k^S - \lambda^S\, \mu_J t\,. \tag{5.4}$$

N_t is a poisson process with intensity λ^S defined by (3.16).[10] As explained in Sect. 3.1.1, the jump component is modeled as compensated process in (5.4) so that the incorporation of the jump term does not change the expected value of X and we keep the martingale property of the discounted derivative process under $\mathbb{Q}$. J_k^S denotes the jump size of the k-th jump which is lognormally distributed via[11]

$$\ln(1 + J^S) \sim N(\ln(1 + \mu_J) - \frac{1}{2}\,\sigma_J^2, \sigma_J^2)\,. \tag{5.5}$$

μ_J is the expected jump size and σ_J its volatility. The jump process is assumed to be independent from the continuous part. We plug (5.4) in (5.3). Itô's lemma for the

[9] More information concerning the simulation of jump processes is given in Cont and Tankov (2003).

[10] The application to more sophisticated square-root or OU stochastic volatility models is straightforward.

[11] This specification of lognormal jumps traces back to Bates (1996b, 2000). BCC (1997) and DPS (2000) also incorporated this type of jump in a square-root stochastic volatility model.

transform $X_t = \ln(S_t)$ leads to

$$dX_t = (r - \frac{1}{2}\sigma^2 - \lambda^X \mu_J)\, dt + \sigma\, dW_t^X + dN_t \ln(1 + J^S)\,, \tag{5.6}$$

where $\lambda^X = \lambda^S$, $dW_t^X = dW_t^S$ is only a change of notation.

We omit the FPDE for this simple model setup. The guess for the characteristic function of the diffusion component is $\Phi^d = \exp\{i\phi X_t + B(\tau)\}$. This leads to the ODE

$$\frac{\mathrm{d}B(\tau)}{\mathrm{d}\tau} = i\phi\left(r - \frac{1}{2}\sigma^2 - \lambda^X \mu_J\right) - \frac{1}{2}\phi^2\sigma^2\,.$$

A straightforward integration leads to the Black-Scholes characteristic function (with an adapted drift term)[12]

$$\Phi^d = \exp\left\{i\phi X_t + i\phi\left(r - \frac{1}{2}\sigma^2 - \lambda^X \mu_J\right)\tau - \frac{1}{2}\phi^2\sigma^2\tau\right\}\,. \tag{5.7}$$

Since the jump component is independent from the diffusion component, we can apply the solution for the characteristic function of the diffusion component Φ^d and multiply it with the characteristic function of the jump component Φ^{J^X} according to (3.18)[13]:

$$\Phi(\phi, t, T) = \Phi^d(\phi, t, T) \cdot \Phi^{J^X}(\phi, t, T)\,, \tag{5.8}$$

with

$$\Phi^{J^X}(\phi, t, T) = \exp\left\{(T-t)\lambda^X(\exp[i\phi\{\ln(1+\mu_J) - \frac{1}{2}\sigma_J^2\} - \frac{1}{2}\sigma_J^2\phi^2] - 1)\right\}\,. \tag{5.9}$$

5.2.2 Mean-Reverting Assets

Let us now consider jumps when the underlying price process under $\mathbb{Q}$ shows mean reversion. As pointed out in Das (2002) and previously in Sect. 5.1, the jump affects the subsequent behavior of the mean-reverting drift term and is therefore not independent from the continuous part. The incorporation of jumps with the multiplication of characteristic functions according to (5.8) is not appropriate. Following

[12] The drift term adaption traces back to the specification of the jump process as compensated process (5.4).

[13] A more detailed discussion concerning the multiplication of characteristic functions for independent factors is given in Zhu (2000).

(3.1), we specify the price process of the underlying as

$$dS_t = \eta\{\overline{S} - S_t\}\, S_t\, dt + \sqrt{V_t}\, S_t\, dW_t^S + S_t\, dP_t^S\,, \tag{5.10}$$

where the jump component is defined by (5.4) and (5.5). We plug (5.4) in (5.10) and obtain

$$dX_t = (\eta\{\overline{X} - X_t\} - \frac{1}{2}\, V_t - \lambda^X\, \mu_J)\, dt + \sqrt{V_t}\, dW_t^X + dN_t \ln(1 + J^S)\,, \tag{5.11}$$

where $\lambda^X = \lambda^S$, $dW_t^X = dW_t^S$ as in the previous subsection.

Now consider for example the square-root stochastic volatility model or the OU stochastic volatility model as discussed in Sects. 4.1 and 4.2. For the square-root model, the FPDE is given by

$$\begin{aligned}\frac{\partial \Phi}{\partial t} &+ (\eta\{\overline{X} - X_t\} - \frac{1}{2}\, V_t - \lambda^X \mu_J)\frac{\partial \Phi}{\partial X} + \kappa(\theta - V_t)\frac{\partial \Phi}{\partial V} + \frac{1}{2}\, V_t\, \frac{\partial^2 \Phi}{\partial X^2} \\ &+ \frac{1}{2}\, \zeta^2\, V_t\, \frac{\partial^2 \Phi}{\partial V^2} + \rho V_t \zeta \frac{\partial^2 \Phi}{\partial X\, \partial V} + \lambda^X\, \mathbb{E}^{\mathbb{Q}}[(\Phi(X_t + J^X) - \Phi(X_t))] = 0\,,\end{aligned}$$

where $J^X = \ln(1 + J^S)$. We apply the exponential affine guess (4.5) for Φ and obtain the following set of ODEs.

$$\begin{aligned}\frac{\mathrm{d}B(\tau)}{\mathrm{d}\tau} &= -\frac{1}{2} i\phi e^{-\eta\tau} + \frac{1}{2}(i\phi)^2 e^{-2\eta\tau} - \kappa B(\tau) + \frac{1}{2}\zeta^2 B^2(\tau) + \rho\zeta i\phi e^{-\eta\tau} B(\tau) \\ \frac{\mathrm{d}C(\tau)}{\mathrm{d}\tau} &= \left(\eta\overline{X} - \lambda^X \mu_J\right) i\phi e^{-\eta\tau} + \kappa\theta B(\tau) + \lambda^X \mathbb{E}^{\mathbb{Q}}\left[\exp\{i\phi e^{-\eta\tau} J^X\} - 1\right]\end{aligned} \tag{5.12}$$

We observe that the ODE for $B(\tau)$ is identical to (4.7) in Sect. 4.1. The remaining expectation in the ODE for $C(\tau)$ can be solved because the jump J^X is assumed to be normally distributed with parameters $\ln(1 + \mu_J) - 0.5\sigma_J^2$ and σ_J^2. The resulting ODE is given by

$$\begin{aligned}\frac{\mathrm{d}C(\tau)}{\mathrm{d}\tau} &= \left(\eta\overline{X} - \lambda^X \mu_J\right) i\phi e^{-\eta\tau} + \kappa\theta B(\tau) + \\ &+ \lambda^X \exp\left\{i\phi e^{-\eta\tau}[\ln(1 + \mu_J) - \frac{1}{2}\sigma_J^2] - \frac{1}{2}\phi^2 e^{-2\eta\tau}\sigma_J^2\right\} - \lambda^X\,.\end{aligned} \tag{5.13}$$

The three nested exponential functions of the integration variable τ inhibit a closed-form solution for (5.13). Hence, we solve the ODE system with a Runge-Kutta-algorithm.

For the OU stochastic volatility model, the jump term affects only the function $D(\tau)$. The ODEs for $B(\tau)$ and $C(\tau)$ are given in (4.20), and the ODE for

$D(\tau)$ changes to

$$\frac{\mathrm{d}D(\tau)}{\mathrm{d}\tau} = \left(\eta\overline{X} - \lambda^X \mu_J\right) i\phi e^{-\eta\tau} + \kappa\theta C(\tau) + \zeta^2 B(\tau) + \frac{1}{2}\zeta^2 C^2(\tau) + \\ + \lambda^X \exp\left\{ i\phi e^{-\eta\tau}[\ln(1+\mu_J) - \frac{1}{2}\sigma_J^2] - \frac{1}{2}\phi^2 e^{-2\eta\tau}\sigma_J^2 \right\} - \lambda^X , \quad (5.14)$$

Since there is no closed-form solution available, the computation will be done with numerical integration methods.

5.2.3 Comparison with the Monte-Carlo Solution

Following the jump-adapted derivative-free time discretization scheme of Bruti-Liberati and Platen (2006) as described in Sect. 5.1, we simulated the SDE system with an underlying process according to (5.11) and subordinated CIR variance process as in (4.1).[14] The parameter values are $S = 80$, $\overline{S} = 85$, $\eta = 1$, $T - t = 0.5$, $\zeta = 0.2$, $\sqrt{V} = 0.2$, $\kappa = 1$, $\rho = -0.5$, $\theta = 0.05$, $\mu_J = 0.1$, $\sigma_J = 0.3$, $\lambda^X = 2$.

The results of the MC simulation are shown in Fig. 5.4. A comparison with the continuous square-root stochastic volatility model in Fig. 4.3 shows that the incorporation of the jump has a large impact on the shape of the distribution. The distribution of S_T shows positive skewness (2.358) and a much higher kurtosis (17.470) compared to the continuous model with a skewness of -0.083 and a kurtosis of 3.173, which is close to a normal distribution (see also Sect. 4.1.3). The expected number of jumps in the considered time interval $T - t = 0.5$ is 1. Though the process is driven back to the long-term equilibrium level $\overline{S} = 85$ after a jump, the impact of the mean reversion in the drift term is much smaller, since the mean reversion cannot remove jumps which occur shortly before maturity. This property results in a smaller value for the RK solution F of the futures price compared to the continuous model since jumps occur both upwards and downwards and weaken the impact of the mean-reverting drift term which, in our case, pushes the process upwards to the equilibrium level $\overline{S} = 85$.

The higher variance and kurtosis influence the confidence interval for $\mathbb{E}[S_T]$. The confidence interval is larger and the MC value $\mathbb{E}[S_T] = 81.1426$ is not that close to the Runge-Kutta solution $F = 81.1338$ as in Chap. 4. Nevertheless, the semi-analytical value lies within the confidence interval [81.1227; 81.1624]. Obviously, option values are highly increased compared to the reference model in Sect. 4.1 due to the higher volatility caused by the jumps.

[14] In the following, we focused on CIR variance as reference model. Since the impact of the model extensions is similar for both stochastic volatility models, we omit the presentation of MC simulations for the OU stochastic volatility case.

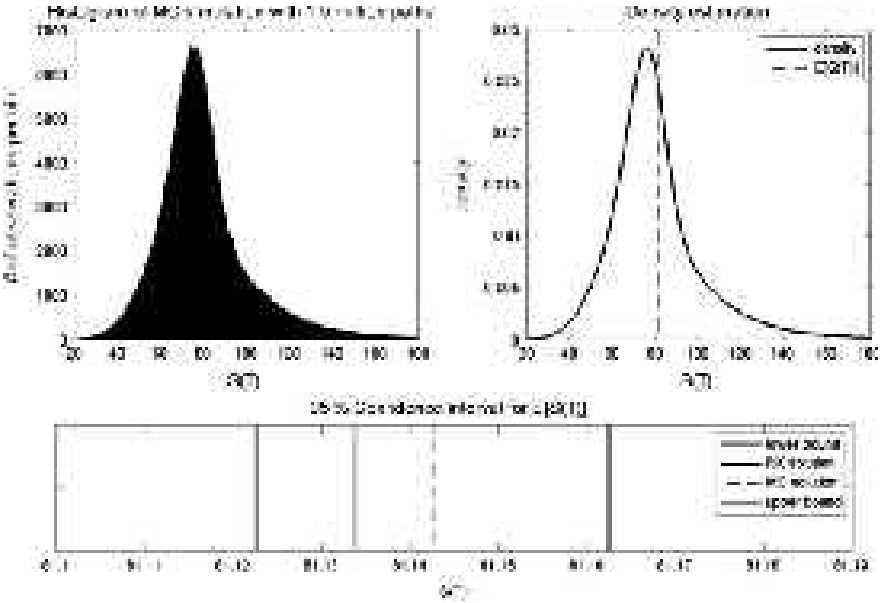

Fig. 5.4 Histogram, density function and confidence interval for the OU model with square-root stochastic volatility and lognormal jumps of the underlying

5.3 Exponentially and Γ-Distributed Jumps in the Variance Process

Following DPS (2000), we incorporate exponentially distributed jumps in the variance process in the square-root stochastic volatility model. The system of SDEs reads

$$\begin{aligned} dX_t &= (\eta\{\overline{X} - X_t\} - \frac{1}{2} V_t)\, dt + \sqrt{V_t}\, dW_t^X \\ dV_t &= \kappa(\theta - V_t)dt + \zeta \sqrt{V_t}\, dW_t^V + dP_t^V , \end{aligned} \tag{5.15}$$

where

$$P_t^V = \sum_{k=1}^{N_t} J_k^V , \tag{5.16}$$

with N_t being a Poisson process with intensity λ^V.

5.3.1 Exponentially Distributed Jumps

The jump size J_k^V of the compound Poisson process P_t^V is exponentially distributed with parameter $\gamma > 0$. Hence, the jumps in variance are only allowed to be positive.

With this jump distribution, one avoids the unpleasant case of a negative variance after a large downward jump. The first moment of this distribution is $\mathbb{E}[J^V] = \frac{1}{\gamma}$, the variance is given by $\text{var}(J^V) = (\frac{1}{\gamma})^2$.

The FPDE according to (3.36) is

$$\frac{\partial \Phi}{\partial t} + (\eta\{\overline{X} - X_t\} - \frac{1}{2}V_t)\frac{\partial \Phi}{\partial X} + \kappa(\theta - V_t)\frac{\partial \Phi}{\partial V} + \frac{1}{2}V_t\frac{\partial^2 \Phi}{\partial X^2} + \frac{1}{2}\zeta^2 V_t\frac{\partial^2 \Phi}{\partial V^2} + \rho V_t \zeta \frac{\partial^2 \Phi}{\partial X \partial V} + \lambda^V \mathbb{E}^{\mathbb{Q}}[(\Phi(V_t + J^V) - \Phi(V_t))] = 0\,, \quad (5.17)$$

with the first terms identical to Sect. 4.1 and the new jump term

$$\lambda^V \mathbb{E}^{\mathbb{Q}}[(\Phi(V_t + J^V) - \Phi(V_t))]\,.$$

We apply the exponential affine guess (4.5) for Φ in (5.17). After simplifying, we obtain

$$\lambda^V \exp\{i\phi A(\tau)X_t + B(\tau)V_t + C(\tau)\} \cdot \left(\mathbb{E}^{\mathbb{Q}}\left[\exp\left\{B(\tau)\,J^V\right\}\right] - 1\right)\,.$$

The remaining expectation is solved under the constraint that the distribution of J^V is exponential (see also DPS (2000)). After dividing by Φ, we obtain for the jump term

$$\lambda^V \left(\mathbb{E}^{\mathbb{Q}}\left[\exp\left\{B(\tau)\,J^V\right\}\right] - 1\right) = \lambda^V \left(\frac{\gamma}{\gamma - B(\tau)} - 1\right)\,. \quad (5.18)$$

We notice that the jump term is not added to the terms containing X_t or V_t and therefore the jump affects only the function $C(\tau)$. The corresponding ODE is

$$\frac{\mathrm{d}C(\tau)}{\mathrm{d}\tau} = \eta\overline{X}i\phi e^{-\eta\tau} + \kappa\theta B(\tau) + \lambda^V \left(\frac{\gamma}{\gamma - B(\tau)} - 1\right)\,. \quad (5.19)$$

Since there is no closed-form solution available for (5.19), we have to solve the ODE system with numerical integration methods.

5.3.2 Γ-Distributed Jumps

Let us now consider the incorporation of Γ-distributed jumps. As mentioned before, this jump setup traces back to Kispert (2005) and can be seen as a generalization of exponential distributed jumps. The jump in variance is now assumed to be $\Gamma(\gamma, \xi)$-distributed ($\gamma > 0$, $\xi > 0$). For $\xi = 1$, the $\Gamma(\gamma, 1)$-distribution is an exponential distribution with parameter γ. As in the case of the exponential distribution, this jump specification allows only for positive jumps with $\mathbb{E}[J^V] = \frac{\xi}{\gamma}$ and $\text{var}(J^V) = \frac{\xi}{\gamma^2}$. For this type of variance jump, the proceeding is very similar to exponential

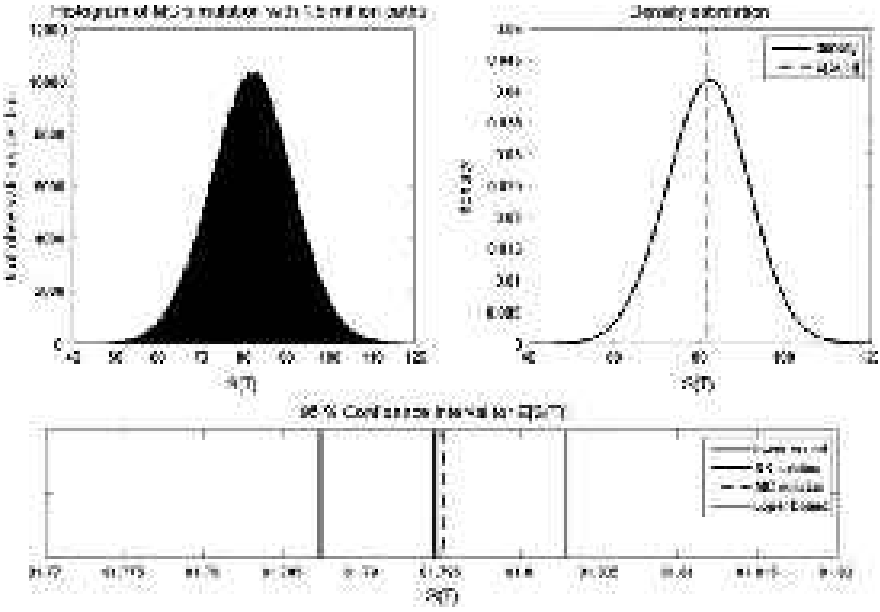

Fig. 5.5 Histogram, density function and confidence interval for the OU model with square-root stochastic volatility and exponential distributed jumps in the variance process

variance jumps and the ODE for $C(\tau)$ is given by[15]

$$\frac{\mathrm{d}C(\tau)}{\mathrm{d}\tau} = \eta\overline{X}i\phi e^{-\eta\tau} + \kappa\theta B(\tau) + \lambda^V\left[\left(1-\frac{1}{\gamma}B(\tau)\right)^{-\xi} - 1\right]. \qquad (5.20)$$

5.3.3 Comparison with the Monte-Carlo Solution

Due to the similarity of the model setups, we decided to provide the MC simulation results only for exponentially distributed jumps. A comparison between exponential and Γ jumps is given in Sect. 5.4.2. The parameter values are the following: $S = 80$, $\overline{S} = 85$, $\eta = 1$, $T - t = 0.5$, $\zeta = 0.2$, $\sqrt{V} = 0.2$, $\kappa = 1$, $\rho = -0.5$, $\theta = 0.05$, $\gamma = 200$, $\lambda^V = 2$. The expected number of jumps per path in the time interval $T-t$ is therefore 1 and the expected jump size is 0.005.

Due to the relatively small jump event, the incorporation of the exponential jump in the variance process does not change that much than jumps in the underlying process. The results of the MC simulation are shown in Fig. 5.5 and are similar to the continuous model in Sect. 4.1. The shape of the distribution is close to normal

[15] Cf. Kispert (2005).

with a skewness of -0.055 and a kurtosis of 3.178 and only slightly different from the square-root stochastic volatility model without jumps (skewness of -0.083 and kurtosis of 3.173). An at-the-money call option is therefore only somewhat more expensive than in the reference model (4.6726 compared to 4.5770).

Due to the small kurtosis, the confidence interval $[81.7887; 81.8044]$ is smaller than in Sect. 5.2.3. The MC value for $\mathbb{E}[S_T]$ is 81.7966 and close to the Runge-Kutta solution $F = 81.7956$.

5.4 Jumps in Both the Underlying and Variance Process

5.4.1 Independent Jumps

Now consider the case where jumps are allowed both in the underlying and the variance process. The system of SDEs is given by

$$\begin{aligned} dX_t &= \left(\eta\{\overline{X} - X_t\} - \frac{1}{2}V_t\right)dt + \sqrt{V_t}\,dW_t^X + dP_t^X \\ dV_t &= \kappa(\theta - V_t)dt + \zeta\sqrt{V_t}\,dW_t^V + dP_t^V\,, \end{aligned} \tag{5.21}$$

with P_t^X and P_t^V specified according to (5.4) and (5.16).

When the two jump processes are assumed to be independent from each other and from the continuous part, we face the following FPDE:

$$\begin{aligned} &\frac{\partial\Phi}{\partial t} + (\eta\{\overline{X} - X_t\} - \frac{1}{2}V_t - \lambda^X\mu_J)\frac{\partial\Phi}{\partial X} + \kappa(\theta - V_t)\frac{\partial\Phi}{\partial V} \\ &\quad + \frac{1}{2}V_t\frac{\partial^2\Phi}{\partial X^2} + \frac{1}{2}\zeta^2 V_t\frac{\partial^2\Phi}{\partial V^2} + \rho V_t\zeta\frac{\partial^2\Phi}{\partial X\,\partial V} \\ &\quad + \lambda^V\,\mathbb{E}^{\mathbb{Q}}[(\Phi(X_t, V_t + J^V) - \Phi(X_t, V_t))] \\ &\quad + \lambda^X\,\mathbb{E}^{\mathbb{Q}}[(\Phi(X_t + J^X, V_t) - \Phi(X_t, V_t))] = 0\,. \end{aligned}$$

Again, the ODE for $B(\tau)$ is identical to Sect. 4.1 and the two jump terms together with the adaption of the drift term are incorporated in the ODE for $C(\tau)$. In the case of exponential distributed variance jumps, we obtain

$$\begin{aligned} \frac{\mathrm{d}C(\tau)}{\mathrm{d}\tau} &= \left(\eta\overline{X} - \lambda^X\mu_J\right)i\phi e^{-\eta\tau} + \kappa\theta B(\tau) + \lambda^V\left(\frac{\gamma}{\gamma - B(\tau)} - 1\right) \\ &\quad + \lambda^X\exp\left\{i\phi e^{-\eta\tau}[\ln(1+\mu_J) - \frac{1}{2}\sigma_J^2] - \frac{1}{2}\phi^2 e^{-2\eta\tau}\sigma_J^2\right\} - \lambda^X\,. \end{aligned} \tag{5.22}$$

And for Γ-distributed variance jumps, the ODE reads

$$\frac{\mathrm{d}C(\tau)}{\mathrm{d}\tau} = \left(\eta\overline{X} - \lambda^X \mu_J\right) i\phi e^{-\eta\tau} + \kappa\theta B(\tau) + \lambda^V \left[\left(1 - \frac{1}{\gamma} B(\tau)\right)^{-\xi} - 1\right] + \lambda^X \exp\left\{i\phi e^{-\eta\tau}[\ln(1+\mu_J) - \frac{1}{2}\sigma_J^2] - \frac{1}{2}\phi^2 e^{-2\eta\tau}\sigma_J^2\right\} - \lambda^X . \quad (5.23)$$

Comparison with the Monte-Carlo Solution

As in the previous section, the MC simulation deals with exponential distributed variance jumps. The parameter settings are $S = 80$, $\overline{S} = 85$, $\eta = 1$, $T - t = 0.5$, $\zeta = 0.2$, $\sqrt{V} = 0.2$, $\kappa = 1$, $\rho = -0.5$, $\theta = 0.05$, $\gamma = 200$, $\lambda^X = 2$, $\lambda^V = 2$, $\mu_J = 0.1$, $\sigma_J = 0.3$. As in every setting in this chapter, the number of jumps averages out at 1 both for the underlying and the subordinated process.

The shape of the distribution of S_T and the 95% confidence interval for F are shown in Fig. 5.6. As expected, the shape of the distribution is similar to Sect. 5.2.3, but with a higher skewness (2.612 compared to 2.358) and kurtosis (24.021 compared to 17.470) due to the additional jump in variance.

The model with both jumps results in a high variance of the MC sample. Therefore, the 95% confidence interval [81.1141; 81.1541] is the largest of our models. The Runge-Kutta solution for F is 81.1287 and somewhat close to the MC solu-

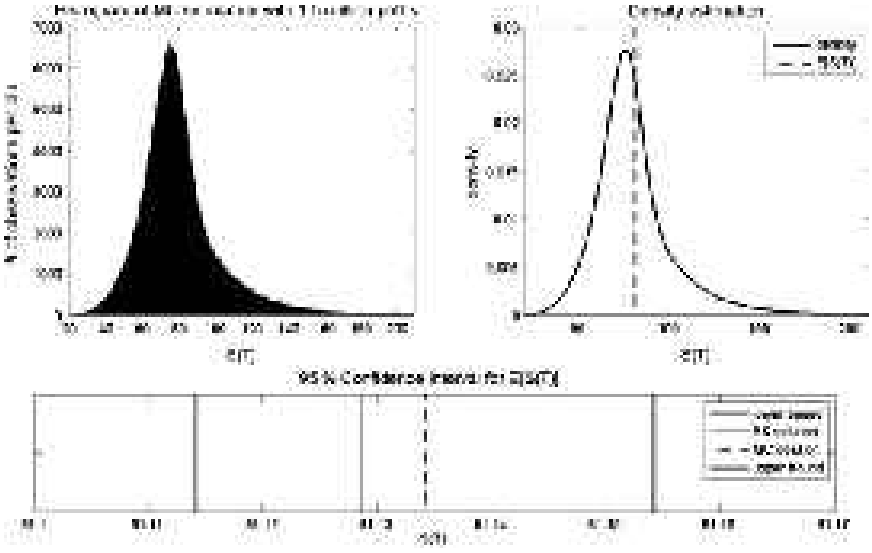

Fig. 5.6 Histogram, density function and confidence interval for the OU model with square-root stochastic volatility and independent jumps in the log-underlying and variance process

tion which is 81.1341. Due to the high variance caused by the two jump processes, an at-the-money call is more expensive than in Sect. 5.2.3 (8.4711 compared to 8.4149).

5.4.2 Correlated Jumps

DPS (2000) also incorporate the case where the jump sizes of the jumps in X_t and V_t are allowed to be correlated. In this model, the two jumps occur always simultaneously. Hence, P_t^X and P_t^V refer to only one Poisson process with intensity λ^ρ. This Poisson process is again assumed to be independent from the diffusion component.

Exponentially Distributed Variance Jumps

The jump size J^V is exponentially distributed with parameter γ. When a certain jump J_k^V is realized, the corresponding jump J_k^S is distributed according to

$$\ln(1+J_k^S) \sim N\left(\ln(1+\mu_J) - \frac{1}{2}\sigma_J^2 + \rho_J \cdot J_k^V, \sigma_{J,\rho}^2\right). \tag{5.24}$$

The FPDE is given by

$$\begin{aligned}
&\frac{\partial\Phi}{\partial t} + (\eta\{\overline{X} - X_t\} - \frac{1}{2}V_t - \lambda^\rho \frac{\mu_J\gamma + \rho_J}{\gamma - \rho_J})\frac{\partial\Phi}{\partial X} + \kappa(\theta - V_t)\frac{\partial\Phi}{\partial V} \\
&\quad + \frac{1}{2}V_t\frac{\partial^2\Phi}{\partial X^2} + \frac{1}{2}\xi^2 V_t\frac{\partial^2\Phi}{\partial V^2} + \rho V_t\xi\frac{\partial^2\Phi}{\partial X\,\partial V} \\
&\quad + \lambda^\rho \mathbb{E}^{\mathbb{Q}}\left[\mathbb{E}^{\mathbb{Q}}[(\Phi(X_t + J^X, V_t + J^V) - \Phi(X_t, V_t))|J^V = J_k^V]\right] = 0\,.
\end{aligned}$$

Note that the drift term correction is now (see DPS (2000))

$$-\lambda^\rho \frac{\mu_J\gamma + \rho_J}{\gamma - \rho_J}\,dt\,,$$

which incorporates both expected jump sizes and their correlation. With $\rho_J = 0$ we have $-\lambda\mu_J\,dt$ as in Sect. 5.2.

The jump components are again incorporated in the ODE for $C(\tau)$:

$$\begin{aligned}
\frac{\mathrm{d}C(\tau)}{\mathrm{d}\tau} &= \left(\eta\overline{X} - \lambda^\rho \frac{\mu_J\gamma + \rho_J}{\gamma - \rho_J}\right) i\phi e^{-\eta\tau} + \kappa\theta B(\tau) \\
&\quad + \lambda^\rho \mathbb{E}^{\mathbb{Q}}\left[\mathbb{E}^{\mathbb{Q}}[\exp\{i\phi A(\tau)J^X + B(\tau)J^V\}|J^V = J_k^V]\right] - \lambda^\rho\,.
\end{aligned} \tag{5.25}$$

To solve for the first expectation in (5.25), we set $A(\tau) = \exp(-\eta\tau)$ in (5.25) and use the distribution law in (5.24) to obtain for the jump term

$$\lambda^\rho \mathbb{E}^{\mathbb{Q}}\left[\exp\{i\phi e^{-\eta\tau}(\ln(1+\mu_J) - \frac{1}{2}\sigma_J^2 + \rho_j J_k^V) - \frac{1}{2}\phi^2\sigma_J^2 e^{-2\eta\tau} + B(\tau)J_k^V\}\right] - \lambda^\rho. \tag{5.26}$$

Since J_k^V is exponentially distributed with parameter γ, one can solve the remaining expectation to obtain for (5.26)[16]

$$\frac{\lambda^\rho\,\gamma\exp\{i\phi e^{-\eta\tau}(\ln(1+\mu_J) - \frac{1}{2}\sigma_J^2) - \frac{1}{2}\phi^2\sigma_J^2 e^{-2\eta\tau}\}}{\gamma - i\phi e^{-\eta\tau}\rho_J - B(\tau)} - \lambda^\rho\,. \tag{5.27}$$

The ODE for $B(\tau)$ is again identical to (4.7) in Sect. 4.1 and the ODE for $C(\tau)$ is given by

$$\begin{aligned}\frac{\mathrm{d}C(\tau)}{\mathrm{d}\tau} &= \left(\eta\overline{X} - \lambda^\rho\,\frac{\mu_J\gamma + \rho_J}{\gamma - \rho_J}\right) i\phi e^{-\eta\tau} + \kappa\theta B(\tau) \\ &\quad + \lambda^\rho\,\frac{\gamma\exp\left\{i\phi e^{-\eta\tau}(\ln(1+\mu_J) - \frac{1}{2}\sigma_J^2) - \frac{1}{2}\phi^2\sigma_J^2 e^{-2\eta\tau}\right\}}{\gamma - i\phi e^{-\eta\tau}\rho_J - B(\tau)} - \lambda^\rho\,. \end{aligned}\tag{5.28}$$

Γ-Distributed Variance Jumps

Now consider the jump sizes J_k^V to be Γ-distributed with parameters γ and ξ as in the previous sections. The distribution law for a price jump contingent on a realized variance jump as described in (5.24) holds analogously.

The FPDE is given by

$$\begin{aligned}&\frac{\partial\Phi}{\partial t} + \left[\eta\{\overline{X} - X_t\} - \frac{1}{2}V_t - \lambda^\rho\left(\frac{1+\mu_J}{\left(1-\frac{\rho_J}{\gamma}\right)^\xi} - 1\right)\right]\frac{\partial\Phi}{\partial X} \\ &\quad + \kappa(\theta - V_t)\frac{\partial\Phi}{\partial V} + \frac{1}{2}V_t\,\frac{\partial^2\Phi}{\partial X^2} + \frac{1}{2}\zeta^2 V_t\,\frac{\partial^2\Phi}{\partial V^2} + \rho V_t\zeta\frac{\partial^2\Phi}{\partial X\,\partial V} \\ &\quad + \lambda^\rho\,\mathbb{E}^{\mathbb{Q}}\left[\mathbb{E}^{\mathbb{Q}}[(\Phi(X_t + J^X, V_t + J^V) - \Phi(X_t, V_t))|J^V = J_k^V]\right] = 0\,.\end{aligned}$$

[16] See also DPS (2000).

The drift term correction for this type of jump specification is[17]

$$-\lambda^{\rho}\left(\frac{1+\mu_J}{\left(1-\frac{\rho_J}{\gamma}\right)^{\xi}}-1\right)dt\,.$$

Note that for $\xi = 1$, the drift term correction is identical to the previous paragraph and for $\rho_J = 0$, the drift term correction is again given by $-\lambda\mu_J\,dt$ as in Sect. 5.2.[18]

The proceeding is similar to the previous paragraph. Equations (5.25) (with different correction term) and (5.26) hold analogously. When the variance jump in (5.26) is Γ-distributed, the ODE for $C(\tau)$ is given by

$$\begin{aligned}\frac{\mathrm{d}C(\tau)}{\mathrm{d}\tau} &= \left[\eta\overline{X}-\lambda^{\rho}\left(\frac{1+\mu_J}{\left(1-\frac{\rho_J}{\gamma}\right)^{\xi}}-1\right)\right]i\phi e^{-\eta\tau}+\kappa\theta B(\tau)\\ &\quad+\lambda^{\rho}\frac{\exp\left\{i\phi e^{-\eta\tau}(\ln(1+\mu_J)-\frac{1}{2}\sigma_J^2)-\frac{1}{2}\phi^2\sigma_J^2e^{-2\eta\tau}\right\}}{\left(1-\frac{1}{\gamma}\{i\phi e^{-\eta\tau}\rho_J+B(\tau)\}\right)^{\xi}}-\lambda^{\rho}\,. \quad (5.29)\end{aligned}$$

Both (5.28) and (5.29) are solved with numerical integration routines.

Comparison with the Monte-Carlo Solution

We firstly run a MC simulation for exponentially distributed variance jumps with parameter values $S = 80$, $\overline{S} = 85$, $\eta = 1$, $T - t = 0.5$, $\zeta = 0.2$, $\sqrt{V} = 0.2$, $\kappa = 1$, $\rho = -0.5$, $\theta = 0.05$, $\gamma = 200$, $\lambda^{\rho} = 2$, $\mu_J = 0.1$, $\sigma_J = 0.3$, $\rho_J = 0.5$. As in the previous section, the expected number of jump events per path is 1. Both the underlying and the variance jump refer to one jump event.

We choose a positive ρ_J to account for the fact that in commodity markets, an upward price jump is likely to be associated with an upward jump in volatility and vice versa. The so-called leverage effect which denotes negative correlation between price and volatility movements mainly is a feature of financial asset markets.

The results are displayed in Fig. 5.7. We observe that correlated simultaneous jumps have a smaller impact than independent jumps. Hence, the results are closer to the model with lognormal jumps. We notice a somewhat higher skewness (2.424 compared to 2.358 in Sect. 5.2.3) and kurtosis (18.767 compared to 17.470 in Sect. 5.2.3) due to the additional simultaneous jump in variance.

[17] Cf. also DPS (2000).

[18] The equality of the correction terms for $\xi = 1$ is required since the $\Gamma(\gamma, 1)$-distribution is an exponential distribution with parameter γ.

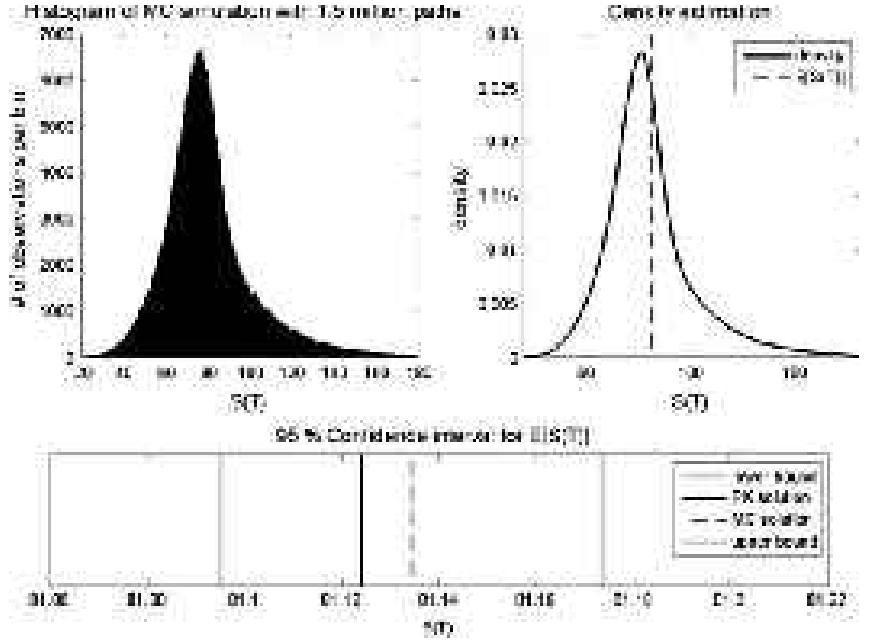

Fig. 5.7 Histogram, density function and confidence interval for the OU model with square-root stochastic volatility and correlated jumps with exponentially distributed variance jumps

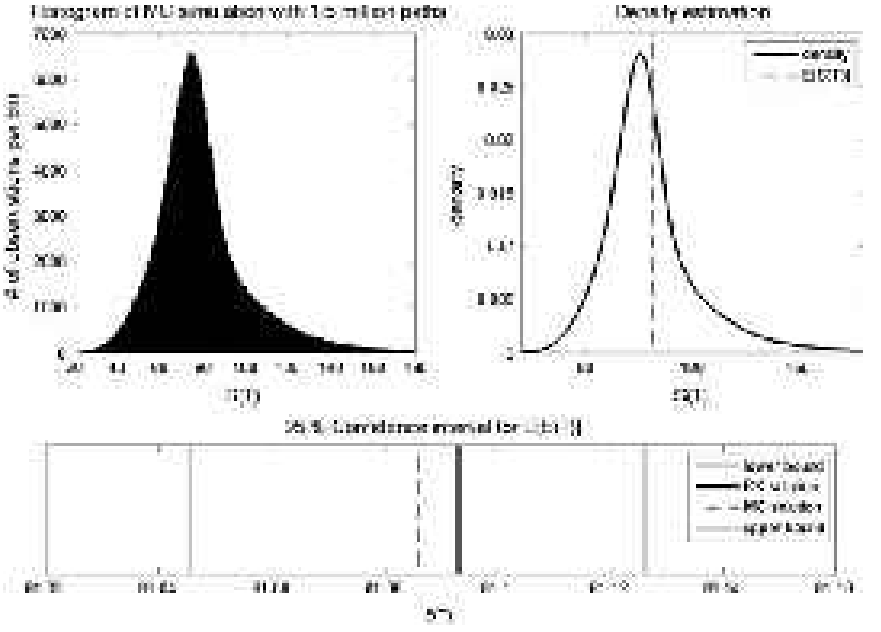

Fig. 5.8 Histogram, density function and confidence interval for the OU model with square-root stochastic volatility and correlated jumps with Γ-distributed variance jumps

The value for F is 81.1239 and close to the value with lognormal jumps (81.1338). The Runge-Kutta solution lies within the confidence interval [81.0949; 81.1735], but is not that close to the MC solution which is 81.1342. An at-the-money call is slightly more expensive than in the model with lognormal jumps (8.4681 compared to 8.4149).

In the following, we shortly present the results in the case of Γ-distributed variance jumps. The parameter setting is $S = 80$, $\overline{S} = 85$, $\eta = 1$, $T - t = 0.5$, $\zeta = 0.2$, $\sqrt{V} = 0.2$, $\kappa = 1$, $\rho = -0.5$, $\theta = 0.05$, $\gamma = 100$, $\xi = 2$, $\lambda^{\rho} = 2$, $\mu_J = 0.1$, $\sigma_J = 0.3$, $\rho_J = 0.5$. Hence, the variance jumps exhibit both a higher expected value and a higher standard deviation compared with exponentially distributed jumps with parameter $\gamma = 200$.

The results are displayed in Fig. 5.8. The shape of the distribution is very similar to the setting with exponentially distributed jumps. The skewness is 2.465 and the kurtosis is 18.668 (both values are slightly higher than in Fig. 5.7). The RK value for F is 81.0932, the MC value is 81.0859 with associated confidence interval [81.0456; 81.1262]. Due to higher variance, an at-the-money call is more valuable ($C = 8.6295$).

Chapter 6
Stochastic Equilibrium Level of the Underlying Process

The values of $\overline{S}$ and $\overline{X}$ denote the mean values, i.e. the long-run equilibrium levels, of the price process and the log-price process, respectively. In the preceding chapters, these parameters are held constant, which implies that in the long-run, every shock in the price process is removed due to the mean reversion. In this section, we model the mean of the price process itself as an additional stochastic factor $\mathfrak{X}$, which is equivalent to the assumption that there exist shocks in the price process which persist.

We address both a mean-reverting process and a Brownian motion process with (presumably positive) drift as subordinated equilibrium level process. While the former accounts for additional risk in price variations, the latter can represent inflation effects. The combination with jumps in the equilibrium level process as discussed in Sect. 6.3.2 may account for regime shift risk. For instance, the crude oil price behavior in the last few years can be modeled according to either a large value of the drift component $\mu_{\mathfrak{X}}$ or a large upward jump in the equilibrium level process.

6.1 Constant Volatility

6.1.1 Mean-Reverting Equilibrium Level

We substitute the constant parameter $\overline{X}$ of the log-price process with the stochastic equilibrium level $\mathfrak{X}$. The SDEs of the log-price process and subordinated equilibrium level process are modeled as follows:

$$\begin{aligned} dX_t &= (\eta\{\mathfrak{X}_t - X_t\} - \frac{1}{2}V_t)\,dt + \sqrt{V_t}\,dW_t^X \\ d\mathfrak{X}_t &= \kappa_{\mathfrak{X}}(\theta_{\mathfrak{X}} - \mathfrak{X}_t)\,dt + \sigma_{\mathfrak{X}}\,dW_t^{\mathfrak{X}}, \end{aligned} \tag{6.1}$$

where the two Brownian motions are allowed to be correlated via $dW_t^X \cdot dW_t^{\mathfrak{X}} = \rho_{\mathfrak{X}}\,dt$. The equilibrium level follows itself a mean reverting process. This model

B. Lutz, *Pricing of Derivatives on Mean-Reverting Assets*,
Lecture Notes in Economics and Mathematical Systems,
DOI 10.1007/978-3-642-02909-7_6,

setup has already been proposed in Realdon (2007) for commodity price processes.[1] Korn (2005) specifies the equilibrium level process also as Ornstein–Uhlenbeck process, but models the log-price process similar to Schwartz and Smith as additionally composed process of a short-term and a long-term component. The FPDE for (6.1) is given by

$$\frac{\partial \Phi}{\partial t} + \left(\eta\{\mathfrak{X}_t - X_t\} - \frac{1}{2}\,V_t\right)\frac{\partial \Phi}{\partial X} + \kappa_{\mathfrak{X}}(\theta_{\mathfrak{X}} - \mathfrak{X}_t)\frac{\partial \Phi}{\partial \mathfrak{X}} + \frac{1}{2}\,V_t\,\frac{\partial^2 \Phi}{\partial X^2} + \frac{1}{2}\,\sigma_{\mathfrak{X}}^2\,\frac{\partial^2 \Phi}{\partial \mathfrak{X}^2} + \rho_{\mathfrak{X}}\sqrt{V_t}\,\sigma_{\mathfrak{X}}\frac{\partial^2 \Phi}{\partial X\,\partial \mathfrak{X}} = 0\,. \tag{6.2}$$

As in Sect. 4.1.2, the guess for Φ is exponential affine and of the form $\Phi = \exp\{i\,\phi\,e^{-\eta\tau}\,X_t + B(\tau)\,\mathfrak{X}_t + C(\tau)\}$. Under the restriction that $\eta \neq \kappa_{\mathfrak{X}}$, the solution for $B(\tau)$ is given by[2]

$$B(\tau) = \frac{\eta i \phi}{\eta - \kappa_{\mathfrak{X}}}\,(e^{-\kappa_{\mathfrak{X}}\tau} - e^{-\eta\tau})\,. \tag{6.3}$$

Realdon presents the ODE for $C(\tau)$ and solves for this function using numerical Runge-Kutta integration. However, it is possible to express the solution for $C(\tau)$ analytically:

$$\begin{aligned} C(\tau) = {} & \frac{i\phi}{2\eta}\,V_t\,(e^{-\eta\tau} - 1) + \frac{\eta\theta_{\mathfrak{X}} i\phi}{\eta - \kappa_{\mathfrak{X}}}\,(1 - e^{-\kappa_{\mathfrak{X}}\tau}) + \frac{\kappa_{\mathfrak{X}}\theta_{\mathfrak{X}} i\phi}{\eta - \kappa_{\mathfrak{X}}}\,(e^{-\eta\tau} - 1) \\ & + \frac{\phi^2}{4\eta}\,V_t\left(e^{-2\eta\tau} - 1\right) + \frac{\sigma_{\mathfrak{X}}^2\eta^2\phi^2}{2(\eta - \kappa_{\mathfrak{X}})^2}\left[\frac{1}{2\kappa_{\mathfrak{X}}}\left(e^{-2\kappa_{\mathfrak{X}}\tau} - 1\right)\right. \\ & \left. - \frac{2}{\kappa_{\mathfrak{X}} + \eta}\left(e^{-(\kappa_{\mathfrak{X}} + \eta)\tau} - 1\right) + \frac{1}{2\eta}\left(e^{-2\eta\tau} - 1\right)\right] \\ & + \frac{\rho_{\mathfrak{X}}\sigma_{\mathfrak{X}}\eta\phi^2}{\eta - \kappa_{\mathfrak{X}}}\sqrt{V_t}\left[\frac{1}{\kappa_{\mathfrak{X}} + \eta}\left(e^{-(\kappa_{\mathfrak{X}} + \eta)\tau} - 1\right) - \frac{1}{2\eta}\left(e^{-2\eta\tau} - 1\right)\right]. \end{aligned} \tag{6.4}$$

Special Case: $\eta = \kappa_{\mathfrak{X}}$

The special case solution presented in this paragraph is not included in Realdon. Under the restriction that the two adjustment speed parameters η and $\kappa_{\mathfrak{X}}$ are equal,

[1] However, the model setup in (6.1) does not entirely coincide with Realdon due to the term $-0.5V_t\,dt$ in the process for X_t. As already mentioned in Chap. 4, the additional term seems to be more reasonable when the model setup is based on the price process of the underlying with subsequent log-transformation.

[2] See Realdon (2007).

the solutions in (6.3) and (6.4) are not defined. The solutions for the two functions $B(\tau)$ and $C(\tau)$ are given as follows:

$$B(\tau) = \eta i \phi \tau e^{-\eta\tau}, \tag{6.5}$$

$$C(\tau) = \frac{i\phi}{\eta}\left(e^{-\eta\tau} - 1\right)\left(\frac{1}{2}V_t - \kappa_{\mathfrak{X}}\theta_{\mathfrak{X}}\right) - \tau\kappa_{\mathfrak{X}}\theta_{\mathfrak{X}} i\phi e^{-\eta\tau} + \frac{1}{4}\phi^2\sigma_{\mathfrak{X}}\tau e^{-2\eta\tau}$$
$$\times\left(\sigma_{\mathfrak{X}} + \eta\tau\sigma_{\mathfrak{X}} + 2\rho_{\mathfrak{X}}\sqrt{V_t}\right) + \frac{\phi^2}{4\eta}\left(e^{-2\eta\tau} - 1\right)\left(V_t + \frac{1}{2}\sigma_{\mathfrak{X}}^2 + \rho_{\mathfrak{X}}\sqrt{V_t}\sigma_{\mathfrak{X}}\right) \tag{6.6}$$

Realdon (2007) points out that this model is very tractable for the computation of options on futures since the distribution of X_T and $\mathfrak{X}_T$ conditional on initial values $X_t, \mathfrak{X}_t$ is Gaussian, but he is not able to express the variance of X_T in closed form.

6.1.2 Brownian Motion with Drift

Now consider a different specification of the subordinated equilibrium level process:

$$dX_t = \left(\eta\{\mathfrak{X}_t - X_t\} - \frac{1}{2}V_t\right)dt + \sqrt{V_t}\,dW_t^X$$
$$d\mathfrak{X}_t = \mu_{\mathfrak{X}}\,dt + \sigma_{\mathfrak{X}}\,dW_t^{\mathfrak{X}}. \tag{6.7}$$

Apart from the term $-\frac{1}{2}V_t\,dt$, the specification in (6.7) is similar to Schwartz and Smith (2000), though they work with a price process which is additionally composed of a zero mean Ornstein–Uhlenbeck process for the deviations from the long-run equilibrium and the attractor itself which follows the same SDE as in (6.7).[3] The drift in the subordinated process can be taken as inflation effect, when working with non-inflation-adjusted data.[4]

The setting in (6.7) is not fully equivalent to the setup in Schwartz and Smith, as one can see in the following.[5] The two processes in Schwartz and Smith are

$$d\chi^* = -\kappa^*\chi^* dt + \sigma_{\chi^*} dW_t^{\chi^*} \tag{6.8}$$

[3] Korn (2005) also comments on the equivalence of (6.7) to the Schwartz and Smith setup.

[4] A similar specification of the subordinated process for the long-term equilibrium level is given in Pilipović (1998). This model setup does not incorporate stochastic volatility.

[5] Schwartz and Smith (2000) demonstrate that their model setup is equivalent to the stochastic convenience yield model of Gibson and Schwartz (1990).

for the short-term deviations and

$$d\xi^* = \mu_{\xi^*}\,dt + \sigma_{\xi^*}\,dW_t^{\xi^*} \tag{6.9}$$

for the long-term equilibrium level.[6] The definitions of the equilibrium dynamics in (6.7) and (6.9) are identical. As for the price process, since $X_t = \chi_t^* + \xi_t^*$, the dynamics are given by

$$\begin{aligned} dX_t &= d\chi_t^* + d\xi_t^* \\ &= \left(-\kappa^*\chi^* + \mu_{\xi^*}\right)dt + \sigma_{\chi^*}\,dW_t^{\chi^*} + \sigma_{\xi^*}\,dW_t^{\xi^*}. \end{aligned} \tag{6.10}$$

We observe that the volatility terms will be equivalent for

$$\sqrt{V_t}\,dW_t^X = \sigma_{\chi^*}\,dW_t^{\chi^*} + \sigma_{\xi^*}\,dW_t^{\xi^*}.$$

The drift term in (6.10) will be equivalent to (6.7) if

$$-\eta\chi_t^* - \frac{1}{2}\,V_t = -\kappa^*\chi_t^* + \mu_{\xi^*}$$

holds.[7] Since the equivalence of the equilibrium levels requires $\mu_{\xi^*} = \mu_{\mathfrak{X}}$ to hold, it is not entirely possible to express the setup in (6.7) in terms of the parameters of Schwartz and Smith (2000), at least as long as $\mu_{\xi^*} = \mu_{\mathfrak{X}} \neq -\frac{1}{2}\,V_t$, which is a reasonable restriction.

To calculate the characteristic function, we set up the correspondent FPDE to (6.7) which is given by

$$\begin{aligned} &\frac{\partial\Phi}{\partial t} + \left(\eta\{\mathfrak{X}_t - X_t\} - \frac{1}{2}\,V_t\right)\frac{\partial\Phi}{\partial X} + \mu_{\mathfrak{X}}\frac{\partial\Phi}{\partial\mathfrak{X}} \\ &\quad + \frac{1}{2}\,V_t\,\frac{\partial^2\Phi}{\partial X^2} + \frac{1}{2}\,\sigma_{\mathfrak{X}}^2\,\frac{\partial^2\Phi}{\partial\mathfrak{X}^2} + \rho_{\mathfrak{X}}\sqrt{V_t}\,\sigma_{\mathfrak{X}}\frac{\partial^2\Phi}{\partial X\,\partial\mathfrak{X}} = 0\,. \end{aligned} \tag{6.11}$$

The guess for Φ is the same as in Sect. 6.1.1. The solutions for the functions $B(\tau)$ and $C(\tau)$ with respect to the boundary conditions are given as follows:

$$B(\tau) = i\phi\,(1 - e^{-\eta\tau}) \tag{6.12}$$

[6] For notational convenience, we arrange the Schwartz and Smith model parameters in this subsection with an asterisk.

[7] Note that the short term deviations χ_t^* are linked to the model parameters in (6.7) via $\chi_t^* = X_t - \mathfrak{X}_t$.

$$C(\tau) = \mu_{\mathfrak{X}} i\phi\tau - \frac{1}{2}\sigma_{\mathfrak{X}}^2\phi^2\tau + \frac{i\phi}{\eta}\left(e^{-\eta\tau} - 1\right)\left[\frac{1}{2}V_t + \mu_{\mathfrak{X}} + i\phi\sigma_{\mathfrak{X}}^2 - \rho_{\mathfrak{X}}\sqrt{V_t}\,\sigma_{\mathfrak{X}} i\phi\right] + \frac{\phi^2}{4\eta}\left(1 - e^{-2\eta\tau}\right)\left[2\rho_{\mathfrak{X}}\sqrt{V_t}\,\sigma_{\mathfrak{X}} - V_t - \sigma_{\mathfrak{X}}^2\right]. \quad (6.13)$$

6.2 Integration of Square-Root Stochastic Volatility

6.2.1 Mean-Reverting Equilibrium Level

In this section, the process assumptions as described in Sect. 6.1 are extended by square-root stochastic volatility. For arithmetic reasons, we slightly modify the volatility of the equilibrium level process. We arrive at a three factor model driven by the following system of SDEs:

$$\begin{aligned} dX_t &= (\eta\{\mathfrak{X}_t - X_t\} - \frac{1}{2}V_t)\,dt + \sqrt{V_t}\,dW_t^X \\ d\mathfrak{X}_t &= \kappa_{\mathfrak{X}}(\theta_{\mathfrak{X}} - \mathfrak{X}_t)\,dt + \sigma_{\mathfrak{X}}\sqrt{V_t}\,dW_t^{\mathfrak{X}} \\ dV_t &= \kappa(\theta - V_t)dt + \zeta\sqrt{V_t}\,dW_t^V\,. \end{aligned} \quad (6.14)$$

The Brownian motions are allowed to be pairwise correlated via

$$\begin{aligned} dW_t^X \cdot dW_t^V &= \rho dt \\ dW_t^X \cdot dW_t^{\mathfrak{X}} &= \rho_{\mathfrak{X}} dt \\ dW_t^{\mathfrak{X}} \cdot dW_t^V &= \rho_{\mathfrak{X}V}\,dt\,. \end{aligned}$$

The FPDE for this setting reads

$$\begin{aligned} &\frac{\partial\Phi}{\partial t} + \left(\eta\{\mathfrak{X}_t - X_t\} - \frac{1}{2}V_t\right)\frac{\partial\Phi}{\partial X} + \mu_{\mathfrak{X}}\frac{\partial\Phi}{\partial\mathfrak{X}} + \kappa(\theta - V_t)\frac{\partial\Phi}{\partial V} \\ &\quad + \frac{1}{2}V_t\frac{\partial^2\Phi}{\partial X^2} + \frac{1}{2}\sigma_{\mathfrak{X}}^2\frac{\partial^2\Phi}{\partial\mathfrak{X}^2} + \frac{1}{2}\zeta^2 V_t\frac{\partial^2\Phi}{\partial V^2} + \rho V_t\zeta\frac{\partial^2\Phi}{\partial X\,\partial V} \\ &\quad + \rho_{\mathfrak{X}} V_t\,\sigma_{\mathfrak{X}}\frac{\partial^2\Phi}{\partial X\,\partial\mathfrak{X}} + \rho_{\mathfrak{X}V}V_t\sigma_{\mathfrak{X}}\zeta\frac{\partial^2\Phi}{\partial V\,\partial\mathfrak{X}} = 0\,. \end{aligned} \quad (6.15)$$

We apply a guess for Φ of the form $\Phi = \exp\{i\phi e^{-\eta\tau}X_t + B(\tau)\mathfrak{X}_t + C(\tau)V_t + D(\tau)\}$. The solution for $B(\tau)$ is given by (6.3), respectively by (6.5), when $\eta = \kappa_{\mathfrak{X}}$ holds. Unfortunately, two subordinated mean-reverting processes inhibit a closed-form solution for $C(\tau)$ and $D(\tau)$ in terms of hypergeometric functions. The ODEs for the two remaining functions are given by

$$\frac{\mathrm{d}C(\tau)}{\mathrm{d}\tau} = -\frac{1}{2}\,i\phi e^{-\eta\tau} + \frac{1}{2}\,(i\phi)^2 e^{-2\eta\tau} + \frac{1}{2}\sigma_{\mathfrak{X}}^2 B^2(\tau) + \rho_{\mathfrak{X}}\sigma_{\mathfrak{X}} i\phi e^{-\eta\tau} B(\tau)$$

$$+ \left[\rho\zeta i\phi e^{-\eta\tau} - \kappa + \rho_{\mathfrak{X}V}\zeta\sigma_{\mathfrak{X}} B(\tau)\right] C(\tau) + \frac{1}{2}\,\zeta^2 C^2(\tau) \tag{6.16}$$

$$\frac{\mathrm{d}D(\tau)}{\mathrm{d}\tau} = \kappa\theta C(\tau) + \kappa_{\mathfrak{X}}\theta_{\mathfrak{X}} B(\tau)\,. \tag{6.17}$$

6.2.2 Brownian Motion with Drift

Now consider the integration of square-root stochastic volatility in the SDE system defined by (6.7).[8]

$$\begin{aligned} dX_t &= (\eta\{\mathfrak{X}_t - X_t\} - \frac{1}{2}\,V_t)\,dt + \sqrt{V_t}\,dW_t^X \\ d\mathfrak{X}_t &= \mu_{\mathfrak{X}}\,dt + \sigma_{\mathfrak{X}}\,\sqrt{V_t}\,dW_t^{\mathfrak{X}} \\ dV_t &= \kappa(\theta - V_t)dt + \zeta\,\sqrt{V_t}\,dW_t^V\,. \end{aligned} \tag{6.18}$$

Again, the Brownian motions are allowed to be pairwise correlated as in the previous subsection. The FPDE is similar to (6.15). For this model setting, it is possible to derive a solution for Φ in terms of hypergeometric functions similar to Sect. 4.1. The insertion of the corresponding partial derivatives in (6.15) leads to the well-known solution $B(\tau) = i\phi(1 - e^{-\eta\tau})$ together with a system of two ODEs:

$$\begin{aligned} \frac{\mathrm{d}C(\tau)}{\mathrm{d}\tau} &= -\frac{1}{2}\,i\phi e^{-\eta\tau} + \frac{1}{2}\,(i\phi)^2 e^{-2\eta\tau} + \frac{1}{2}\sigma_{\mathfrak{X}}^2 (i\phi)^2\,(1 - e^{-\eta\tau})^2 \\ &\quad + \rho_{\mathfrak{X}}\sigma_{\mathfrak{X}}(i\phi)^2 e^{-\eta\tau}\,(1 - e^{-\eta\tau}) + [\rho\zeta i\phi e^{-\eta\tau} - \kappa \\ &\quad + \rho_{\mathfrak{X}V}\zeta\sigma_{\mathfrak{X}} i\phi\,(1 - e^{-\eta\tau})]\,C(\tau) + \frac{1}{2}\,\zeta^2 C^2(\tau) \\ \frac{\mathrm{d}D(\tau)}{\mathrm{d}\tau} &= \kappa\theta C(\tau) + \mu_{\mathfrak{X}} i\phi\,(1 - e^{-\eta\tau})\,, \end{aligned} \tag{6.19}$$

with boundary conditions $C(0) = D(0) = 0$.

Consider the first in (6.19). We make the same transformation $G(\tau) = \exp\{-\int \frac{1}{2}\,\zeta^2 C(\tau)\,d\tau\}$ and substitution $\upsilon = i\phi\,e^{-\eta\tau}$ as in Sect. 4.1.2 to obtain a linear homogenous second order equation of the form

[8] The volatility of the equilibrium level process is modified as in the previous subsection.

$$\eta^2\upsilon^2\frac{\mathrm{d}^2G(\upsilon)}{\mathrm{d}\upsilon^2}+\eta\left[\upsilon^2\left\{\rho\zeta-\rho_{\mathfrak{x}V}\zeta\sigma_{\mathfrak{x}}\right\}+\upsilon\left\{\eta+\rho_{\mathfrak{x}V}\zeta\sigma_{\mathfrak{x}}i\phi-\kappa\right\}\right]\frac{\mathrm{d}G(\upsilon)}{\mathrm{d}\upsilon}$$
$$+\frac{1}{2}\zeta^2\left[\upsilon^2\left\{\frac{1}{2}+\frac{1}{2}\sigma_{\mathfrak{x}}^2-\rho_{\mathfrak{x}}\sigma_{\mathfrak{x}}\right\}+\upsilon\left\{\rho_{\mathfrak{x}}\sigma_{\mathfrak{x}}i\phi-i\phi\sigma_{\mathfrak{x}}^2-\frac{1}{2}\right\}\right.$$
$$\left.+\frac{1}{2}\sigma_{\mathfrak{x}}^2(i\phi)^2\right]G(\upsilon)=0\,. \tag{6.20}$$

Now substitute $G(\upsilon)=\upsilon^pH(\upsilon)$, where[9]

$$p=\frac{1}{2\eta}\left(\rho_{\mathfrak{x}V}\zeta\sigma_{\mathfrak{x}}i\phi-\kappa\pm\sqrt{\left(\rho_{\mathfrak{x}V}\zeta\sigma_{\mathfrak{x}}i\phi-\kappa\right)^2-\sigma_{\mathfrak{x}}^2\zeta^2(i\phi)^2}\right). \tag{6.21}$$

The substitution with one of the two possible values for p as defined by the $\pm$-sign in (6.21) leads to

$$\eta^2\upsilon\frac{\mathrm{d}^2H(\upsilon)}{\mathrm{d}\upsilon^2}+\eta\left[\upsilon\left\{\rho\zeta-\rho_{\mathfrak{x}V}\zeta\sigma_{\mathfrak{x}}\right\}+2\eta p+\eta+\rho_{\mathfrak{x}V}\zeta\sigma_{\mathfrak{x}}i\phi-\kappa\right]\frac{\mathrm{d}H(\upsilon)}{\mathrm{d}\upsilon}$$
$$+\left[\frac{1}{2}\zeta^2\upsilon\left\{\frac{1}{2}+\frac{1}{2}\sigma_{\mathfrak{x}}^2-\rho_{\mathfrak{x}}\sigma_{\mathfrak{x}}\right\}+\eta\left\{\rho\zeta-\rho_{\mathfrak{x}V}\zeta\sigma_{\mathfrak{x}}\right\}p\right.$$
$$\left.+\frac{1}{2}\zeta^2\left\{\rho_{\mathfrak{x}}\sigma_{\mathfrak{x}}i\phi-i\phi\sigma_{\mathfrak{x}}^2-\frac{1}{2}\right\}\right]H(\upsilon)=0\,. \tag{6.22}$$

For both values of p, the substitution $G(\upsilon)=\upsilon^pH(\upsilon)$ transforms (6.20) into (6.22). After the backward substitutions, both alternatives should lead to the same result. We tested both values for p and obtained the same solutions, as expected. However, the choice of the plus sign is superior for two reasons. Firstly, our tests did not reveal a case where the algorithm fails when the plus sign is chosen, and secondly, the special case 1 solution can only occur when the minus sign is applied (see also Sect. 6.2.2).[10] Hence, the special case 1 solution can be omitted when p is determined by the plus sign.

The structure of (6.22) is equivalent to (4.9) in Chap. 4. Hence, we present a general case and two special case solutions in line with the proceeding in Chap. 4. It is worth noting that to the best of our knowledge, the extension of a mean reverting price process with both stochastic equilibrium level and stochastic volatility is presented in the following paragraphs in the first place.

[9] See Polyanin and Zaitsev (2003), p. 229.

[10] Contrary, the application of the minus sign may lead to convergence difficulties in the "hyper" subroutine of the translated Fortran code in Barrowes (2004).

General Case Solution

The restriction for the general case solution for (6.22) is that

$$\rho^2 - 1 + \sigma_{\mathfrak{X}}^2(\rho_{\mathfrak{X}V}^2 - 1) - 2\sigma_{\mathfrak{X}}(\rho\rho_{\mathfrak{X}V} - \rho_{\mathfrak{X}}) \neq 0$$

holds. One subset of parameter settings which fulfill this condition is obviously $\rho \neq \pm 1$ and $\rho_{\mathfrak{X}V} \neq \pm 1$ together with $\rho_{\mathfrak{X}} \neq \rho \cdot \rho_{\mathfrak{X}V}$.

Under the additional restriction that the parameter b which is defined below is neither zero nor a negative integer, the solution for $H(\upsilon)$ is given by[11]

$$H(\upsilon) = \exp\{d\,\upsilon\}\left[\mathfrak{C}_1 M\left(a, b, c\upsilon\right) + \mathfrak{C}_2 U\left(a, b, c\upsilon\right)\right], \tag{6.23}$$

where

$$a = \frac{f}{\eta\zeta\sqrt{\rho^2 - 1 - 2\sigma_{\mathfrak{X}}(\rho_{\mathfrak{X}V} - \rho_{\mathfrak{X}}) + \sigma_{\mathfrak{X}}^2(\rho_{\mathfrak{X}V}^2 - 1)}}$$

$$b = 2p + \frac{1}{\eta}\left(\eta - \kappa + \rho_{\mathfrak{X}V}\zeta\sigma_{\mathfrak{X}} i\phi\right)$$

$$c = \frac{\zeta\sqrt{\rho^2 - 1 - 2\sigma_{\mathfrak{X}}(\rho_{\mathfrak{X}V} - \rho_{\mathfrak{X}}) + \sigma_{\mathfrak{X}}^2(\rho_{\mathfrak{X}V}^2 - 1)}}{-2\eta}$$

$$d = \frac{\zeta}{2\eta}\left[\sqrt{\rho^2 - 1 - 2\sigma_{\mathfrak{X}}(\rho_{\mathfrak{X}V} - \rho_{\mathfrak{X}}) + \sigma_{\mathfrak{X}}^2(\rho_{\mathfrak{X}V}^2 - 1)} - (\rho - \rho_{\mathfrak{X}V}\sigma_{\mathfrak{X}})\right],$$

and

$$f = \frac{\zeta}{2}\left[\eta - \kappa + \rho_{\mathfrak{X}V}\zeta\sigma_{\mathfrak{X}} i\phi\right]\left[\sqrt{\rho^2 - 1 - 2\sigma_{\mathfrak{X}}(\rho_{\mathfrak{X}V} - \rho_{\mathfrak{X}}) + \sigma_{\mathfrak{X}}^2(\rho_{\mathfrak{X}V}^2 - 1)}\right.$$

$$\left. - (\rho - \rho_{\mathfrak{X}V}\sigma_{\mathfrak{X}})\right] + \frac{1}{2}\zeta^2\left(\rho_{\mathfrak{X}}\sigma_{\mathfrak{X}} i\phi - i\phi\sigma_{\mathfrak{X}}^2 - \frac{1}{2}\right).$$

The application of the backward substitutions $G(\upsilon) = \upsilon^p H(\upsilon)$, $\upsilon = i\phi e^{-\eta\tau}$ and

$$C(\tau) = -\frac{2}{\zeta^2}\frac{G'(\tau)}{G(\tau)}$$

[11] Polyanin and Zaitsev (2003), p. 225.

leads to

$$C(\tau) = \frac{2\eta}{\zeta^2}\Bigg[p + \frac{d}{c}\,g(\tau) + ag(\tau)\,\frac{\mathfrak{C}b^{-1}M\,(1+a,1+b,g(\tau)) - U\,(1+a,1+b,g(\tau))}{\mathfrak{C}M\,(a,b,g(\tau)) + U\,(a,b,g(\tau))}\Bigg], \tag{6.24}$$

with auxiliary function

$$g(\tau) = c\,i\phi\,e^{-\eta\tau}$$

and integration constant

$$\mathfrak{C} = \frac{\mathfrak{C}_1}{\mathfrak{C}_2} = \frac{ag(0)U\,(1+a,1+b,g(0)) - \left(p + \frac{d}{c}\,g(0)\right)U\,(a,b,g(0))}{\frac{a}{b}\,g(0)M\,(1+a,1+b,g(0)) + \left(p + \frac{d}{c}\,g(0)\right)M\,(a,b,g(0))}.$$

The insertion of (6.24) in the second ODE in (6.19) together with the application of the boundary condition leads to

$$D(\tau) = \frac{2\kappa\theta}{\zeta^2}\left[\eta p\tau + d\,i\phi\,(1-e^{-\eta\tau}) - \ln\left(\frac{\mathfrak{C}M\,(a,b,g(\tau)) + U\,(a,b,g(\tau))}{\mathfrak{C}M\,(a,b,g(0)) + U\,(a,b,g(0))}\right)\right] + \frac{\mu_{\mathfrak{X}} i\phi}{\eta}\,(\tau\eta + e^{-\eta\tau} - 1)\,. \tag{6.25}$$

Special Case 1 Solution

The first parameter restriction for the special case 1 solution is equivalent to the general case condition, which implies that

$$\rho^2 - 1 + \sigma_{\mathfrak{X}}^2(\rho_{\mathfrak{X}V}^2 - 1) - 2\sigma_{\mathfrak{X}}(\rho\rho_{\mathfrak{X}V} - \rho_{\mathfrak{X}}) \neq 0$$

holds. Additionally, we now presume that the Kummer function parameter b is zero or a negative integer. Since b depends on p, which is itself a solution of a quadratic equation, the condition for b being zero or a negative integer is up to the $\pm$-sign in (6.21).

$$b = 1 \pm \sqrt{(\rho_{\mathfrak{X}V}\zeta\sigma_{\mathfrak{X}} i\phi - \kappa)^2 - \sigma_{\mathfrak{X}}^2\zeta^2(i\phi)^2} \neq 0, -1, -2, \ldots \tag{6.26}$$

The square root in (6.26) provides positive real numbers or imaginary numbers, but not negative real numbers. Therefore, negative integer solutions for b are only possible when the minus sign in (6.26), respectively in (6.21), is chosen. Our tests did not reveal cases where the choice of the plus sign in (6.26) fails to provide accurate solutions. Hence, we assert that a full presentation of this special case is not needed and restrict ourselves to the general solution for $H(\upsilon)$[12]:

$$H(\upsilon) = e^{d\upsilon}\,(c\upsilon)^{1-b}\,[\mathcal{C}_1 M\,(a-b+1, 2-b, c\upsilon) + \mathcal{C}_2 U\,(a-b+1, 2-b, c\upsilon)]\,, \tag{6.27}$$

with the same parameters a, b, c and d as in the previous paragraph.

Special Case 2 Solution

Under the condition that

$$\rho^2 - 1 + \sigma_{\mathfrak{x}}^2(\rho_{\mathfrak{x}V}^2 - 1) - 2\sigma_{\mathfrak{x}}(\rho\rho_{\mathfrak{x}V} - \rho_{\mathfrak{x}}) = 0$$

holds, the solution for $H(\upsilon)$ is given in terms of Bessel functions (see also Sect. 4.2.3).

$$H(\upsilon) = \exp\left\{\frac{\zeta}{2\eta}\,(\rho_{\mathfrak{x}V}\sigma_{\mathfrak{x}} - \rho)\,\upsilon\right\}\,\upsilon^{\frac{q}{2}}\,\left[\mathcal{C}_1 J_q\left(2\sqrt{z\upsilon}\right) + \mathcal{C}_2 Y_q\left(2\sqrt{z\upsilon}\right)\right]\,, \tag{6.28}$$

where

$$q = 1 - 2p - \frac{1}{\eta}\,(\eta - \kappa + \rho_{\mathfrak{x}V}\zeta\sigma_{\mathfrak{x}} i\phi) \tag{6.29}$$

$$z = \frac{\zeta}{2}\,(\eta - \kappa + \rho_{\mathfrak{x}V}\zeta\sigma_{\mathfrak{x}} i\phi)\,(\rho_{\mathfrak{x}V}\sigma_{\mathfrak{x}} - \rho) + \frac{1}{2}\,\zeta^2\left(\rho_{\mathfrak{x}}\sigma_{\mathfrak{x}} i\phi - i\phi\sigma_{\mathfrak{x}}^2 - \frac{1}{2}\right)\,.$$

Note that the Bessel functions in this subsection are of complex order and complex argument.[13] The order of the Bessel functions in (6.28) is given by (6.29). Equation

[12] Polyanin and Zaitsev (2003), p. 222.

[13] The Matlab® package only includes Bessel functions of real order. We tested two ways to calculate complex order Bessel functions. Firstly, we implemented a Maple™ call which on the one hand offers high accuracy, but on the other hand is conducted with long computation time (though this calculation method is still slightly faster than numerical integration methods). Secondly, we used Matlab® source code provided by H. Cai from Northwestern University at Chicago (Cai (2006), this code is available via the Matlab® central file exchange). We slightly modified the code to achieve higher accuracy. The modified code provides identical results up to the twelfth decimal place and is about six times faster than the Maple™ function calls. However, the calculation still takes much more time when working with complex order Bessel functions instead of real order Bessel functions as given in Sect. 4.2.3.

(6.29) is a real number for all reasonable parameter settings when $\phi = -i$ holds, i.e. in the case of the calculation of futures prices. For other values of ϕ, (6.29) is a complex number when $\rho_{\mathfrak{X}V} \neq 0$, $\zeta \neq 0$ and $\sigma_{\mathfrak{X}} \neq 0$ holds. The latter two restrictions are less interesting since they refer to deterministic subordinated processes. Hence, the order of the Bessel functions is always a complex number when the correlation of the two subordinated stochastic processes is nonzero.

The application of the backward substitutions as in the first paragraph of this subsection leads to

$$C(\tau) = \frac{2\eta p}{\zeta^2} + \frac{1}{\zeta}\left(\rho_{\mathfrak{X}V}\sigma_{\mathfrak{X}} - \rho\right) i\phi e^{-\eta\tau} + \frac{2\eta}{\zeta^2} h(\tau) \frac{\mathcal{C} J_{q-1}\left(2h(\tau)\right) + Y_{q-1}\left(2h(\tau)\right)}{\mathcal{C} J_q\left(2h(\tau)\right) + Y_q\left(2h(\tau)\right)}, \tag{6.30}$$

with auxiliary function

$$h(\tau) = \sqrt{z\, i\phi\, e^{-\eta\tau}}$$

and integration constant

$$\mathcal{C} = \frac{\mathcal{C}_1}{\mathcal{C}_2} = \frac{\frac{2\eta}{\zeta^2} h(0) Y_{q-1}\left(2h(0)\right) - \left[\frac{1}{\zeta}(\rho - \rho_{\mathfrak{X}V}\sigma_{\mathfrak{X}}) i\phi - \frac{2\eta p}{\zeta^2}\right] Y_q\left(2h(0)\right)}{\left[\frac{1}{\zeta}(\rho - \rho_{\mathfrak{X}V}\sigma_{\mathfrak{X}}) i\phi - \frac{2\eta p}{\zeta^2}\right] J_q\left(2h(0)\right) - \frac{2\eta}{\zeta^2} h(0) J_{q-1}\left(2h(0)\right)}.$$

Apply the solution for $C(\tau)$ as given in (6.30) in the second ODE in (6.19) to obtain

$$\begin{aligned} D(\tau) = {} & \frac{2\kappa\theta}{\zeta^2}\left(p + \frac{q}{2}\right)\tau + \frac{\kappa\theta}{\eta\zeta}\left(\rho_{\mathfrak{X}V}\sigma_{\mathfrak{X}} - \rho\right) i\phi\left(1 - e^{-\eta\tau}\right) \\ & - \frac{2\kappa\theta}{\zeta^2} \ln\left(\frac{\mathcal{C} J_q\left(2h(\tau)\right) + Y_q\left(2h(\tau)\right)}{\mathcal{C} J_q\left(2h(0)\right) + Y_q\left(2h(0)\right)}\right) + \frac{\mu_{\mathfrak{X}} i\phi}{\eta}\left(\tau\eta + e^{-\eta\tau} - 1\right). \end{aligned} \tag{6.31}$$

Comparison with the Monte-Carlo Solution

We simulated the evolution of the SDE system in (6.18) with the following parameter setting: $S = 80$, $\mathfrak{X} = 85$, $\eta = 1$, $T - t = 0.5$, $\zeta = 0.2$, $\sqrt{V} = 0.2$, $\kappa = 1$, $\rho = -0.5$, $\theta = 0.05$, $\mu_{\mathfrak{X}} = 0.1$, $\sigma_{\mathfrak{X}} = 0.2$, $\rho_{\mathfrak{X}V} = 0.5$, $\rho_{\mathfrak{X}} = 0.3$. The parameter setting refers to the general case solution as given in (6.24) and (6.25).

Since we have to simulate three pairwise correlated Brownian motions, we firstly applied a Cholesky decomposition of the correlation matrix.[14] The output of the Cholesky decomposition is a lower triangular matrix $\mathbf{L}$ which can be used

[14] Under the restrictions that the Matrix $\mathbf{M}$ is Hermitian and positive definite, the Cholesky decomposition can be applied. Since a Hermitian matrix with real entries is symmetric, these restrictions are always fulfilled by a valid correlation matrix. The matrix is decomposed according to $\mathbf{M} = \mathbf{L}\mathbf{L}^T$, where $\mathbf{L}^T$ is the transpose of $\mathbf{L}$.

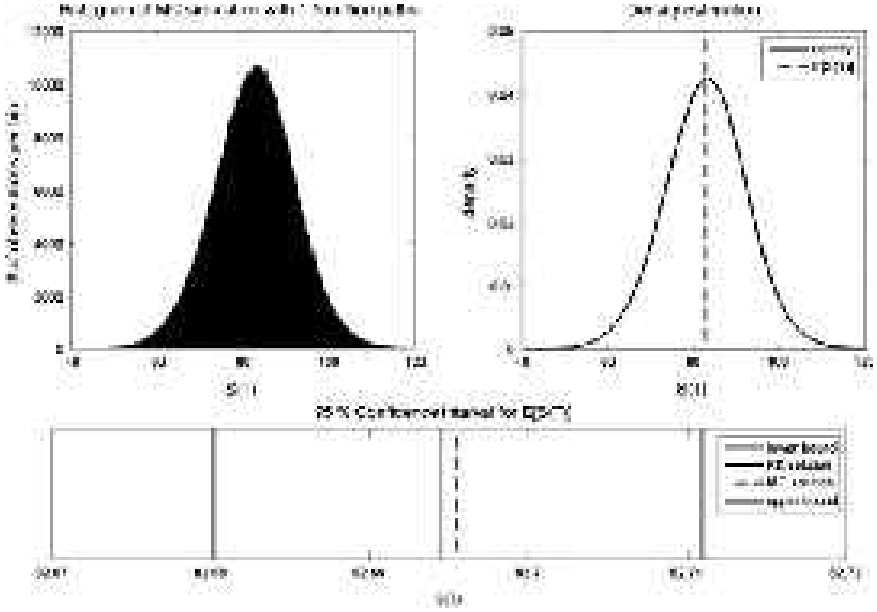

Fig. 6.1 Histogram, density function and confidence interval for the OU model with stochastic equilibrium level and square-root stochastic volatility

to transform a vector of independent pseudo random numbers $\tilde{\mathbf{z}}$ into a vector $\mathbf{L}\tilde{\mathbf{z}}$ with the wanted covariance properties. The results of the simulation are displayed in Fig. 6.1.

The shape of the distribution is quite similar to the square-root stochastic volatility case without stochastic equilibrium level. The skewness is -0.031 compared with -0.083 in Sect. 4.1.3, while the kurtosis is slightly larger (3.201 compared with 3.173). The overall volatility of the underlying is also larger, which results in a bigger confidence interval for F. The 95 % confidence interval for the spot price at time T is $[82.6801, 82.7109]$. As expected, the analytical value $F = 82.6945$ lies within the confidence interval and matches quite well the MC solution which is 82.6955.

The price of a European call is higher than in the reference case ($C = 5.1905$ compared with 4.5770 in Sect. 4.1.3).

6.3 Other Model Extensions

There are numerous possibilities to combine the basic setup of this chapter, a mean reverting price process with subordinated stochastic equilibrium level process, with other stochastic factors. In this section, we discuss the combination with

Ornstein–Uhlenbeck stochastic volatility as well as with different types of jumps as discussed in Chap. 5. In all these cases, one needs numerical integration schemes as discussed in Sect. 3.6 to recover the solutions of the ODE systems.

6.3.1 Ornstein–Uhlenbeck Stochastic Volatility

The adaption of the SDE system (6.18) in the previous section to Ornstein–Uhlenbeck stochastic volatility is given as follows:

$$\begin{aligned} dX_t &= (\eta\{\mathfrak{X}_t - X_t\} - \frac{1}{2}\sigma_t^2)\,dt + \sigma_t\,dW_t^X \\ d\mathfrak{X}_t &= \mu_{\mathfrak{X}}\,dt + \sigma_{\mathfrak{X}}\,dW_t^{\mathfrak{X}} \\ d\sigma_t &= \kappa(\theta - \sigma_t)dt + \zeta\,dW_t^{\sigma}\,. \end{aligned} \tag{6.32}$$

We omit the presentation of the FPDE which is very similar to Sect. 6.2.2. We apply the exponential linear-quadratic guess

$$\Phi = \exp\left\{i\phi e^{-\eta\tau}X_t + i\phi(1-e^{-\eta\tau})\mathfrak{X}_t + C(\tau)\sigma_t^2 + D(\tau)\sigma_t + E(\tau)\right\}$$

and arrive at the wanted system of ODEs:

$$\begin{aligned} \frac{\mathrm{d}C(\tau)}{\mathrm{d}\tau} &= -\frac{1}{2}i\phi e^{-\eta\tau} - 2\kappa C(\tau) - \frac{1}{2}\phi^2 e^{-2\eta\tau} + 2\zeta^2 C^2(\tau) + 2\rho\zeta i\phi e^{-\eta\tau}C(\tau) \\ \frac{\mathrm{d}D(\tau)}{\mathrm{d}\tau} &= 2\kappa\theta C(\tau) - \kappa D(\tau) + 2\zeta^2 C(\tau)D(\tau) + \rho\zeta i\phi e^{-\eta\tau}D(\tau) \\ &\quad - \rho_{\mathfrak{X}}\sigma_{\mathfrak{X}}\phi^2 e^{-\eta\tau}(1-e^{-\eta\tau}) + 2\rho_{\mathfrak{X}\sigma}\zeta\sigma_{\mathfrak{X}}i\phi(1-e^{-\eta\tau})C(\tau) \\ \frac{\mathrm{d}E(\tau)}{\mathrm{d}\tau} &= \kappa\theta D(\tau) + \mu_{\mathfrak{X}}i\phi(1-e^{-\eta\tau}) - \frac{1}{2}\sigma_{\mathfrak{X}}^2\phi^2(1-2e^{-\eta\tau}+e^{-2\eta\tau}) + \zeta^2 C(\tau) \\ &\quad + \frac{1}{2}\zeta^2 D^2(\tau) + \rho_{\mathfrak{X}\sigma}\zeta\sigma_{\mathfrak{X}}i\phi(1-e^{-\eta\tau})D(\tau)\,, \end{aligned} \tag{6.33}$$

where $\rho_{\mathfrak{X}\sigma}dt = dW_t^{\sigma}dW_t^{\mathfrak{X}}$. As in Sect. 4.2, this ODE system has to be solved with numerical integration methods.

Of course, it is also possible to combine a mean-reverting stochastic equilibrium level with Ornstein–Uhlenbeck stochastic volatility. The resulting ODE system has also to be solved with Runge-Kutta integration. Since the adaption is very similar to the ODE system already presented in this subsection, we omit the presentation of the ODE system for both mean-reverting stochastic equilibrium level and OU stochastic volatility in this place.

6.3.2 Model Extensions with Jump Components

The incorporation of jump components as discussed in Chap. 5 in the framework of this chapter leads also to ODE systems which have to be solved with the Runge-Kutta algorithm. The jump components affect the ODE of the function which is associated with none of the state variables, i.e. the function corresponding with constants.[15]

For lognormally distributed jumps in the price process, one has to incorporate the term

$$\lambda^X \exp\left\{ i\phi e^{-\eta\tau}\left[\ln(1+\mu_J) - \frac{1}{2}\sigma_J^2\right] - \frac{1}{2}\phi^2 e^{-2\eta\tau}\sigma_J^2\right\} - \lambda^X . \tag{6.34}$$

In case of exponentially or Γ-distributed jumps in the variance process, the term (5.18) (respectively the jump term in (5.20)) is added to the ODE of the appropriate function. Independent jumps in both the price and variance process can be incorporated by adding both terms to the ODE. Correlated jumps in the price and variance process can be considered by adding (5.27) (respectively by adding the jump term in (5.29) when considering Γ-distributed variance jumps). Note that in case of jumps in the price process, one has also to bear in mind the drift term correction as discussed in Chap. 5.

Finally, we consider lognormally distributed jumps in the subordinated process of the equilibrium level. Not surprisingly, the jump term which is added to the constant function ODE is similar to (6.34) and reads

$$\begin{aligned}\lambda^{\mathfrak{X}} \exp\{ i\phi(1-e^{-\eta\tau})\left[\ln(1+\mu_J^{\mathfrak{X}}) - \frac{1}{2}(\sigma_J^{\mathfrak{X}})^2\right] \\ - \frac{1}{2}\phi^2(1-2e^{-\eta\tau}+e^{-2\eta\tau})(\sigma_J^{\mathfrak{X}})^2\} - \lambda^{\mathfrak{X}} ,\end{aligned} \tag{6.35}$$

where $\lambda^{\mathfrak{X}}$ is the intensity of the equilibrium level jump process and the jump in $\mathfrak{X}$ is normally distributed with parameters $\ln\left(1+\mu_J^{\mathfrak{X}}\right) - 0.5(\sigma_J^{\mathfrak{X}})^2$ and $(\sigma_J^{\mathfrak{X}})^2$.

[15] This is the function $C(\tau)$ in Sect. 6.1.2, $D(\tau)$ in Sect. 6.2.2 and $E(\tau)$ in Sect. 6.3.1.

Chapter 7
Deterministic Seasonality Effects

Seasonality in price movements and volatility is an important difference between certain commodity classes and standard financial assets. Especially for agricultural commodities, one observes a repeating cyclical pattern of decreasing prices at the harvesting period and after the harvest and a peak in prices a few months before the harvest. Empirically, one can observe the seasonality in the term structure of futures prices for agricultural goods such as wheat or soybeans. While agricultural and animal products do show a seasonality effect, other groups of commodities such as metals or other raw materials do not.[1] Furthermore, electricity futures prices share both a mean reverting and a seasonal property, due to the cyclical behavior of consumption which is mainly driven by the seasonal evolution of temperatures.[2]

The case of soybeans is investigated by Richter and Sørensen (2002), who model the soybean price process with subordinated stochastic volatility and convenience yield processes. They incorporate seasonality in the convenience yield process. The price process is not mean-reverting and the seasonality effect makes an indirect impact on prices through the convenience yield process and through a seasonal impact of volatility. Richter and Sørensen provide an empirical survey with a parameter estimation based on soybean futures and options on futures prices.

A similar model setup can be found in Sørensen (2002), who incorporates the seasonality effect directly in the price process. The log-price process is additionally composed of a Black and Scholes SDE, the deterministic seasonality component and a third component which is driven by a zero mean Ornstein–Uhlenbeck process. Sørensen provides an empirical analysis based on corn, wheat and soybean futures prices.

A direct implementation of a deterministic seasonality component can also be found in Lucia and Schwartz (2002), who examine the seasonal behavior of electricity futures in the Nord Pool power exchange.[3] They model the log-price basically as

[1] See Fama and French (1987) for an empirical evidence of this finding. Seasonality in agricultural commodity futures is consistent with studies by Chatrath et al. (2002) and Adrangi and Chatrath (2003).

[2] See e.g. Lucia and Schwartz (2002).

[3] Nord Pool is the power exchange of the Nordic power market, including Denmark, Finland, Norway and Sweden.

B. Lutz, *Pricing of Derivatives on Mean-Reverting Assets*,
Lecture Notes in Economics and Mathematical Systems,
DOI 10.1007/978-3-642-02909-7_7,

a sum of a constant level parameter, a deterministic seasonal component and a zero mean Ornstein–Uhlenbeck process.

7.1 Seasonality in the Log-Price Process

In the following, we incorporate a deterministic seasonal component directly in the log-price process. Our approach follows Richter and Sørensen (2002) and Sørensen (2002) as for the specification of the seasonal component, though their models cannot be recovered within the framework of this section, since they either implement the seasonal component in the subordinated process (see Sect. 7.2) or in the log-price process, but without mean-reversion of the underlying.

We specify the log-price process as

$$dX_t = (\mathfrak{S}_t^X + \eta\{\overline{X} - X_t\} - \frac{1}{2} V_t)\, dt + \sqrt{V_t}\, dW_t^X\,, \tag{7.1}$$

where $\mathfrak{S}_t^X$ is the deterministic seasonal component defined by

$$\mathfrak{S}_t^X = \Lambda_1^X \cos\big(2\pi t\big) + \Lambda_2^X \sin\big(2\pi t\big)\,. \tag{7.2}$$

Hence, the increment of X_t is additionally determined by a seasonal component which has the form of a sinusoidal curve subject to calendar time t which repeats its cycle each year. The seasonal increment will be negative after and positive before the harvesting period. The sign and the ratio of Λ_1^X and Λ_2^X determine the displacement of the curve on the time-abscissa, while the absolute value of the two parameters determines the amplitude of the curve, i.e. the overall impact of the seasonal component.[4]

The impact of a seasonal component is demonstrated in Figs. 7.1 and 7.2. In Fig. 7.1, the density evolution of a price process governed by (7.1) and (7.2) is displayed. The parameter values are set to $\Lambda_1^X = \Lambda_2^X = 0.5$, $S = 80$, $\overline{S} = 85$, $\eta = 1$, $\sqrt{V} = 0.2$. The darker the color of the graph, the higher is the density. The corresponding density values are shown on the bar on the right.

One observes firstly the seasonal component, which leads to a cyclical pattern of the density, and secondly the diffusion component, which leads to increasing uncertainty with proceeding time. At least in the first months, the shape of the distribution is clearly flattened by the diffusion component. After round about one year, the shape of the curve remains more or less constant (apart from seasonal fluctuation) since the diffusion is compensated by the mean reversion.

[4] If both values are positive, a ratio $\Lambda_1^X/\Lambda_2^X \approx 0$ refers to a sinus curve, while a ratio of 1 refers to a phase shift of $0.25\,\pi$, for example. The phase shift is important to match the sinus curve with the date of the harvesting period within the year.

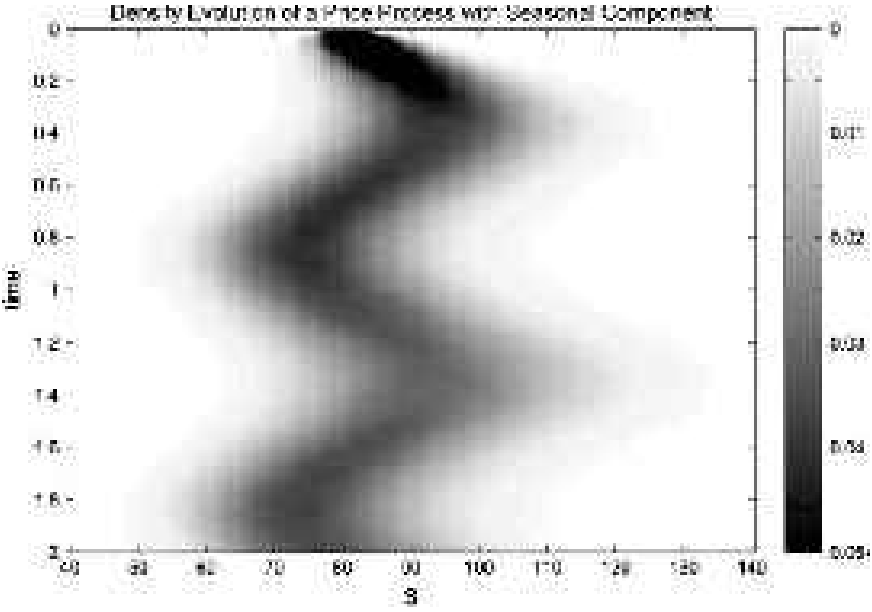

Fig. 7.1 Density evolution of a price process with seasonal component

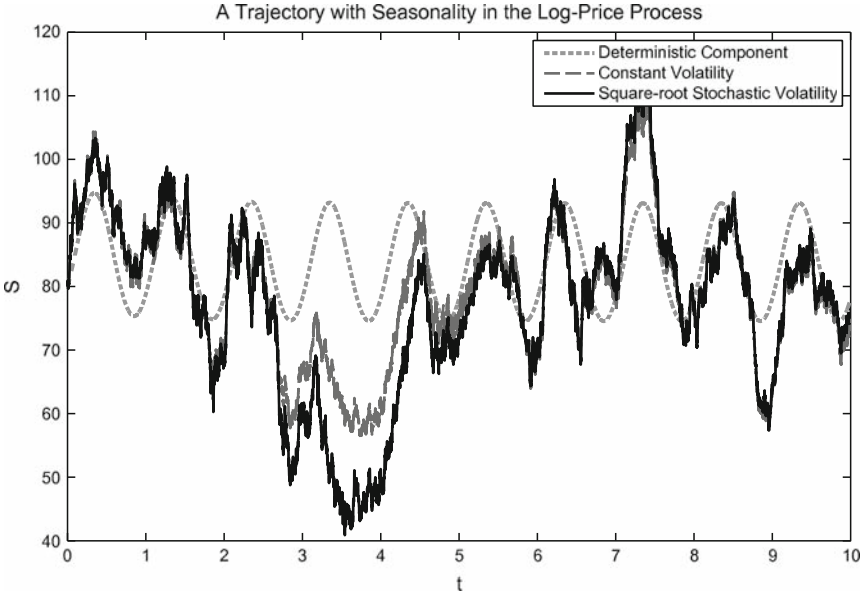

Fig. 7.2 A trajectory with seasonality in the log-price process

In Fig. 7.2, we demonstrate the impact of seasonality on one trajectory with both constant and square-root stochastic volatility. The trajectory has been generated with a strong scheme of order 1. The deterministic component consists of the drift term in (7.1) which incorporates seasonality and mean reversion. The parameter settings are $\Lambda_1^X = \Lambda_2^X = 0.5$, $S = 80$, $\overline{S} = 85$, $\eta = 1$, $\zeta = 0.2$, $\sqrt{V} = 0.2$, $\kappa = 1$, $\rho = -0.5$, $\theta = 0.05$. In the stochastic volatility case, the deviations from the cycle around the long-run mean are larger since the variance process is driven to the mean $\theta = 0.05$ which lies above the initial value $V_t = 0.04$ (which is also the value of V_t in the constant volatility case). The displacement of the sinus curve could refer to the situation that the actual date lies a few months after the harvesting period, since the deterministic component has its seasonal minimum at $t \approx 0.8, 1.8, 2.8$, etc. (t denotes calendar time in years).

7.1.1 Constant Volatility

When we suppose constant volatility, the process is fully described by (7.1) and (7.2). The FPDE depends on terms containing X_t and on terms with constant parameters. The usual guess is exponential affine and takes therefore the form $\Phi(t, X_t) = \exp\{i\phi A(\tau)X_t + B(\tau)\}$. The boundary conditions are $A(0) = 1$ and $B(0) = 0$. The function $B(\tau)$ fulfills the ODE

$$\frac{\mathrm{d}B(\tau)}{\mathrm{d}\tau} = \left(\Lambda_1^X \cos\big(2\pi(T-\tau)\big) + \Lambda_2^X \sin\big(2\pi(T-\tau)\big) + \eta\overline{X} - \frac{1}{2}V_t\right) i\phi e^{-\eta\tau} - \frac{1}{2}V_t\phi^2 e^{-2\eta\tau}, \tag{7.3}$$

and $A(\tau) = e^{-\eta\tau}$ as in the previous model settings. The solution for (7.3) with respect to the boundary condition is given by

$$\begin{aligned} B(\tau) = {} & \left[\overline{X} - \frac{V_t}{2\eta}\right]\big[i\phi - l(\tau)\big] - \frac{V_t}{4\eta}\Big[\phi^2 + [l(\tau)]^2\Big] \\ & + \frac{i\phi}{\eta^2 + 4\pi^2}\Bigg[\Lambda_1^X\Bigg\{\eta\Big(\cos\big(2\pi T\big) - e^{-\eta\tau}\cos\big(2\pi(T-\tau)\big)\Big) + 2\pi\Big(\sin\big(2\pi T\big) \\ & - e^{-\eta\tau}\sin\big(2\pi(T-\tau)\big)\Big)\Bigg\} + \Lambda_2^X\Bigg\{2\pi\Big(e^{-\eta\tau}\cos\big(2\pi(T-\tau)\big) - \cos\big(2\pi T\big)\Big) \\ & + \eta\Big(\sin\big(2\pi T\big) - e^{-\eta\tau}\sin\big(2\pi(T-\tau)\big)\Big)\Bigg\}\Bigg], \end{aligned} \tag{7.4}$$

where $l(\tau)$ is an auxiliary function defined by

$$l(\tau) = i\phi e^{-\eta\tau}.$$

Typically, option prices are calculated for the actual date, i.e. $t = 0$. Using $\tau = T - t$ and setting $t = 0$, (7.4) simplifies to

$$\begin{aligned} B(\tau) = &\left[\overline{X} - \frac{V_t}{2\eta}\right]\big[i\phi - l(\tau)\big] - \frac{V_t}{4\eta}\Big[\phi^2 + [l(\tau)]^2\Big] \\ &+ \frac{i\phi}{\eta^2 + 4\pi^2}\Bigg[\Lambda_1^X\Big\{\eta\big(\cos\big(2\pi\tau\big) - e^{-\eta\tau}\big) + 2\pi\sin\big(2\pi\tau\big)\Big\} \\ &+ \Lambda_2^X\Big\{2\pi\big(e^{-\eta\tau} - \cos\big(2\pi\tau\big)\big) + \eta\sin\big(2\pi\tau\big)\Big\}\Bigg]. \end{aligned} \tag{7.5}$$

Hence, assuming an Ornstein–Uhlenbeck process with a seasonal increment for the log-price without subordinated process leads to an analytic solution for the characteristic function which is straightforward and fast to compute. Option and futures prices are recovered within a fraction of a second. In fact, the incorporation of a deterministic seasonal increment in the log-price process still enables the same solution methods as without seasonal component, as we will see in the following.

7.1.2 Square-Root Stochastic Volatility

Now consider a log-price process specified by (7.1) and (7.2) with a subordinated square-root stochastic volatility process as defined in (4.1). The exponential affine guess is $\Phi(t, X_t, V_t) = \exp\{i\phi A(\tau)X_t + B(\tau)V_t + C(\tau)\}$ with boundary conditions $A(0) = 1$, $B(0) = 0$ and $C(0) = 0$ as in Sect. 4.1. The solution for the first function is again $A(\tau) = e^{-\eta\tau}$, while the solution for $B(\tau)$ is given by (4.11) (respectively (4.13) or (4.15), depending on the parameter settings). The seasonal component affects the ODE for $C(\tau)$ which is now given by

$$\frac{\mathrm{d}C(\tau)}{\mathrm{d}\tau} = \Big(\eta\overline{X} + \Lambda_1^X\cos\big(2\pi(T-\tau)\big) + \Lambda_2^X\sin\big(2\pi(T-\tau)\big)\Big)i\phi e^{-\eta\tau} + \kappa\theta B(\tau)\,. \tag{7.6}$$

The general case solution for (7.6) under the constraint that $t = 0$ is

$$\begin{aligned} C(\tau) = &\,\overline{X}\big[i\phi - l(\tau)\big] + \big[c(\tau) - c(0)\big]\cdot\left[\frac{\kappa\theta}{\zeta\eta}\left(1 - \frac{\rho}{\sqrt{\rho^2-1}}\right)\right] - \frac{2\kappa\theta}{\zeta^2} \\ &\times\ln\left[\frac{\mathcal{C}M(a,b,c(\tau)\frac{\zeta}{\eta}) + U(a,b,c(\tau)\frac{\zeta}{\eta})}{\mathcal{C}M(a,b,c(0)\frac{\zeta}{\eta}) + U(a,b,c(0)\frac{\zeta}{\eta})}\right] + \frac{i\phi}{\eta^2+4\pi^2}\Bigg[\Lambda_1^X\Big\{\eta\big(\cos\big(2\pi\tau\big) \\ &- e^{-\eta\tau}\big) + 2\pi\sin\big(2\pi\tau\big)\Big\} + \Lambda_2^X\Big\{2\pi\big(e^{-\eta\tau} - \cos\big(2\pi\tau\big)\big) + \eta\sin\big(2\pi\tau\big)\Big\}\Bigg], \end{aligned} \tag{7.7}$$

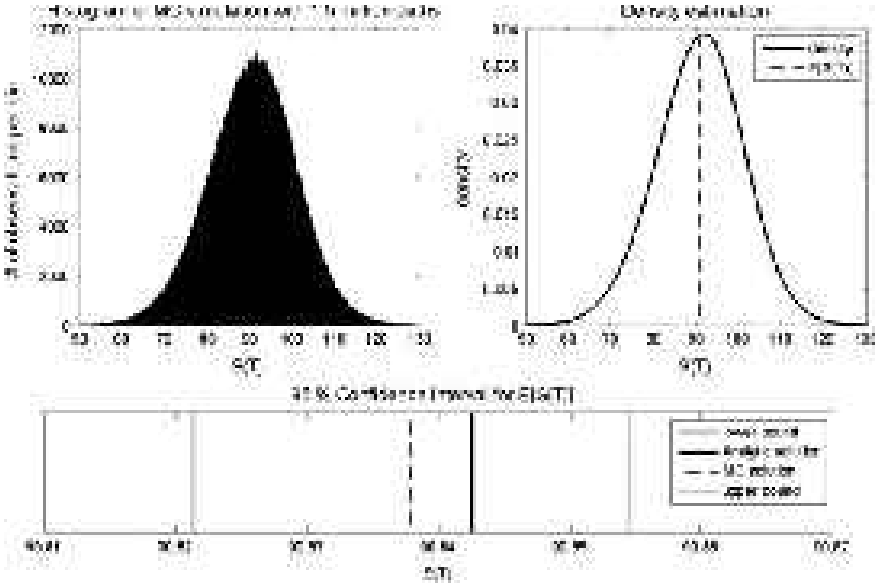

Fig. 7.3 Histogram, density function and confidence interval for the OU model with seasonality component in the price process and square-root stochastic volatility

with the auxiliary function $c(\tau)$ and the constants a, b and $\mathcal{C}$ as defined in Appendix section "Solution for B and C in the Square-Root Stochastic Volatility Framework with Imperfectly Correlated Brownian Motions" in Chap. 4.[5] Since the solutions for the special cases which are discussed in case 2 of sections "Case 2: κ/η is a Positive Integer" as well as in "Solution for B and C in the Square-Root Stochastic Volatility Framework with Perfectly Correlated Brownian Motions" in Appendix of Chap. 4 are analogous, we omit their presentation in this place.

Comparison with the Monte-Carlo Solution

The results of a MC simulation are displayed in Fig. 7.3. The parameter values are set to $S = 80, \overline{S} = 85, \eta = 1, T - t = 0.5, \zeta = 0.2, \sqrt{V} = 0.2, \kappa = 1$, $\rho = -0.5, \theta = 0.05, \Lambda_1^X = \Lambda_2^X = 0.5$. This parameter setting refers to the special case 1 solution which is not explicitly presented in this section.[6] One observes that the distribution is shifted to the right, but a moderate seasonality effect changes the

[5] The parameter conditions for the general case are $\rho \neq \pm 1$ and $(\kappa/\eta) \notin \mathbb{N}$ (see Sect. 4.1.2 and Appendix section "Solution for B and C in the Square-Root Stochastic Volatility Framework with Imperfectly Correlated Brownian Motions" in Chap. 4).

[6] The MC solution for the corresponding square-root stochastic volatility model without seasonality effect in Appendix of Chap. 4 refers also to the special case 1 solution.

shape of the distribution only slightly. The distribution is somewhat closer to normal with a skewness of -0.049 and a kurtosis of 3.131.

7.1.3 Other Model Extensions

The incorporation of a seasonal component in the log-price process together with other model extensions such as Ornstein–Uhlenbeck stochastic volatility or jump effects as discussed in Chap. 5 is easily achieved by adapting the corresponding ODE and solving the ODE system with a Runge-Kutta algorithm. The necessary adaption is done e.g. as in (4.7) and (7.6) by adding the seasonal component to the term $\eta\overline{X}$ as follows:

$$\eta\overline{X} \to \eta\overline{X} + \Lambda_1^X \cos\bigl(2\pi(T-\tau)\bigr) + \Lambda_2^X \sin\bigl(2\pi(T-\tau)\bigr).$$

Since the structure of the solution is largely identical, we omit the presentation of MC simulations for these model extensions. The distribution is shifted upwards or downwards depending on the seasonality component, but as long as these variations account only for a fraction of the price process, the shape of the distribution is only slightly changed.

7.2 Seasonal Impact of Volatility

7.2.1 Seasonal Variance According to Richter and Sørensen

An example for the modeling of a seasonal volatility effect is given in Richter and Sørensen (2002). Their model setting is identical to ours except for the mean reversion in the drift term. An empirical evidence of this topic is given in Crain and Lee (1996), who report a seasonal volatility effect in wheat spot and futures markets.

The underlying log-price process is modeled as follows:

$$dX_t = \left(\eta\{\overline{X} - X_t\} - \frac{1}{2}\exp\bigl\{2\mathfrak{S}_t^V\bigr\}\,V_t\right)dt + \exp\bigl\{\mathfrak{S}_t^V\bigr\}\sqrt{V_t}\,dW_t^X, \qquad (7.8)$$

where the seasonal component is of the same form as in the previous section.

$$\mathfrak{S}_t^V = \Lambda_1^V \cos\bigl(2\pi t\bigr) + \Lambda_2^V \sin\bigl(2\pi t\bigr) \qquad (7.9)$$

The seasonal component in (7.9) enters the log-price process via an exponential function which ensures that the impact of volatility is always positive. The volatility parameter itself may be deterministic or stochastic.

In this model setting, there is no closed-form solution available, not even in the simple case of deterministic volatility. If we assume that the model is fully described by (7.8) and (7.9), volatility is deterministic and the exponential affine guess for the characteristic function is $\Phi(t, X_t) = \exp\{i\phi A(\tau)X_t + B(\tau)\}$ with boundary conditions $A(0) = 1$ and $B(0) = 0$. The solution for the first function is again $A(\tau) = e^{-\eta\tau}$, while the ODE for the second function is

$$\frac{\mathrm{d}B(\tau)}{\mathrm{d}\tau} = \eta\overline{X}i\phi e^{-\eta\tau} - \frac{1}{2}\exp\{2\mathfrak{S}_t^V\}V_t i\phi e^{-\eta\tau} - \frac{1}{2}\exp\{2\mathfrak{S}_t^V\}V_t\phi^2 e^{-2\eta\tau}\,. \quad (7.10)$$

Since there is no closed-form solution available for (7.10), one has to solve the ODE system with Runge-Kutta-methods. Of course, this is also possible for more sophisticated model settings, e.g. with square-root stochastic volatility.[7] One can extend every model of Chaps. 4 and 5 by simply multiplying each volatility parameter with factor $\exp\{\mathfrak{S}_t^V\}$ (or equivalently, each variance parameter with factor $\exp\{2\mathfrak{S}_t^V\}$) in the ODEs and then solving the system with Runge-Kutta algorithms.

7.2.2 Modeling of Seasonality in the Variance Process

An alternative approach of a seasonal impact of volatility is a direct implementation of a seasonal component in the variance process. By this means, we are able to provide an analytic solution in case of deterministic volatility. To the best of our knowledge, the discussion of this model setup is new in this work. The shape of the variance function is different to the approach of Richter and Sørensen, since the exponential function in (7.8) leads to large peaks, while the setting in (7.12) describes a sinus curve with equal upward and downward movement.

The evolution of the price process is again given by

$$dX_t = \left(\eta\{\overline{X} - X_t\} - \frac{1}{2}V_t\right)dt + \sqrt{V_t}\,dW_t^X\,, \quad (7.11)$$

with subordinated deterministic variance

$$dV_t = \kappa\big(\theta[1 + \mathfrak{S}_t^V] - V_t\big)dt\,. \quad (7.12)$$

The seasonality component is defined by (7.9). The parameters Λ_1^V and Λ_2^V are restricted to $\Lambda_1^V \in (-1;1)$, $\Lambda_2^V \in (-1;1)$ and $|\Lambda_1^V| + |\Lambda_2^V| \leq 1$, which assures that $\mathfrak{S}_t^V \geq -1$ and therefore, that V_t is always nonnegative. The FPDE for this setting is

$$\frac{\partial\Phi}{\partial t} + \left(\eta\{\overline{X} - X_t\} - \frac{1}{2}V_t\right)\frac{\partial\Phi}{\partial X} + \kappa\left(\theta[1 + \mathfrak{S}_t^V] - V_t\right)\frac{\partial\Phi}{\partial V} + \frac{1}{2}V_t\frac{\partial^2\Phi}{\partial X^2} = 0\,. \quad (7.13)$$

[7] Richter and Sørensen (2002) implement square-root stochastic volatility, for example.

An exponential affine guess of the form

$$\Phi(t, X_t, V_t) = \exp\{i\phi A(\tau)X_t + B(\tau)V_t + C(\tau)\}$$

leads to the following ODEs (remember that $A(\tau) = e^{-\eta\tau}$):

$$\begin{aligned}\frac{\mathrm{d}B(\tau)}{\mathrm{d}\tau} &= -\frac{1}{2}i\phi e^{-\eta\tau} + \frac{1}{2}(i\phi)^2 e^{-2\eta\tau} - \kappa B(\tau)\\ \frac{\mathrm{d}C(\tau)}{\mathrm{d}\tau} &= \eta\overline{X}i\phi e^{-\eta\tau} + \kappa\theta[1 + \mathfrak{S}_t^V]B(\tau)\,.\end{aligned} \tag{7.14}$$

The general solution for the first ODE is

$$B(\tau) = \mathcal{D}e^{-\kappa\tau} + e^{-\kappa\tau}\int e^{\kappa\tau}\left(-\frac{1}{2}i\phi e^{-\eta\tau} + \frac{1}{2}(i\phi)^2 e^{-2\eta\tau}\right)\mathrm{d}\tau\,, \tag{7.15}$$

where $\mathcal{D}$ is the integration constant which is defined by the boundary condition $B(0) = 0$. The solutions for the two ODEs depends on the adjustment speed parameters κ and η.

General Case Solution

Under the constraints that $\kappa \neq \eta$, $\kappa \neq 2\eta$ and $t = 0$, the solutions for the ODEs in (7.14) are given by

$$B(\tau) = \frac{\mathfrak{a}}{\kappa\theta}\left(e^{-\kappa\tau} - e^{-\eta\tau}\right) + \frac{\mathfrak{b}}{\kappa\theta}\left(e^{-2\eta\tau} - e^{-\kappa\tau}\right) \tag{7.16}$$

and

$$\begin{aligned}C(\tau) = {} & i\phi\overline{X}\big[1 - e^{-\eta\tau}\big] + \mathfrak{a}\Big[\frac{1}{\eta}\big(e^{-\eta\tau} - 1\big) - \frac{1}{\kappa}\big(e^{-\kappa\tau} - 1\big)\Big] + \mathfrak{b}\Big[\frac{1}{\kappa}\big(e^{-\kappa\tau} - 1\big)\\ & - \frac{1}{2\eta}\big(e^{-2\eta\tau} - 1\big)\Big] + \Lambda_1^V\mathfrak{a}\big[\mathfrak{s}\{\kappa\, m(\tau) + 2\pi\sin(2\pi\tau)\} - \mathfrak{u}\{2\pi\sin(2\pi\tau)\\ & + \eta\, n(\tau)\}\big] + \Lambda_1^V\mathfrak{b}\big[\mathfrak{w}\{2\eta\big(\cos(2\pi\tau) - e^{-2\eta\tau}\big) + 2\pi\sin(2\pi\tau)\}\\ & - \mathfrak{s}\{2\pi\sin(2\pi\tau) + \kappa m(\tau)\}\big] + \Lambda_2^V\mathfrak{a}\big[\mathfrak{s}\{\kappa\sin(2\pi\tau) - 2\pi m(\tau)\}\\ & + \mathfrak{u}\{2\pi n(\tau) - \eta\sin(2\pi\tau)\}\big] + \Lambda_2^V\mathfrak{b}\big[\mathfrak{w}\{2\pi\big(e^{-2\eta\tau} - \cos(2\pi\tau)\big)\\ & + 2\eta\sin(2\pi\tau)\} + \mathfrak{s}\{2\pi m(\tau) - \kappa\sin(2\pi\tau)\}\big],\end{aligned} \tag{7.17}$$

with the auxiliary functions

$$\begin{aligned}m(\tau) &= \cos(2\pi\tau) - e^{-\kappa\tau}\\ n(\tau) &= \cos(2\pi\tau) - e^{-\eta\tau}\end{aligned}$$

and constants with integration parameter ϕ

$$\mathfrak{a} = \frac{\kappa\theta i\phi}{2(\kappa-\eta)} \qquad \mathfrak{b} = -\frac{\kappa\theta\phi^2}{2\kappa-4\eta},$$

and without ϕ

$$\mathfrak{s} = \frac{1}{\kappa^2+4\pi^2} \qquad \mathfrak{u} = \frac{1}{\eta^2+4\pi^2} \qquad \mathfrak{w} = \frac{1}{4\eta^2+4\pi^2}.$$

Special Case 1: $\eta = \kappa$

In this special case, we substitute the parameter η. The solution for $B(\tau)$ with respect to the boundary condition simplifies to

$$B(\tau) = e^{-\kappa\tau}\left[\frac{\phi^2}{2\kappa}\left(e^{-\kappa\tau}-1\right) - \frac{1}{2}i\phi\tau\right]. \tag{7.18}$$

The solution for the second ODE under the constraint that $t = 0$ is given by

$$\begin{aligned} C(\tau) = {} & i\phi\overline{X}\left[1-e^{-\kappa\tau}\right] + \frac{\theta i\phi}{4\kappa}\left[\left(e^{-\kappa\tau}-1\right)\left(2-2i\phi\right) + i\phi\left(e^{-2\kappa\tau}-1\right)\right. \\ & \left. + 2\kappa\tau e^{-\kappa\tau}\right] - \frac{1}{2}\Lambda_1^V\mathfrak{s}\,\theta\phi^2\left[\kappa m(\tau) + 2\pi\sin(2\pi\tau)\right] + \Lambda_1^V\mathfrak{c}\left[\kappa\left(e^{-2\kappa\tau}\right.\right. \\ & \left.\left. - \cos(2\pi\tau)\right) - \pi\sin(2\pi\tau)\right] - \frac{1}{2}\Lambda_2^V\mathfrak{s}\,\theta\phi^2\left[\kappa\sin(2\pi\tau) - 2\pi m(\tau)\right] \\ & + \Lambda_2^V\mathfrak{c}\left[\pi\left(\cos(2\pi\tau) - e^{-2\kappa\tau}\right) - \kappa\sin(2\pi\tau)\right] + \frac{1}{2}\Lambda_1^V\mathfrak{s}\,\kappa\theta i\phi\left[\kappa\tau e^{-\kappa\tau}\right. \\ & \left. - \mathfrak{s}\left\{4\kappa\pi\sin(2\pi\tau) + \left(\kappa^2-4\pi^2\right)m(\tau)\right\}\right] + \frac{1}{2}\Lambda_2^V\mathfrak{s}\,\kappa\theta i\phi\left[\mathfrak{s}\left\{4\kappa\pi m(\tau)\right.\right. \\ & \left.\left. - \left(\kappa^2-4\pi^2\right)\sin(2\pi\tau)\right\} - 2\pi\tau e^{-\kappa\tau}\right], \end{aligned} \tag{7.19}$$

where

$$\mathfrak{c} = -\frac{\theta\phi^2}{4\kappa^2+4\pi^2}.$$

Special Case 2: $2\eta = \kappa$

The substitution $2\eta = \kappa$ in (7.15) leads to the special case 2 solution for $B(\tau)$:

$$B(\tau) = \frac{i\phi}{2\kappa}e^{-\kappa\tau}\left(2 + i\phi\kappa\tau - 2\exp\left\{\frac{1}{2}\kappa\tau\right\}\right). \tag{7.20}$$

Again, we present the solution for $C(\tau)$ under the constraint that $t = 0$:

$$
\begin{aligned}
C(\tau) = {} & i\phi\overline{X}\left(1 - e^{-\frac{1}{2}\kappa\tau}\right) + \frac{i\phi\theta}{2\kappa}\left[(2 + i\phi)(1 - e^{-\kappa\tau}) - e^{-\kappa\tau} i\phi\kappa\tau\right. \\
& \left. + 4\left(e^{-\frac{1}{2}\kappa\tau} - 1\right)\right] + \Lambda_1^V \mathfrak{s}\, i\phi\kappa\theta\left[\left(1 + \frac{1}{2}\,\mathfrak{s}\, i\phi(\kappa^2 - 4\pi^2)\right) m(\tau) - \frac{1}{2} i\phi\kappa\tau e^{-\kappa\tau}\right. \\
& \left. + 2\pi \sin(2\pi\tau)\left(\frac{1}{\kappa} + \mathfrak{s} i\phi\kappa\right)\right] + \Lambda_2^V \mathfrak{s} i\phi\kappa\theta\left[i\phi\pi\tau e^{-\kappa\tau} - 2\pi\left(\frac{1}{\kappa} + \mathfrak{s}\, i\phi\kappa\right) m(\tau)\right. \\
& \left. - \sin(2\pi\tau)\left(1 + \frac{1}{2}\,\mathfrak{s}\, i\phi(\kappa^2 - 4\pi^2)\right)\right] + \Lambda_1^V \mathfrak{d}\left[2\kappa\left(e^{-\frac{1}{2}\kappa\tau} - \cos(2\pi\tau)\right)\right. \\
& \left. - 8\pi \sin(2\pi\tau)\right] + \Lambda_2^V \mathfrak{d}\left[8\pi\left(\cos(2\pi\tau) - e^{-\frac{1}{2}\kappa\tau}\right) - 2\kappa \sin(2\pi\tau)\right], \qquad (7.21)
\end{aligned}
$$

where

$$
\mathfrak{d} = \frac{i\phi\theta}{\kappa^2 + 16\pi^2}\,.
$$

As in the previous section, the characteristic function for deterministic volatility, defined by (7.16) and (7.17), provides a computation of option and futures prices within a fraction of a second. We tested the accuracy of our solutions in (7.16) and (7.17) as well as the special cases (7.18)–(7.21) by performing Runge-Kutta calculations of the ODE system in (7.14), which leads to virtually identical results.

Model Extensions

The combination of seasonality in the log-price process according to (7.1) and (7.2) and seasonal deterministic volatility according to (7.9) and (7.12) is also possible and leads to a closed-form solution for the characteristic function. The system of ODEs is given by

$$
\begin{aligned}
\frac{\mathrm{d}B(\tau)}{\mathrm{d}\tau} &= -\frac{1}{2} i\phi e^{-\eta\tau} + \frac{1}{2}(i\phi)^2 e^{-2\eta\tau} - \kappa B(\tau) \\
\frac{\mathrm{d}C(\tau)}{\mathrm{d}\tau} &= \left[\eta\overline{X} + \mathfrak{S}_t^X\right] i\phi e^{-\eta\tau} + \kappa\theta\left[1 + \mathfrak{S}_t^V\right] B(\tau)\,, \qquad (7.22)
\end{aligned}
$$

which is very similar to (7.14). The solution for $B(\tau)$ is unchanged and in the general case with $\kappa \neq \eta$, $\kappa \neq 2\eta$ and $t = 0$ given by (7.16) (respectively by (7.18) or (7.20) for the two special cases). The solution for $C(\tau)$ under the constraint that $t = 0$ corresponds to (7.17) (respectively to (7.19) or (7.21) for the special cases) with an additional term which is given by

$$
\mathfrak{u}\, i\phi\, \Lambda_1^X\left[\eta n(\tau) + 2\pi \sin(2\pi\tau)\right] + \mathfrak{u}\, i\phi\, \Lambda_2^X\left[\eta \sin(2\pi\tau) - 2\pi n(\tau)\right]. \qquad (7.23)
$$

Model extensions with stochastic volatility or jump features are possible, but always require the computation of the characteristic function with Runge-Kutta-methods. The incorporation of seasonal volatility in the models of Chaps. 4 and 5 can be done by changing the mean reversion level θ of the variance (respectively volatility) process to $\theta[1 + \mathfrak{S}_t^V]$ in the corresponding ODEs.

Chapter 8
Conclusion

In this thesis, we discussed and extended existing pricing models for derivatives on mean-reverting assets. The pricing formulas are based on the Fourier inversion approach of Heston (1993), whereas the specification of the underlying price process traces back to the incomplete market setup in Ross (1997) and model 1 in Schwartz (1997).

In Chap. 2, we discussed the sources and empirical evidence of mean reversion in asset prices. As sources of mean reversion, we identified convenience yield effects and negative correlation between prices and risk premia as well as interest rates. We shortly addressed convenience yield models as a second alternative to achieve mean reversion in prices through an additional subordinated process. Compared with the modeling of mean reversion by an OU price process, convenience yield models show less stringent mean reversion unless the (log-) price is directly included in the convenience yield process. The fact that the model manages with less parameters could be an advantage of OU price processes compared with convenience yield models. Furthermore, the convenience yield is not an observable economic variable, which makes it difficult to judge whether the model setup matches the empirical facts or not.

Various studies revealed that mean reversion mainly is a feature of commodity futures and spot prices and is at most weakly supported in financial asset markets. The Samuelson hypothesis, which postulates that futures prices are less volatile with increasing time to maturity, and the Kaldor-Working hypothesis, which postulates that the convenience yield depends inversely upon the level of inventories, both are empirical facts which are an implication of mean reversion. Therefore, these hypotheses accompany the existence of mean reversion and are supported in commodity markets and rejected in financial asset markets.

The design of the foundations of derivative pricing in Chap. 3 was twofold: In the first part, we showed the setup in a world with complete markets and subsequently demonstrated analogously the pricing of derivatives in incomplete markets. Following Ross (1997), we assumed that the drift of the price process under the risk-neutral measure is mean-reverting and therefore not equal to the risk-free interest rate, which would be the case when markets are complete. We presented the

B. Lutz, *Pricing of Derivatives on Mean-Reverting Assets*,
Lecture Notes in Economics and Mathematical Systems,
DOI 10.1007/978-3-642-02909-7_8, © Springer-Verlag Berlin Heidelberg 2010

Fourier inversion approach of Heston (1993) for the pricing of European options. We also showed how the characteristic function can be useful for the specification of derivative prices. The Fourier inversion approach supports a rich spectrum of process specifications and is not restricted to Gaussian densities.

The second part of Chap. 3 focused on various numerical methods to integrate the Fourier integral and systems of ordinary differential equations. We discussed various algorithms to integrate the Fourier integral in option pricing formulas. For the evaluation of a single option price, we suggested to apply a Gauss-Laguerre quadrature scheme. Since the integration nodes of this algorithm are not equidistant, the algorithm achieves moderate to high accuracy with only a few nodes per integral.[1] The fact that the density of the nodes weakens with the integration parameter ϕ while the computation time per node increases with ϕ is an additional advantage regarding computation time.

When multiple option prices over the whole spectrum of strike prices are required, it is convenient to apply Fast Fourier algorithms. We presented the Fast Fourier algorithm which was introduced in finance by Carr and Madan (1999). This algorithm has the deficiency that the distance of the nodes over the ϕ-axis and the strike axis cannot be chosen independently. As a result of this fact, increasing the accuracy leads to the calculation of option prices which are not needed because of unrealistic strikes. This deficiency can be remedied with the application of the Fractional Fast Fourier algorithm of Bailey and Swartztrauber (1991), which was adopted in finance by Chourdakis (2004).

As for the integration of ODE systems, we argued that the choice of the correct solver depends on the stiffness of the ODE system. Following Ekeland et al. (1998) and Huang and Yu (2007), we chose the eigenvalues of the Jacobi matrix as indicator of stiffness. Stiffness is supported by a negative real part of one or more eigenvalues. The larger the absolute value of the negative real part, the higher the stiffness of the ODE system. Our tests revealed that the ODE systems of our model setups prove to be nonstiff or at most moderately stiff. Hence, one should choose ODE solvers for nonstiff systems, namely the ode45 or the ode113 Matlab® algorithm. While ode45 is based on the Dormand and Prince (1980) pair of embedded Runge-Kutta formulae, ode113 is an Adams-Bashforth-Moulton predictor-corrector scheme. The predictor-corrector scheme proved to be superior with respect to computation time. It is worth noting that this solver also needs Runge-Kutta calculations at the start of the integration to initialize.

In Chaps. 4–7, we discussed various model setups for the pricing of commodity derivatives. We began with the incorporation of stochastic volatility in Chap. 4, therefore extending the models of Ross (1997) and Schwartz (1997). We compared our findings with a similar attempt of Tahani (2004). We were able to show that the model setup of Tahani fails to provide realistic option prices for reasonable parameter values, particularly the linear homogeneity property of option prices is not fulfilled. Due to an uncoupling of the mean reversion and the equilibrium level

[1] Depending on the desired accuracy, 15–40 nodes are sufficient.

parameter, we were able to remedy the deficiencies of the Tahani model. Furthermore, we provided closed-form solutions for the square-root stochastic volatility case, following Repplinger (2008). The solutions are given in terms of Kummer functions for the general case and the special case 1, respectively Bessel functions for the special case 2 which is determined by $\rho = \pm 1$. Following Tahani (2004) and Zhu (2000), we also incorporated Ornstein–Uhlenbeck stochastic volatility. In this model setup, the guess for the characteristic function is exponential linear-quadratic. A closed-form solution is only possible for the help functions $A(\tau)$ and $B(\tau)$, but not for the other two help functions. Hence, the solution for the characteristic function with OU stochastic volatility is given by numerical integration algorithms.

In the appendix of the chapter, we also compared the computation time of the standard numerical integration algorithm ode45 with the closed-form solution in terms of hypergeometric functions. This comparison is only possible for model setups which incorporate square-root stochastic volatility and no jumps, i.e., the models in Sects. 4.1.2 (square-root stochastic volatility), 6.2.2 (square-root stochastic volatility and stochastic non-mean-reverting equilibrium level) and the second paragraph in 7.1 (square-root stochastic volatility with seasonality effects). We compared the computation time of ode45 with the hypergeometric function solution of the former model. Apart from a special case, the solution is given in terms of Kummer functions.[2] Concerning computation time, the numerical algorithm ode45 proved to be approximately six times faster compared to Kummer functions.

In Chap. 5, we addressed the incorporation of jump components in the square-root stochastic volatility framework. We followed Bates (1996a, 1996b, 2000), Duffie, Pan and Singleton (2000) and Kispert (2005) as for the specification of the jump elements. We incorporated lognormally distributed jumps in the price process, exponentially and Γ-distributed jumps in the variance process and combinations of price and variance jumps. Due to the use of numerical ODE integration schemes, we are able to provide solutions for combinations of jumps with both mean reversion in the price process and stochastic volatility. We extended the results of the above-mentioned papers, since the authors only arranged mean reversion with jumps or non-mean-reverting price processes with stochastic volatility and jumps.

Mean-reverting price processes reduce the uncertainty about future price distributions, since every shock in the price process will be removed in the long run. In Chap. 6, we assumed the long-run equilibrium level of the price process to be stochastic, which is equivalent to the assumption of shocks in the price process which persist. We discussed two setups for the subordinated stochastic equilibrium level process: (a) an Ornstein–Uhlenbeck process and (b) Brownian motion with drift. We compared our model setups with similar specifications in Schwartz and Smith (2000) and Realdon (2007). We also addressed extensions of the stochastic equilibrium level setup with stochastic volatility and jumps. For the non-mean-reverting subordinated process together with square-root stochastic volatility, we

[2] The special case is determined by $\rho = \pm 1$. The solution for this special case is given in terms of Bessel functions. The calculation with Bessel functions is much faster than numerical integration.

were able to derive a closed-form solution based on hypergeometric functions similar to the square-root stochastic volatility case in Chap. 4.

Chapter 7 dealt with seasonality effects both in the price and the variance process. We firstly mentioned that seasonality effects are only important in markets with cyclical behavior, e.g., in electricity markets due to seasonal weather changes and agricultural commodity markets due to harvest cycles. Subsequently, we implemented a seasonal component according to Richter and Sørensen (2002) and Sørensen (2002) in a mean-reverting log-price process. The implementation of the seasonal term did not change the shape of the distribution of S_T intensely, it is mainly shifted upwards or downwards according to the seasonal cycle. We discussed this model setup both with constant volatility and square-root stochastic volatility. Since the deterministic seasonal component did not change the structure of the solution, we were able to provide closed-form solutions for both specifications of volatility.

Subsequently, we addressed the modeling of seasonal components in the variance process. We firstly followed Richter and Sørensen and implemented the seasonality effect by means of an exponential function to ensure that variance remains positive. However, a closed-form solution for this model setup is not possible, not even in the simplest case of deterministic volatility. Hence, we applied numerical integration methods to provide the solution for the characteristic function. We further suggested another alternative to achieve seasonality in the variance process. This variance process is also ensured to be nonnegative, but forgoes the use of exponential functions.[3] Due to this slightly simpler model setup, we were able to provide closed-form solutions both for the deterministic and the square-root stochastic volatility case. We also outlined the extensions of the model setups in the previous chapters (i.e., OU stochastic volatility, different jump components, stochastic equilibrium level) with deterministic seasonality effects.

Finally, we want to address some further aspects which are left for future research. Firstly, the empirical testing of the performance of the discussed models would be an interesting topic. Generally speaking, the incorporation of stochastic volatility and jump components should lead to a better empirical model performance. It should be expected that the stochastic equilibrium level models in Chap. 6 perform better for crude oil derivatives than standard OU models. On the other hand, the implementation of too much factors bears the risk of model overspecification.

There are also some further model extensions possible. Firstly, the assumption of deterministic interest rates can be suspended. Models with different specifications of stochastic interest rates can be found in Zhu (2000) as well as DPS (2000), among others.[4] Another possible extension accounts for the empirical fact that there exist periods in which large price moves occur with high frequency, followed

[3] The shape of this seasonal variance component is sinusoidal, whereas the setup of Richter and Sørensen leads to a peaked seasonal component due to the exponential function.

[4] Zhu (2000) addresses not only a square-root process, but also an OU and a double square-root process as subordinated interest rate process.

by other periods of low price variations. Models with a stochastic jump intensity can capture this pattern. This model feature is already discussed in Fang (2002) and Kangro, Pärna and Sepp (2004) for non-mean-reverting assets. Geman and Roncoroni (2006) incorporate a deterministic jump intensity process in the context of the pricing of electricity derivatives.

References

1. Abramowitz M, Stegun I (1970) Handbook of mathematical functions, 9th edn. Dover, New York
2. Adrangi B, Chatrath A (2003) Non-linear dynamics in futures prices: evidence from the coffee, sugar and cocoa exchange. Appl Finan Econ 13:245–256
3. Amin K, Ng V, Pirrong C (1995) Valuing energy derivatives. In: Jameson R (ed) Managing energy price risk. Risk Publications, London
4. Anderson R Danthine J (1983) The time pattern of hedging and the volatility of futures prices. Rev Econ Stud 50:249–266
5. Anthony M, MacDonald R (1998) On the mean reverting properties of target zone exchange rates: Some evidence from the ERM. Eur Econ Rev 42:1493–523
6. Anthony M, MacDonald R (1999) The width of the band and exchange rate mean reversion: Some further ERM-based results. J Int Money Finance 18:411–428
7. Bailey DH, Swartztrauber PN (1991) The Fractional fourier transform and applications. SIAM Review 33(3):389–404
8. Bakshi G, Cao C, Chen Z (1997) Empirical performance of alternative option pricing models. J Finance 52:2003–2049
9. Bakshi G, Madan D (2000) Spanning and derivative security valuation. J Finan Econ 55: 205–238
10. Ball C, Roma A (1994) Stochastic volatility and option pricing. J Finan Quant Anal 29: 589–607
11. Barone-Adesi G, Whaley RE (1987) Efficient analytic approximation of American option values. J Finance 42:301–320
12. Barrowes B (2004) Matlab® code for the generalized hypergeometric function. Available via the Matlab® Central File Exchange. http://www.mathworks.com/matlabcentral/fileexchange/ loadFile.do?objectId=5616&objectType=file. Cited 12 Feb 2008
13. Bates DS (1996a) Dollar jump fears, 1984-1992: distributional abnormalities implicit in currency futures options. J Int Money Finance 15:65–93
14. Bates DS (1996b) Jumps and stochastic volatility: Exchange rate processes implicit in deutschemark options. Rev Finan Stud 9:69–108
15. Bates DS (2000) Post-'87 crash fears in the S & P 500 futures options market. J Econometrics 94:181–238
16. Bauer H (1992) Maß- und Integrationstheorie. Walter de Gruyter, Berlin
17. Baxter M, Rennie A (1996) Financial Calculus: An introduction to derivative pricing. Cambridge University Press, Cambridge
18. Benavides G (2002) The theory of storage and price dynamics of agricultural commodity futures: The case of corn and wheat, EFA 2002 Berlin Meetings Discussion Paper
19. Bessembinder H, Coughenour JF, Seguin PJ, Smoller MM (1995) Mean reversion in equilibrium asset prices: Evidence from the futures term strucure. J Finance 50:361–375

20. Bessembinder H, Coughenour JF, Seguin PJ, Smoller MM (1996) Is there a term structure of futures volatilities? Reevaluating the Samuelson hypothesis. J Derivatives, Winter 1996, 45–58
21. Bjerksund P, Ekern S (1995) Contingent claims evaluation of mean-reverting cash flows in shipping. In: Trigeorgis L (ed) Real Options in Capital Investment: Models, Strategies, and Applications. Preager
22. Björk T (2005) Arbitrage theory in continuous time, 2nd edn. Oxford University Press, Oxford
23. Black F, Scholes MS (1973) The pricing of options and corporate liabilities. J Polit Economy 81:637–654
24. Breeden DT (1979) An intertemporal asset pricing model with stochastic consumption and investment opportunities. J Finan Econ 7:265–296
25. Brennan MJ, Schwartz ES (1985) Evaluating natural resource investments. J Bus 58:135–157
26. Brennan MJ (1991) The price of convenience and the valuation of commodity contingent claims. In: Lund D, Øksendal B (eds) Stochastic Models and Option Values. North Holland, Amsterdam
27. Broadie M, Detemple J (1996) American option valuation: new bounds, approximations, and a comparison of existing methods. Rev Finan Stud 9:1211–1250
28. Bronstein IN, Semendjajew KA, Musiol G, Mühlig H (2001) Taschenbuch der Mathematik, 5th edn. Verlag Harri Deutsch, Frankfurt (Main)
29. Bruti-Liberati N, Platen E (2006) Approximation of jump diffusions in finance and economics, QFRC Research Paper 176, University of Technology, Sydney
30. Bühler W, Korn O, Schöbel R (2004) Hedging long-term forwards with short-term futures; A two-regime approach. Rev Derivatives Res 7:185–212
31. Cai H (2006) Matlab® code for the Bessel function of complex order and argument. Available via the Matlab® Central File Exchange. http://www.mathworks.com/matlabcentral/fileexchange/ loadFile.do?objectId=9515&objectType=file. Cited 12 Feb 2008
32. Carr P, Madan D (1999) Option valuation using the fast fourier transform. Journal of Computational Finance 3:463–520
33. Casassus J, Collin-Dufresne P (2004) Stochastic convenience yield implied from commodity futures and interest rates. J Finance 60:2283–2331
34. Cerny A (2004) Introduction to fast fourier transform in finance. Journal of Derivatives 12(1):73–88
35. Chatrath A, Adrangi B, Dhanda KK (2002) Are commodity prices chaotic? Agr Econ 27: 123–137
36. Chourdakis K (2004) Option pricing using the fractional FFT. Journal of Computational Finance 8:1–18
37. Collin-Dufresne P, Goldstein R (2002) Do bonds span the fixed income markets? Theory and evidence for unspanned stochastic volatility. J Finance 57:1685–1730
38. Cont R (2001) Empirical properties of asset returns: stylized facts and statistical issues. Quant Finance 1:223–236
39. Cont R, Tankov P (2003) Financial modelling with jump processes. Chapman & Hall / CRC, London
40. Cox JC, Ingersoll JE, Ross SA (1981) The relation between forward prices and futures prices. J Finan Econ 9:321–346
41. Cox JC, Ingersoll JE, Ross SA (1985) A theory of the term structure of interest rates. Econometrica 53:385–407
42. Crain SJ, Lee JH (1996) Volatility in wheat spot and futures markets, 1950–1993: Government farm programs, seasonality, and causality. J Finance 51:325–343
43. Das SR (2002) The surprise element: jumps in interest rates. J Econometrics 106:27–65
44. Deaton A, Laroque G (1992) On the behaviour of commodity prices. Rev Finan Stud 59:1–23
45. Deaton A, Laroque G (1996) Competitive storage and commodity price dynamics. J Polit Economy 104:896–923
46. Delbaen F, Schachermayer W (1994) A general version of the fundamental theorem of asset pricing. Mathematische Annalen 300:463–520

47. Delbaen F, Schachermayer W (1998) The fundamental theorem of asset pricing for unbounded stochastic processes. Mathematische Annalen 312:215–250
48. Dormand JR, Prince PJ (1980) A family of embedded Runge-Kutta formulae. Journal of Computational and Applied Mathematics 6:19–26
49. Duffee GR (2002) Term premia and interest rate forecasts in affine models. J Finance 57: 405–443
50. Duffie D, Pan J, Singleton K (2000) Transform analysis and asset pricing for affine jump-diffusions. Econometrica 68:1343–1376
51. Duffie D (2001) Dynamic asset pricing theory, 3rd edn. Princeton University Press, Princeton
52. Ekeland K, Owren B, Øines E (1998) Stiffness detection and estimation of dominant spectra with explicit Runge-Kutta methods. ACM Transactions on Mathematical Software 24: 368–382
53. Elliott R, Sick G, Stein M (2003) Modelling electricity price risk. Working Paper, University of Calgary.
54. Eraker B (2004) Do stock prices and volatility jump? reconciling evidence from spot and option prices. J Finance 59:1367–1403
55. Fama EF (1984) Forward and spot exchange rates. J Monet Econ 14:319–338
56. Fama EF, French KR (1987) Commodity futures prices: Some evidence on forecast power, premiums, and the theory of storage. J Bus 60:55–73
57. Fama EF, French KR (1988) Permanent and temporary components of stock prices. J Polit Economy 96:246–273
58. Fang H (2002) Jumps with a stochastic jump rate: An alternative option pricing model, Ph. D. thesis, University of Virginia.
59. Feller W (1951) Two singular diffusion problems. The Annals of Mathematics 54:173–182
60. French KR (1983) A comparison of futures and forward prices. J Finan Econ 12:311–342
61. French KR (2005) Why and when do spot prices of crude oil revert to futures price levels?, Working Paper, *Finance and Economics Discussion Series* 2005-30, Board of Governors of the Federal Reserve System.
62. Geman H, El Karoui N, Rochet J (1995) Changes of numéraire, change of probability measure and option pricing. Journal of Applied Probability 32:443–458
63. Geman H, Roncoroni A (2006) Understanding the fine structure of electricity prices. J Bus 79:1225–1261
64. Gibson R, Schwartz ES (1990) Stochastic convenience yield and the pricing of oil contingent claims. J Finance 45:959–976
65. Glasserman P (2004) Monte Carlo methods in financial engineering. Springer, New York
66. Golub GH, Welsch JH (1969) Calculation of Gauss quadrature rules. Mathematics of Computation 23:221–230
67. Harrison JM, Kreps D (1979) Martingales and arbitrage in multiperiod securities markets. J Econ Theory 20:381–408
68. Harrison JM, Pliska SR (1981) Martingales and stochastic integrals in the theory of continuous trading. Stochastic Processes and their Applications 11:215–260
69. Heath D, Jarrow R, Morton A (1992) Bond pricing and the term structure of interest rates: A new methodology. Econometrica 60:77–105
70. Heston S (1993) A closed-form solution for options with stochastic volatility with applications to bond and currency options. Rev Finan Stud 6:327–343
71. Hilliard JE, Reis JA (1998) Valuation of commodity futures and options under stochastic convenience yields, interest rates, and jump diffusions in the spot. J Finan Quant Anal 33: 61–86
72. Hilliard JE, Reis JA (1999) Jump processes in commodity futures prices and options pricing. Amer J Agr Econ 81:273–286
73. Huang SJ, Yu J (2007) On stiffness in affine pricing models. Journal of Computational Finance 10:99–123
74. Hui CH, Lo CF (2006) Currency barrier option pricing with mean reversion. The Journal of Futures Markets 26:939–958

75. Hull JC, White A (1987) The pricing of options on assets with stochastic volatilities. J Finance 42:281–300
76. Hull JC (2006) Options, futures, and other derivatives, 6th edn. Prentice Hall, New Jersey
77. Jäckel P (2002) Monte Carlo methods in finance. Wiley, Chichester
78. Jarrow RA, Oldfield GD (1981) Forward contracts and futures contracts. J Finan Econ 9: 373–382
79. Kaldor N (1939) Speculation and economic stability. Rev Econ Stud 7:1–27
80. Kamat R, Oren SS (2002) Exotic options for interruptible electricity supply contracts. Operations Research 50:835–850
81. Kangro R, Pärna K, Sepp A (2004) Pricing European-style options under jump diffusion processes with stochastic volatility: Applications of Fourier transform. Acta et Commentationes Universitatis Tartuensis de Mathematica 8:123–133
82. Karatzas I, Shreve SE (1991) Brownian motion and stochastic calculus. Springer, New York
83. Kispert W (2005) Financial contracts on electricity in the nordic power market, Ph. D. Thesis, University of Tübingen.
84. Kloeden PE, Platen E (1999) Numerical solution of stochastic differential equations, 3rd edn. Springer, Berlin
85. Korn O (2005) Drift matters: An analysis of commodity derivatives. J Futures Markets 25:211–241
86. Lee RW (2004) Option pricing by transform methods: Extensions, unification, and error control. Journal of Computational Finance 7:51–86
87. Lewis A (2000) Option valuation under stochastic volatility. Finance Press
88. Lewis A (2001) A simple option formula for general jump-diffusion and other exponential Lévy processes, SSRN Working Paper and optioncity.net
89. Longstaff FA, Schwartz ES (1995) Valuing credit derivatives. Journal of Fixed Income 5:6–12
90. Lucia JJ, Schwartz ES (2002) Electricity prices and power derivatives: Evidence from the Nordic Power Exchange. Rev Derivatives Res 5:5–50
91. Madan DB, Seneta E (1990) The variance gamma model for share market returns. J Bus 63:511–524
92. Madan DB, Carr P, Chang EC (1998) The variance gamma process and option pricing. Eur Finance Rev 2:79–105
93. Malliaris AG, Brock WA (1991) Stochastic methods in economics and finance, 6th edn. North-Holland, New York
94. Marsaglia G, Tsang WW (2000) The Ziggurat method for generating random variables. J Statistical Software 5:1–7
95. Musiela M, Rutkowski M (2005) Martingale methods in financial modelling, 2nd edn. Springer, Berlin
96. Merton RC (1973) Theory of rational option pricing. Bell Journal of Economics and Management Science 4:141–183
97. Merton RC (1976) Option pricing when underlying stock returns are discontinuous. J Finan Econ 3:125–144
98. Miltersen KR, Schwartz ES (1998) Pricing of options on commodity futures with stochastic term structures of convenience yields and interest rates. J Finan Quant Anal 33:33–59
99. Namias V (1980) The fractional order Fourier transform and its application to quantum mechanics. IMA Journal of Applied Mathematics 25:241–265
100. Øksendal B (2000) Stochastic differential equations, 5th edn. Springer, Berlin
101. Pilipović D (1998) Energy Risk. Valuing and managing energy derivatives. McGraw-Hill, New York
102. Polyanin AD Zaitsev VF (2003) Handbook of exact solutions for ordinary differential equations, 2nd Edn. Chapman & Hall/CRC Press, Boca Raton
103. Poterba JM, Summers LH (1988) Mean reversion in stock prices: evidence and implications. J Finan Econ 22:27–59
104. Press WH, Teukolsky SA, Vetterling WT, Flannery BP (1997) Numerical recipes in C, 2nd edn. Cambridge University Press, Cambridge

105. Realdon M (2007) Revisiting the pricing of commodity futures and forwards, Working Paper, University of Southampton
106. Repplinger D (2008) Option pricing of fixed income derivatives with random fields and unspanned stochastic volatility, Ph. D. Thesis, University of Tübingen
107. Richter M Sørensen C (2002) Stochastic volatility and seasonality in commodity futures and options: The case of soybeans, Working Paper, Copenhagen Business School
108. Ross SA (1997) Hedging Long-Run Commitments: Exercises in Incomplete Market Pricing. Economic Notes by Banca Monte dei Paschi di Siena SpA 26:385–420
109. Routledge B, Seppi D, Spatt C (2000) Equilibrium forward curves for commodities. Journal of Finance 55(3):1297–1338
110. Samuelson PA (1965) Proof that properly anticipated prices fluctuate randomly. Industrial Management Review 6:41–49
111. Schaich E, Münnich R (2001) Mathematische Statistik für Ökonomen, Vahlen, München
112. Schöbel R (1992) Arbitrage pricing in commodity futures markets: Is it feasible? *Presentation at the Conference on Mathematical Finance*, Oberwolfach, August 23–29, 1992.
113. Schöbel R, Zhu J (1999) Stochastic volatility with an Ornstein–Uhlenbeck process: An extension. Eur Finance Rev 3:23–46
114. Schwartz ES (1997) The stochastic behavior of commodity prices: Implications for valuation and hedging. J Finance 52:923–972
115. Schwartz ES, Smith JE (2000) Short-term variations and long-term dynamics in commodity prices. Management Science 46:893–911
116. Scott LO (1997) Pricing stock options in a jump-diffusion model with stochastic volatility and interest rates: applications of Fourier inversion methods. Math Finance 7:413–426
117. Shampine LF, Reichelt MW (1997) The MATLAB ODE suite. SIAM Journal on Scientific Computing 18:1–22
118. Shreve ES (2004) Stochastic calculus for finance II - continuous-time models. Springer, New York
119. Sørensen C (1997) An equilibrium approach to pricing foreign currency options. Eur Finan Manage 3:63–84
120. Sørensen C (2002) Modeling seasonality in agricultural commodity futures. J Futures Markets 22:393–426
121. Stein E, Stein J (1991) Stock price distributions with stochastic volatility: an analytic approach. Rev Finan Stud 4:727–752
122. Stroud A (1974) Numerical quadrature and solution of ordinary differential equations. Springer, New York
123. Sundaram RK (1997) Equivalent martingale measures and risk-neutral pricing: An expository note. J Derivatives, Fall, 85–98
124. Tahani N (2004) Valuing credit derivatives using gaussian quadrature: A stochastic volatility framework. J Futures Markets 24:3–35
125. Vasicek O (1977) An equilibrium characterization of the term structure. J Finan Econ 5: 177–188
126. Weron R, Simonsen I, Wilman P (2003) Modeling high volatile and seasonal markets: evidence from the Nord Pool electricity market. Working Paper, Wroclaw University of Technology, Poland.
127. Working H (1948) Theory of the inverse carrying charge in futures markets. J Farm Econ 30:1–28
128. Working H (1949) The theory of the price of storage. Amer Econ Rev 39:1254–1262
129. Zhu J (2000) Modular pricing of options. Springer, Berlin